2007-12-28

A Role for Histone Modification in the Mechanism of Action of Antidepressant and Stimulant Drugs: a Dissertation

Frederick Albert Schroeder
University of Massachusetts Medical School

A Dissertation Presented

by

Frederick Albert Schroeder

Submitted to the Faculty of the
University of Massachusetts Graduate School of Biomedical Sciences
Worcester, Massachusetts, USA

in partial fulfillment of the requirements for the degree of

DOCTOR OF PHILOSOPHY

December 28, 2007

Program in Neuroscience

A Role for Histone Modification in the Mechanism of Action of Antidepressant and Stimulant Drugs

A Dissertation Presented
By

Frederick Albert Schroeder

Approved as to style and content by:

_____
Alonzo Ross, Ph.D., Chair of Committee

_____
Pradeep Bhide, Ph.D., Member of Committee

_____
Craig L. Peterson, Ph.D., Member of Committee

_____
Ann R. Rittenhouse, Ph.D., Member of Committee

_____
Steven Treistman, Ph.D., Member of Committee

_____
Schahram Akbarian, M.D., Ph.D., Dissertation Mentor

_____
Anthony Carruthers, Ph.D., Dean, Graduate School of Biomedical Sciences

University of Massachusetts Medical School
Doctoral Program in Neuroscience
May 22, 2008

DEDICATION

To my mother and father, for the hereditary effects.

ABSTRACT

Depression and stimulant drug addiction each result in massive losses of health, productivity and human lives every year. Despite decades of research, current treatment regimes for depression are ineffective in approximately half of all patients. Therapy available to stimulant drug addicts is largely ineffective and moreover, dedicated treatments for drug dependence (including abuse of cocaine) are non-existent. Thus, there is a pressing need to further understanding of the molecular mechanisms underlying these disorders in order to develop novel, targeted therapeutic strategies.

Chromatin remodeling, including changes in histone acetylation, has been proposed to play a role in both the etiology and treatment of depression and stimulant abuse. Histone acetyltransferases (HATs) and histone deacetylases (HDACs) regulate numerous cellular processes, including transcription, cell cycle progression and differentiation. Moreover, histone acetylation has been shown to regulate hippocampal neurogenesis, a cellular response associated with the pathogenesis and treatment of depression and stimulant abuse (Hsieh et al., 2004, Yamaguchi et al., 2004, Fischer et al., 2007). Ultimately, such basic cellular processes impact higher order function, namely cognition and emotion.

Indeed, recent studies suggest that HDAC activity in selected forebrain regions, including ventral striatum and hippocampus, modulate stimulant- and antidepressant-induced behavior (Kumar et al., 2005, Tsankova et al., 2006a, Fischer et al., 2007). These reports highlight an association between chromatin remodeling and diverse behavioral changes, including changes induced by the pleiotropic HDAC inhibitor,

sodium butyrate (SB), (Kumar et al., 2005, Tsankova et al., 2006a, Fischer et al., 2007). However, behavioral, brain-metabolic and molecular effects of SB treatment in the context of rodent models of depression, dopaminergic sensitization and repeated cocaine administration remained unclear.

The work described in this thesis illustrates the potential for chromatin modifying drugs in mechanisms underlying the experimental pharmacology of depression and stimulant addiction. Specifically, the data presented here support the view that treatment with the short chain fatty acid, sodium butyrate enhances:

(1) antidepressant-like behavioral effects of the selective serotonin reuptake inhibitor (SSRI), fluoxetine

(2) locomotor sensitization induced by repeated administration of the dopamine D1/D5 receptor agonist SKF82958; and

(3) brain metabolic activation upon repeated cocaine administration as evidenced by fMRI in awake rats.

Furthermore, this report provides evidence that these treatment paradigms will result in chromatin modification changes associated with active transcription, in addition to increased mRNA levels of plasticity-associated genes, including brain-derived neurotrophic factor (BDNF) at key brain regions implicated in the pathogenesis of depression and stimulant addiction.

To date, little is known regarding the underlying mechanisms of action mediating the enhancing effects of sodium butyrate on the various antidepressant- and stimulant-related paradigms. Our findings underscore the potential of chromatin-modifying drugs

to profoundly affect the behavioral response of an animal to antidepressant and stimulant drugs and warrants consideration in the context of developing novel therapeutic strategies.

TABLE OF CONTENTS

LIST OF TABLES

LIST OF FIGURES

COPYRIGHT

CHAPTER I: General Introduction

Depression: Overview

Described by Hippocrates more than 2400 years ago, 'melancholia,' now depression, is a mood disorder affecting nearly one of every six people in the U.S. (Wittchen et al., 1994, Murray and Lopez, 1997, Pincus and Pettit, 2001, Nestler et al., 2002, Greenberg et al., 2003, Kessler et al., 2003, Stewart et al., 2003). Yearly, depression causes a loss of $100 billion in the U.S. alone through decreased productivity and treatment-related costs (Wittchen et al., 1994, Murray and Lopez, 1997, Pincus and Pettit, 2001, Greenberg et al., 2003, Kessler et al., 2003, Stewart et al., 2003). Moreover, the loss of human life remains a solemn reality as suicide rates in depressed patients are estimated as high as 15%. (Michelson et al., 1996, Musselman et al., 1998, Ciechanowski et al., 2000, Schulz et al., 2000). The focus of this section is to provide an overview of depression including proposed pathophysiology, treatment and current tools for depression research.

Etiology of Depression

The presence of a genetic component in the pathoetiology of depression has been recognized, even two millennia ago, based on the observation that the disorder aggregates in families. More formal behavioral genetic studies have established that the concordance rate of depression in monozygotic twins approaches 40-50%, indicating this proportion of the disease is hereditary in nature (Nestler et al., 2002). Moreover, a number of genetic association studies have yielded intriguing data. A recent meta-analysis found a significant association of six susceptibility genes with depression:

APOE, the dopamine D4 receptor, the dopamine and serotonin transporter, *MTHFR*, and the β subunit of G proteins (Lopez-Leon et al., 2007). However, one of the major limitations in the study and development of effective treatment of mood disorders remains the lack of definitive genetic mutations that cause depression.

More recently, human postmortem studies employing microarray technology have underscored the enormous complexity of transcriptional changes associated with depression. For example, a recent small-scale study revealed a subset of genes whose expression was increased in the dorsolateral prefrontal cortex of patients with major depressive disorder. Interestingly, these genes function in stress response (*UCN3, CNR2*) and transcriptional regulation (FOXD3, YWHAH and FBXL10) (Kang et al., 2007). However, it remains to be clarified as to which of these alterations in gene expression represent primary/hereditary deficits, which represent compensatory changes and which are due to environmental factors. As will be highlighted in subsequent sections, environmental factors (such as stress), in conjunction with hereditary genetic deficits, are believed to play a major role in the alterations in transcriptional regulation thought to underlie the pathophysiology of depression.

Environmental factors, particularly emotional stress, are strongly associated with depression. While it is clear that the context and magnitude of stressful stimuli sufficient to induce depression varies greatly between individuals, the relationship between emotional stress and depressive episodes has been established (Nestler et al., 2002). Postmortem brain studies of depressed individuals revealed dramatic physiological differences from non-depressed control brains including neuronal atrophy and cell loss in

limbic brain structures (Manji et al., 2001, Manji and Duman, 2001, Duman and Monteggia, 2006). Importantly, exposure of animals to environmental stress is sufficient to induce depressive-like behavioral changes in addition to cellular deficits mirroring those seen in postmortem brain (Duman, 2004a). Nonetheless, both genetic and environmental factors are likely to involve common brain regions and molecular pathways. Delineation of these individual regions and pathways will help to refine our current understanding of underlying causal mechanisms, and will thus aid in the development of novel, targeted treatments for mood disorders.

Brain regions affected

Given the complex nature of depression, it is not surprising that current information regarding the specific brain regions underlying the disease is limited. While pathological changes have been observed in the brains of depressed patients, these findings are not categorical, and as such do not represent *bona fide* biomarkers for the disease. Postmortem- and structural imaging comparisons have revealed decreased gray matter volumes in subregions of cortex (including prefrontal cortex, PFC), amygdala, hypothalamus and hippocampus (Ongur et al., 1998, Rajkowska et al., 1999, Drevets, 2000, Rajkowska, 2000, Manji et al., 2001, Manaye et al., 2005). These results are supported by neuroimaging studies showing alterations in cerebral blood flow and glucose metabolism in areas of the prefrontal cortex (PFC), hippocampus, striatum, amygdala and thalamus (Manji et al., 2001, Berton and Nestler, 2006, Mah et al., 2007).

Consideration of the normal functions of these regions draws potential relationships to specific emotional symptoms of depression. Reward pathways involving the striatum and amygdala are likely core in mediating depression-associated anhedonia, anxiety and reduced motivation. The hypothalamus may play a role, as imbalances in sleep, appetite and energy in addition to loss of interest in pleasurable activities are prevalent in affected individuals (Nestler et al., 2002). Cognitive and emotional behavior aspects, including memory impairments and feelings of worthlessness, hopelessness, guilt, doom and suicide may be controlled by the frontal cortex and hippocampus. Moreover, connections between these regions via major neurotransmitter pathways highlight putative brain circuitry involved in the pathogenesis and treatment of mood disorders (Nestler et al., 2002, Berton and Nestler, 2006) (**Fig.1-1**). Furthermore, while knowledge of the neuropathology of the depressed brain has come from postmortem examination, much has been determined by comparing the molecular changes evident following effective antidepressant treatment.

Treatment of Depression

Currently, a variety of treatment options for depressed patients provide tools for controlling symptoms in 60-70% of affected individuals. Interventions as simple as increased exercise are part of a battery of non-chemical therapeutic methods also including psychotherapy and electro-convulsive shock therapy (Dunn et al., 2005, Berton and Nestler, 2006). However, the most common form of treatment is antidepressant drug therapy.

As a class of drugs, antidepressants are prescribed more than any other type of medication (Cherry, 2007). Interestingly, since the serendipitous discovery of first-generation antidepressants in the 1950's (the tricyclics and monoamine oxidase inhibitors), little has changed in the design of antidepressant drugs. Early observations of the acute targets of these compounds revealed that they non-specifically inhibited the dopamine-, serotonin-, and norepinephrine-transporters or the monoamine oxidases (Frazer, 1997, Nestler et al., 2002). Details of these mechanistic actions revealed an increase in neurotransmitter signaling and led to the *monoaminergic hypothesis* of depression. This hypothesis states that a key cause of mood disorder is a disregulation of catecholamine and serotonin transporters, in addition to abnormalities in the catabolism of monoamine neurotransmitters (Park et al., 2005, Berton and Nestler, 2006). Improvements in the non-specific activity of first-generation drugs led to *selective* reuptake inhibitors for serotonin or norepinephrine (SSRI / SNRI), second-generation antidepressants which remain widely used. Based on the popularity and general effectivity of these prototypic drugs, current antidepressants are almost exclusively monoamine-targeting (Berton and Nestler, 2006).

However, critics point out that although current drugs are safer than their predecessors, the improvements in efficacy and side-effect profiles have been considered marginal (Berton and Nestler, 2006). Additionally, these drugs have a huge placebo effect; 50% of people respond to antidepressants, but 30% respond to placebo (reviewed by (Rihmer, 2007). Furthermore, many patients who initially obtain pharmaceutical relief from their depression, after months without symptoms, cease treatment. Often,

these patients then relapse into a more severe state of depression (Bockting et al., 2008). Thus, there exists a pressing need to develop advanced, mechanism-based antidepressants for both controlling and maintaining relief from depression.

In recent years, focus has been drawn to the delay in therapeutic efficacy in patients taking antidepressant drugs. That weeks or months of treatment are required for any therapeutic effect suggests that protein expression changes, receptor sensitization and/or cellular changes underlie the action of these drugs (Nelson, 1999, Nestler et al., 2002, Zarate and Quiroz, 2003, Geddes et al., 2004, Wong and Licinio, 2004, Montgomery, 2006). While the monoaminergic hypothesis could account for this, it has been proposed that the mechanisms of antidepressant action in humans involve gene expression changes that correct for underlying transcriptional dysregulation, which, in turn, rectify altered protein levels, and ultimately re-adjust signaling and functional deficits (Manji and Duman, 2001).

Although a comprehensive understanding of the genes and mechanisms underlying these transcriptional changes remains unclear, the recently formulated *neurotrophic hypothesis* considers the effects of antidepressant treatment via plasticity induced by altered expression of critical growth factors. The neurotrophic hypothesis, complementary to the monoaminergic hypothesis, proposes drug action specifically through molecular stimulation of neuronal cell growth and stability (Duman et al., 1997, Altar, 1999). Indeed, chronic antidepressant treatment has been reported to ameliorate depression-associated deficits in glial and neuronal densities in addition to attenuating decreases in neuronal arboring (Manji et al., 2001, Manji and Duman, 2001, Duman and

Monteggia, 2006). Compared to untreated, depressed control brain, antidepressant treatment was found to stimulate cell growth and resiliency in limbic and cortical brain regions (Manji and Duman, 2001) as well as attenuating, or even reversing atrophy of hippocampal cells in depressed patients (Sheline et al., 2003, Vermetten et al., 2003).

With the neurotrophic hypothesis in mind, examination of the cellular and molecular effects associated with the pathophysiology and treatment of depression has included a strong focus on brain derived neurotrophic factor (BDNF). Expressed abundantly in the developing and adult brain in midbrain, amygdala, hypothalamus, cerebral cortex and hippocampus, this neurotrophin and its receptor, TrkB (tropomyosin-related kinase), are highly important for the maturation, function and survival of neurons (Huntley et al., 1992, Masana et al., 1993, Lindsay et al., 1994, Lindvall and Odin, 1994, Nibuya et al., 1995, Chan et al., 2006). In addition to decreased BDNF plasma levels noted in depressed patients (Karege et al., 2002), postmortem studies found elevated BDNF immunoreactivity in hippocampal subregions of depressed patients who were on antidepressant drugs at the time of death (Chen et al., 2001). Moreover, recent reports have linked a non-conservative BDNF polymorphism (Val/Met66) to several forms of major depression (Hwang et al., 2006, Naoe et al., 2007).

Despite these discoveries, the association of BDNF with depression remains inconsistent. Furthermore, given the heterogeneous nature of human mood disorders, clinical research becomes limiting. Thus, more animal work is required in order to examine defined aspects of depression and associated treatment mechanisms.

Animal models of depression

Considerable effort has been given to mirroring the effects of human depression in laboratory animal models. **(Table 1-2)** While rodent models include selectively bred, stress-sensitive subpopulations, these examples are limited (Henn and Vollmayr, 2005). Animal models of depression are based primarily on behavioral changes induced in wild-type strains by environmental stimuli (stress). These models have been approached by recreating particular symptoms of mood disorders in behavioral tests including those designed to address anxiety, despair and learned helplessness (Berton and Nestler, 2006). Moreover, the stress-induced models selected have a strong construct, or face validity, closely paralleling the human disorder.

A classic example of a behavioral-despair model is the forced swim test ("Porsolt's test"). Developed 40 years ago, the forced swim test is based on an animal's response to a stressful, yet inescapable situation – in this case, swimming in a container of water with no exit. Comparison of the time spent swimming with the time spent immobile is used as a measure of depressive-like symptoms (Porsolt et al., 1977b). The general template of this model is recapitulated in the tail-suspension test, and importantly, these behavioral models have excellent predictive validity for providing evidence on the efficacy of antidepressant drugs when applied in humans, particularly in the case of despair-based models and monoaminergic-based treatments (Berton and Nestler, 2006).

Further work in animal models of depression has demonstrated that, analogous to clinical research, antidepressant treatment induces brain region-specific alterations in BDNF expression. In rat hippocampus, mRNA levels of BDNF and TrkB were shown to

be increased by treatment with physical activity, ECT or several antidepressant drugs (Nibuya et al., 1995, Russo-Neustadt et al., 2000). Direct midbrain-infusion of BDNF in rats resulted in antidepressant-like behavioral responses in the forced-swim test and in a learned helplessness model of depression (Siuciak et al., 1996).

Interestingly, expression of BDNF in rat hippocampus following antidepressant treatment was shown to be dynamically regulated with time (Coppell et al., 2003), which may explain some of the variability seen in human postmortem studies. Additionally, although only a single BDNF protein exists, work in rodent models has revealed that several BDNF transcript variants respond differentially to antidepressant treatment, depending on treatment type and duration (Timmusk et al., 1993, Russo-Neustadt et al., 2000, Dias et al., 2003, Tsankova et al., 2006a, Yasuda et al., 2007). Furthermore, mouse models of BDNF and TrkB deficiency have underscored the potential role for this neurotrophin in the development and etiology of depression (Lyons et al., 1999, MacQueen et al., 2001, Rios et al., 2001, Monteggia et al., 2004, Chan et al., 2006), as well as the transcription factor cAMP response element-binding protein (CREB, (Nibuya et al., 1996). Providing support to the neurotrophic hypothesis, these neurotrophins, CREB and its downstream targets (BDNF included) interact through a number of molecular cascades that have been linked to the pathogenesis and treatment of mood disorders.

Cell-surface receptor stimulation by monoamines and growth factors activate intracellular cascades including the cAMP second messenger system, the mitogen activated protein kinase/extracellular signal-regulated kinase (MAPK/ERK) pathway, the

phosphoinositol cycyle, and the GSK-3 (glycogen synthase kinase-3) signaling pathway (reviewed in (Tanis and Duman, 2007). In addition to myriad other effects, each of these pathways can be traced to the downstream-regulation of CREB activity. Thus, a putative mechanistic framework takes shape incorporating antidepressant treatment with receptor signaling, diverse intracellular cascades, and ultimately, regulation of transcription and gene expression.

Stimulant drug abuse: Overview

Addiction to stimulant drugs represents a significant public health issue in terms of medical, psychological and social problems (de Lima et al., 2002). In addition to effects on the primary user, impacts of drug abuse include increased infection of HIV and hepatitis as well as detrimental outcomes of prenatal drug-exposure (Volkow, 2004). The following section, although focusing on cocaine, provides a general mechanistic overview of stimulant addiction as well as underscoring the fact that effective treatment for stimulant abuse *does not exist*.

Brain regions affected and molecular effects of stimulant abuse:

'Psychostimulant' refers to drugs that produce a spectrum of stimulatory effects in humans. These drugs include cocaine, amphetamine, methamphetamine and methylphenidate and can be used therapeutically for ADHD or can be potently addictive (Musto, 1992, Das, 1993, Gonzalez Castro et al., 2000). Each stimulant affects the brain

uniquely, yet have been consistently shown to converge on the reward circuitry of the limbic system (**Fig.1-1**)(Nestler, 2005).

Regulated primarily by dopamine, the mesolimbic reward pathway is believed responsible for the acute reinforcing effects of drugs of abuse (Kreek et al., 2002, Heidbreder and Hagan, 2005). Specifically, acute administration of any drug of abuse functions to activate dopaminergic neurons projecting from the ventral tegmental area (VTA) to the nucleus accumbens (NAc) and other targets in the forebrain (**Fig. 1-1**). Indeed, in the case of cocaine, inhibition of presynaptic transporters of dopamine (DA), serotonin and norepinephrine increases synaptic levels of each of these neurotransmitters (Kreek et al., 2002). However, given the role of dopamine in the brain's reward pathway, a major focus of cocaine addiction research has been in regard to this monoamine.

Decades of research have consistently implicated dopaminergic signaling in the mechanisms underlying cocaine addiction. The link between dopamine and reward was first established, in part, by reports showing that psychostimulant self-administration was reduced with dopamine receptor blockade (Gunne et al., 1972, Wilson and Schuster, 1972, Yokel and Wise, 1976, De Wit and Wise, 1977). Further supportive evidence came from studies showing that chemical lesions of the dopmainergic pathway attenuated cocaine self-administration (Roberts et al., 1977, Roberts et al., 1980, Roberts and Koob, 1982). Extensive structure-function studies of the transporters targeted by cocaine led to the *dopamine hypothesis* named for the high correlation of dopamine transporter (DAT)-blockade studies proposing that cocaine's rewarding effects were a result of DAT-

inhibition-induced increases of synaptic dopamine (Ritz et al., 1988, Spealman et al., 1989).

Indeed, behavioral analysis of DAT knockout mice showed a lack of cocaine-induced locomotor response in comparison to wild type controls (Giros et al., 1996, Sora et al., 1998, Sora et al., 2001). However, in the conditioned place preference (CPP) test, where preference for a drug-associated environment is measured, cocaine-treated DAT knockout mice performed no differently that wildtype control mice (Sora et al., 1998). Furthermore, DAT knockout mice showed no attenuation of cocaine self-administration (Rocha et al., 1998a). Thus, these studies show that DAT knockout mice recapitulate some, but not all of the behavioral effects of cocaine. More recently, self-administration studies in mice lacking one or more types of transporters for dopamine, serotonin and norepinephirne (DAT, SERT, NET) have shown dynamic response to cocaine reinforcement (Rocha et al., 1998b, Xu et al., 2000, Sora et al., 2001). Specifically, although single knockouts of DAT (Rocha et al., 1998b), SERT (Sora et al., 1998), or NET (Xu et al., 2000) showed no change in cocaine-related reward, DAT/SERT double knockout eliminated cocaine reward (Sora et al., 2001), while SERT/NET double knockout enhanced cocaine reward (Hall et al., 2002). These studies provide evidence that multiple neurotransmitter systems are likely involved in the regulation of cocaine abuse. However, additional factors have been implicated in the mechanims that mediate cocaine's effects, in particular, regulation of transcription and gene expression.

The association of changes in transcription and gene expression with administration of addictive substances is not a new idea (reviewed by (Mackler and

Eberwine, 1991). Reports have shown *in vivo,* that acute administration of cocaine induces increased mRNA levels of early response genes, including c-fos (Hope et al., 1992). Work on the transcription factor splice variant, ΔfosB, has demonstrated that chronic treatment with any drug of abuse, including cocaine, induces accumulation of the uniquely stable ΔfosB protein in the NAc, though the mechanisms associated with this accumulation remain unclear (Nestler et al., 2001, McClung et al., 2004). Chronic cocaine administration also induces dynamic gene expression changes in tyrosine hydroxylase (TH), the rate-limiting enzyme in catecholamine biosynthesis (Nestler, 1992, Lu et al., 2003), however these responsive changes in TH may not be surprising given that cocaine is known to block the reuptake transporters of dopamine and norepinephrine. Finally, neurotrophins, including BDNF have been implicated in the development of psychostimulant abuse (Horger et al., 1999, Pierce et al., 1999, Grimm et al., 2003, Lu et al., 2004, Filip et al., 2006, Corominas et al., 2007). These various biochemical changes can be viewed as drug-induced neural plasticity.

Treatment of cocaine abuse:

Efforts to treat cocaine abuse have focused on the dopaminergic system, which via a plasticity-related mechanism becomes dysfunctional following chronic cocaine abuse. Extended cocaine use decreases basal DA signaling, however cocaine or associated environmental cues sensitize DA receptors. These complex effects are thought to contribute to the symptoms of depression and craving experienced during cocaine withdrawal (de Lima et al., 2002). Compensation for these monoaminergic deficits has

been the primary basis for addiction therapy, which utilizes antidepressants and D1-receptor agonists.

First examined in rodent models, single-drug behavioral testing revealed that D1-agoinst treatment, as with cocaine treatment, stimulates locomotor activity (Le Moine et al., 1997, Schindler and Carmona, 2002, Nergardh et al., 2005) (see also Table 1-2). However, evidence that co-administration of D1-agonists *with* cocaine caused decreases in cocaine use prompted clinical attention. Specifically, it was shown that combined treatment with D1-agonists and cocaine decreased cocaine self-administration in non-human primates (Katz and Witkin, 1992, Caine et al., 2000) and rodents (Caine et al., 1999, Self et al., 2000, Chausmer and Katz, 2002) as well as decreasing the subjective effects of cocaine-use in humans (Haney et al., 1999). However, the efficacies of these treatments, in addition to other treatment options, remain dramatically limited. This was highlighted by a recent review of 45 clinical trials of cocaine abuse therapy; many of the treatments utilized antidepressants or dopamine agonists, but unfortunately, the overall conclusion was that there was no significant effect of any addiction-reducing therapy (de Lima et al., 2002).

Indeed, more recent attempts to treat cocaine dependence have used the antiepileptic and mood stabilizer, sodium valproate (SV). An open-label trial of correlated increased valproate plasma levels with cocaine abstinance (Halikas et al., 2001). This effect was supported by mouse behavioral experiments showing that valproate treatment decreases cocaine-induced locomotor activity (Herzog et al., 2007). The mechanisms that underlie these very preliminary findings may include known effects

of SV, including inhibition of protein kinase C, activation of mitogen-activated protein kinases and increased B-cell lymphoma 2-family (Bcl-2)-mediated cell survival as reviewed in (Einat and Manji, 2006), as well as induction of neuronal differentiation inhibition of histone deacetylation (Hsieh et al., 2004). As outlined in the next section, chromatin remodeling, including histone acetylation, has a dynamic role in the regulation of gene transcription and thus, is of particular interest in further determination of the molecular actions and future treatment paradigms of stimulant abuse.

Histone Modification, Chromatin Structure and Function: Overview

Within each cell, gene expression is under exquisite control as evidenced by the myriad cell types within the body, whose unique phenotypes -established during development- result from specific programs of gene expression. Additionally, cells are able to make adjustments to transcription on a more acute time-scale in response to environmental stimuli. Both the establishment of cell-specific gene expression programs during development and more acute, minute-to-minute alterations are regulated by epigenetic changes: chemical modification of DNA and histone proteins. This section will provide a basic overview of histone modification, chromatin structure and the impact these have on transcriptional regulation as well as therapeutic implications for chromatin-modifying drugs in depression and stimulant abuse.

The most basic organizational unit of DNA is the nucleosome: stretches of 147 base pairs (bp) of DNA wrapped 1.7 times around an octameric core of histone proteins comprised of two histone (H) H2A-H2B dimers and an H3-H4 heterotetramer. Between

each nucleosome, short lengths of DNA (10-60bp) link the nucleosomes together forming the familiar 10nm chromatin fiber, which appears as 'beads on a string' (reviewed in (Peterson and Laniel, 2004). Further compaction of chromatin to the 30nm fiber is facilitated by linker histones, and this 30nm fiber is condensed still more by other proteins, resulting in higher-order structures with architecture that remains unclear (Peterson and Laniel, 2004, Wang et al., 2007b). Importantly, while DNA compaction facilitates its efficient packaging in the nucleus, vital cellular functions require mechanisms that de-condense chromatin, making DNA accessible for processes including DNA replication (in dividing cells) and transcription.

As many factors work in concert to condense (close) chromatin, there are several mechanisms that reverse this process, though in a manner of surprising specificity. One such mechanism centers around the core histones – particularly, their individual 15-38bp N-terminal tails. The N-terminal tails of core histones, in addition to the C-terminal tail of H2A, extend outward from their central globular domain and critically impact the formation of higher-order chromatin structure (Luger et al., 1997, Peterson and Laniel, 2004). This relationship was evidenced from studies showing that, *in vitro*, core histones harboring N-terminal tail deletions could not condense beyond the 10nm chromatin fiber (Hansen, 2002, Peterson and Laniel, 2004).

The histone tails are subject to a wide variety of covalent, residue specific modifications, including methylation, phosphorylation and acetylation. These post-translational modifications further impact the role of histone tails in chromatin folding as illustrated by a study showing that increased histone tail acetylation resulted in deficient

formation of 30nm chromatin fibers (Tse et al., 1998). Highly condensed chromatin is thought to result, at least in part, from tail-mediated histone-histone interactions as well as tail-mediated binding of non-histone effector proteins. It should be noted that, although histone modifications do indeed alter amino acid charge and are important for higher-order chromatin structure and function (Hansen, 2002, Kouzarides, 2007), in contrast to previous models, these charge alterations likely have little impact on the wrapping of DNA around the core nucleosome. Deficiencies in 30nm chromatin fiber compaction via histone tail acetylation was recently refined to a single modification; acetylation of histone H4-Lys16 (Shogren-Knaak et al., 2006). This work also illustrated that H4-K16 acetylation prevented the interaction of an effector protein with the chromatin fiber (Shogren-Knaak et al., 2006).

While this novel example suggests a critical regulatory mechanism for the single-residue modification, H4-K16ac, in the regulation of chromatin structure, a hypothesis for a 'histone code' was developed based on the observation that cellular functions appeared to be associated with specific *combinations* of histone tail modifications (Jenuwein and Allis, 2001, Peterson and Laniel, 2004) and has since associated defined histone modification patterns with processes, including transcriptional activation, repression and ATP-dependent chromatin remodeling. However, the *context* in which the histone code is read can result in different cellular functions depending on cell type, non-histone 'effector' proteins present, and the gene under examination (Peterson and Laniel, 2004).

As such, the recognition of histone tail modifications or 'reading' of the histone code represents a highly important step in resultant chromatin structure and function.

Proteins containing small, histone-binding modules represent key players in the reading of the histone code. Specifically, chromodomain-containing proteins can recognize methylated lysine residues and bromodomain-containing proteins result in specific binding to acetylated lysines. Further binding specificity of a module with a particular histone modification can depend on the non-histone binding protein. That Heterochromatin Protein 1 (HP1) and Polycomb proteins both contain chromodomains, yet selectively bind to dimethyl H3Lys9 and dimethyl H3Lys27, respectively, supports the view that combinations of residue modification act as part of a regulatory system to control these interactions (Wang et al., 2007a). Other aspects in the regulation of histone-effector binding and activity include neighboring residues on the N-terminal tail as well as the distinct enzymatic action of the non-histone binding protein. One such example is the protein General Control Nonderepressible 5, a member of the transcriptional activation complex and histone acetyl transferase. This protein preferentially acetylations lysine residues 9 and 14 on the histone H3 N-terminal tail; sites of action distinct from the histone H4 lysines 4, 8, 12, and 16 targeted by the human Nucleosome Acetyltransferaes of H4 HAT complexes, (Peterson and Laniel, 2004).

Importantly, a number of these small histone-binding module-containing proteins are present in ATP-dependent chromatin-remodeling enzyme complexes. Chromatin remodeling is a process generally defined as nucleosomal structural changes including dissociation of DNA-histone contacts, translocation of the nucleosome along DNA, removal of histones from DNA, and exchange of histones for histone variants (Wang et al., 2007a). Mammalian chromatin remodeling ATPases include the switching

defective/sucrose non-fermenting (SWI/SNF) enzymes, both of which contain C-terminal bromodomains (thus binding acetylated histone tails) and primarily promote accessibility for transcription factor binding by disorganizing and reorganizing nucleosomal positioning (Martens and Winston, 2003, Wang et al., 2007b). However it is important to note that these enzymes have also been shown to recruit transcriptional repressors (Ooi et al., 2006). These enzymes and other ATPases- function in concert with histone tail modifications and DNA methylation to alter the structure of the nucleosome by dissociation of the DNA-histone contacts (looping), translocation of the nucleosome along DNA (sliding) and removal and exchange of histones. While histone modifications play a critical role in these processes, it is important to emphasize that *chromatin remodeling* requires ATP-dependent enzymatic activity to bring about such nucleosome structural changes (Wang et al., 2007b).

Histone Acetylation

The study of histone modification has focused on the acetylation of histone tails, particularly of histones H3 and H4. This modification is controlled by the opposing action of two classes of enzymes: histone acetyltransferases (HATs) and histone deacetylases (HDACs). Both HAT- and HDAC-families contain multiple members whose enzymatic targets include not only histones, but also transcription factors (Glozak et al., 2005). Furthermore, some of the more than 20 HAT-family members, including p300/CBP (CREB Binding Protein), General Control Nonderepressible 5 (Gcn5), p300/CBP-associated factor (PCAF) and Steroid receptor coactivator-1 (SRC-1), act as

transcription factors themselves via interaction within the transcription activation complex (Peterson and Laniel, 2004, Black et al., 2006a). Similarly, HDAC-family members have been shown to interact in transcriptional co-repressor complexes with proteins, including Methyl CpG binding protein 2 (MeCP2) and Mothers against decapentaplegic (Mad) (Nan et al., 1997, Sommer et al., 1997).

Further, mutations of either HAT or HDAC family-associated proteins are sufficient to induce specific pathological outcomes. For example, mutations localized to the *CBP* locus have been found in many patients with Rubinstein-Taybi Syndrome, a form of mental retardation (Petrij et al., 1995). Additionally, Rett syndrome, an X-linked neuropsychiatric disorder, is highly correlated with a mutation in the MeCP2 gene (Amir et al., 1999, Akbarian, 2003). Of note, CBP and MeCP2 each have multiple functions, only one of which is the regulation of histone acetylation. However, these clinical associations underscore the critical roles individual chromatin modifying enzymes have in maintaining the plasticity of a cell and its genome.

Indeed, the association between histone hyperacetylation (particularly H3 and H4) on nucleosomes surrounding promoter-region DNA of genes showing increased transcription is well established (Allfrey et al., 1968, Grunstein, 1990, Struhl, 1998, Brown et al., 2000). Additionally, reports associating histone acetylation with the accessibility of DNA and binding of transcription factors (Lee et al., 1993, Vettese-Dadey et al., 1996, Struhl, 1998) are suggestive of a direct transcriptional regulatory mechanism. Nevertheless, while further work is required to elucidate the regulatory roles of dynamic histone acetylation changes at specific gene-promoter sequences,

research has been facilitated by application of pharmacological agents that inhibit HAT or HDAC.

Histone Acetylation: Pharmacology

Examination of *in vitro* and *in vivo* changes induced by altered histone acetylation has relied on several broad-acting histone deacetylase inhibitors (HDACi) including the short chain fatty acids, sodium butyrate (SB) and sodium valproate (SV), in addition to suberoylanilide hydroxamic acid (SAHA) and Trichostatin A (TSA). Each of these compounds robustly disrupts the histone acetylation equilibrium set by HAT and HDAC enzymes. While each HDACi has unique features, these well-known examples inhibit the majority of class I/II HDACs, underscoring their comprehensive action (Davie, 2003, Dokmanovic et al., 2007a). Known HDAC family members, 18 to date, have been segregated into 4 classes based on homology with yeast proteins. A recent review summarizes: Class I (HDAC 1-3, 8) are primarily nuclear and interact with DNA through multi-protein complexes; Class II (HDAC 4-7, 9 and 10) contain motifs for nuclear and cytoplasmic localization, and can thus shuttle between the two; Class III HDACs are NAD-dependent homologs of the yeast protein, Sir2; and the recently created, Class IV HDACs (HDAC 11) have properties of both Class I and II HDACs (Dokmanovic et al., 2007b).

When introduced to mammalian cells *in vitro*, broad-acting HDAC inhibitors robustly increase acetylation levels of H2A, H2B, H3 and H4 (reviewed in (Marks et al., 2001). Interestingly, recent microarray profiling of HDACi-treated mammalian cells

revealed that gene expression changes were only detectable in a small fraction of genes analyzed; whereas 3% of affected genes showed increased transcription, 4% showed a *decrease* in response to HDACi treatment (Mariadason et al., 2000, Nusinzon and Horvath, 2005). Moreover, treatment of adult progenitor cells with valproate, *in vitro,* has been shown to induce neuronal differentiation (Hsieh et al., 2004). Together, these data illustrate that histone hyperacetylation induced by non-specific HDACi has transcriptional effects that are both limited and dynamic and may play a role in the mechanisms underlying neuronal plasticity.

Histone Acetylation: Behavioral Effects

In vivo treatment with the class I/II HDACi, sodium butyrate, revealed further exciting evidence suggesting that HDACi are sufficient to induce not only chromatin modification and changes in gene expression, but also to dramatically alter an animal's behavioral response. At the outset of our studies in 2003, work by Ferrante and colleagues showed that extended SB administration improved neurological and motor deficits in a mouse model of Huntington's disease. Of note, SB readily crosses the blood-brain barrier and is a structural homolog to SV, a small molecule used in clinical treatment of epilepsy and as a mood stabilizer (Egorin et al., 1999, Amann et al., 2007).

More recently, several publications have associated HDACi treatment in rodents with robust behavioral effects; enhancement of cocaine-induced reward (Kumar et al., 2005), antidepressant-like effects in social defeat stress depression models (Tsankova et al., 2006a) (see also Table 1-2) and improved learning and memory (Fischer et al., 2007).

These behavioral results, summarized in the following table, underscore the pleiotropic effects of SB (and other HDACi) and its ability to induce diverse phenotypic response in animal models.

Study	**Class I/II HDACi treatment**	**Behavioral Response**
Kumar et al, ***Neuron* 2005,** v.48(2)	Sodium Butyrate	2-fold **increase** in cocaine-induced locomotor activity
Tsankova et al, ***Nat Neurosci* 2006,** v.9(4)	Sodium Butyrate	2-fold **improvement** in social defeat stress
Fisher et al, ***Nature* 2007,** v.447(7141)	Sodium Butyrate	1.5 / 2-fold **improvement** in associative/spatial learning
Kumar et al, ***Neuron* 2005,** v.48(2)	Trichostatin A	2-fold **increase** in cocaine-induced place preference

Table 1-1: HDACi-induced behavioral changes in mice.

Model	**Main Feature**
Anxiety-based tests -Light Dark Box -Open Field Test	The degree to which aniamls explores a particular environment (open space, brightly lit area, elevated area) is increased by anxiolytic drugs (e.g., benzodiazepines).
Tail Suspension Test	Antidepressants acutely increase the time an animal struggles when suspended by its tail; lack of struggling thought of represent a state of despair.
Forced Swim Test	Antidepressants acutely increase the time an animal struggles in a chamber of water; lack of struggling thought to represent a state of despair.
Chronic mild stress	Animals exposed repeatedly to several unpredictable stresses (cold, disruption of light-dark cycle, footshock, restraint, etc.) show reduced sucrose preference and sexual behavior; however, these endpoints have been difficult to replicate, particularly in mice.
Social Stress	Animals exposed to various types of social stress (proximity to dominant males, odors of natural predators) show behavioral abnormalities; however, such abnormalities have been difficult to replicate, particularly in mice.
Locomotor Activity	Measure animal's response to novel homecage environment
Reward-based tests -Cocaine CPP	Animals show highly reproducible responses to drugs of abuse (or to natural rewards such as food or sex) in classical conditioning and operant conditioning assays.

Table 1-2: Selected behavioral models used in depression and addiction research

Finally, from these collective background data, I sought to determine the biochemical and behavioral effects of a chromatin-modifying drug in the context of animal models of depression and stimulant abuse. Specifically, I hypothesized that systemic treatment with sodium butyrate (SB) as single drug, or in combination with the SSRI, fluoxetine, would improve behavioral response in a mouse model of depression. Further, I proposed that this behavioral response would be observed at doses of SB that increase bulk histone acetylation levels, and would associate with changes in BDNF transcription in the hippocampus and frontal cortex (Chapter II).

Additionally, given the emerging evidence for an impact of HDAC function on the stimulant and rewarding effects of cocaine, I hypothesized that sensitization of the dopaminergic system by combined treatment of SB with the dopamine D_1-receptor agonist, SKF82958 (SKF), would enhance an animal's behavioral response to subsequent cocaine challenge. I also proposed that SB+SKF combination treatment would be associated with changes in transcription of tyrosine hydroxylase and BDNF in addition to chromatin modification changes in the promoter regions of these genes (Chapter III). This hypothesis was expanded in a rodent neuroimaging study to examine the proposal that cotreatment of cocaine with the HDACi, sodium butyrate, would result in increased cocaine-related brain metabolic activation, whereas cotreatment of cocaine with the HATi, curcumin, would result in attenuated cocaine-related brain metabolic response (Chapter IV). Considering the preliminary evidence of HDACi-mediated behavioral changes in the context of both depression- and stimulant-drug abuse mechanisms, it was

interesting to speculate as to the impact of this experimental pharmacology. The details of our findings are outlined below.

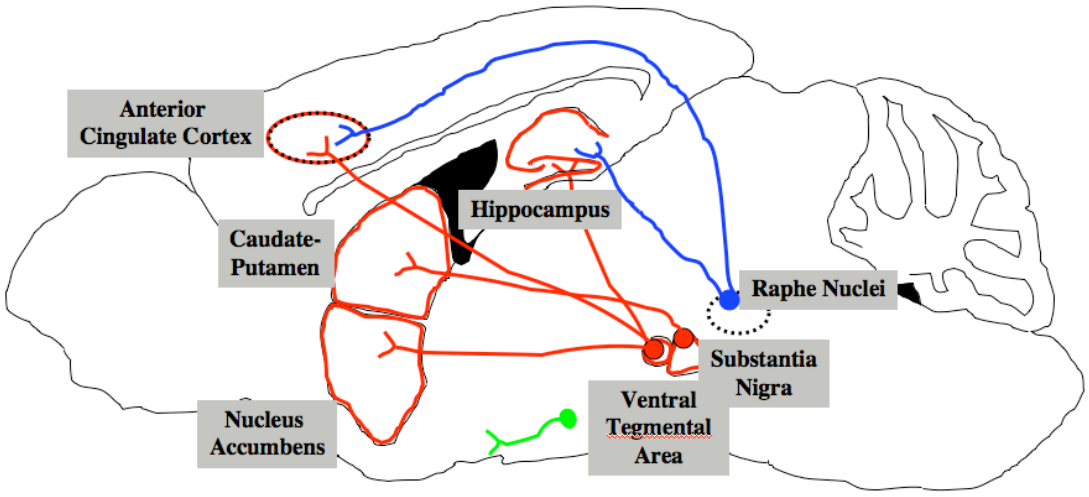

Figure 1-1: Simplified neurotransmitter pathways for serotonin (blue lines) and dopamine (red lines*) in the rodent brain. These basic circuits are highlighted given the importance of serotonin signaling in depression (see Chapter II) as well as dopaminergic signaling in stimulant drug reward and addiction (see Chapters III/IV). It should be appreciated that serotonergic neurons project from the dorsal raphe to extensive forebrain targets that include the hippocampus and frontal cortex. Similarly, dopaminergic neurons project in four major pathways to a number of regions in the forebrain: mesolimbic, mesocortical, nigro-striatal, and tuberoinfundibular (*hypothalamus to median eminence, green).

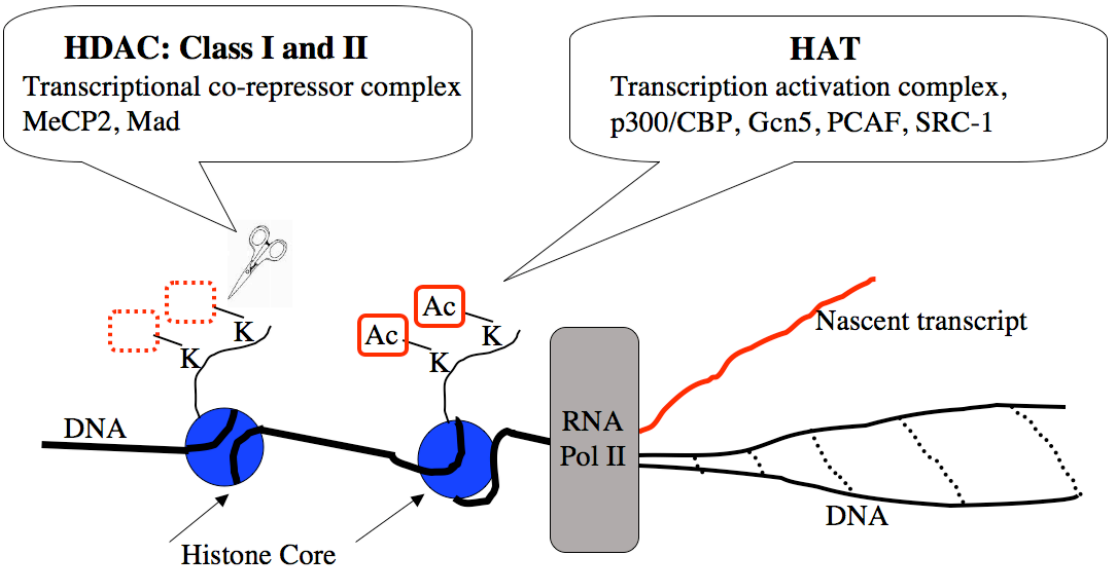

Figure 1-2: Histone tail modification. Modification of histone N-terminal tails, including acetylation (Ac) of lysine residues (K), is involved in the dynamic recruitment of transcriptional regulatory machinery. Histone acetylation is regulated by two families of enzymes, histone deacetylases (HDAC) and histone acetyltransferases (HAT). A major subset of HDACs (most class I and II HDACs) are subject to inhibition by the short chain-fatty acid, sodium butyrate (see Chapters II-IV). Similarly, HAT function can be significantly inhibited by the drug curcumin (see Chapter IV). Inhibition of either enzyme family is sufficient to dynamically alter general levels of histone acetylation.

CHAPTER II:

Antidepressant-Like Effects of the Histone Deacetylase Inhibitor, Sodium Butyrate, in the Mouse

The work presented in this chapter is reproduced from a study by Schroeder et al., published in *Biological Psychiatry* (Schroeder et al., 2007) with minor changes in style and text.

This work was conducted under the direction of Dr. Schahram Akbarian, and it is with gratitude to him and the other authors that I reproduce these data for the purposes of this dissertation. My contributions to this work consisted of conducting all animal and biochemical experiments. Cong Lily Lin contributed in scoring some of the behavioral tests as well as in executing a fraction of the western blotting and quantitative real-time PCR experiments. Dr. Wim Crusio led design of the behavioral test battery and assisted in statistical analysis. The manuscript was primarily prepared by Dr. Akbarian, while I contributed to the Results, Materials and Methods, figures and legends, and provided feedback on other sections.

Abstract

Background: Chromatin remodeling, including changes in histone acetylation, may play a role in the pathophysiology and treatment of depression. We investigated whether the histone deacetylase inhibitor, sodium butyrate (SB), administered as single drug or in combination with the SSRI, fluoxetine, exerts antidepressant-like effects in mice.

Methods: Mice (C57BL/6J) received injections of SB, fluoxetine, or a combination of both drugs either acutely or chronically for a period of 28 days, and were subjected to a battery of tests to measure anxiety and behavioral despair. Histone acetylation, and expression of brain-derived neurotrophic factor, BDNF, was monitored in hippocampus and frontal cortex.

Results: Co-treatment with SB and fluoxetine resulted in a significant, 20-40% decrease in immobility scores in the tail suspension test (TST), a measure for behavioral despair, both acutely and chronically. In contrast, decreased immobility after single drug regimens were limited either to the acute (fluoxetine) or chronic (SB) paradigm. Systemic injection of SB induced short-lasting histone hyperacetylation in hippocampus and frontal cortex. Among the four treatment paradigms that resulted in improved immobility scores in the TST, three were associated with a transient, at least 50% increase in BDNF transcript in frontal cortex, while changes in hippocampus were less consistent.

Conclusions: The histone deacetylase inhibitor, SB, exerts antidepressant-like effects in the mouse. The therapeutic benefits and molecular actions of histone modifying drugs, including co-treatment with SSRIs and other newer generation antidepressants, warrant further exploration in experimental models.

Introduction

Depressive disorders are among the most prevalent causes of illness-induced disability world wide (Murray and Lopez, 1997). Notably, to date, all drugs approved as antidepressant medications are either inhibitors of monoamine transporters or monoamine oxidase (Cryan and Mombereau, 2004, Berton and Nestler, 2006) and take 6 – 8 weeks to exert their effects (Wong and Licinio, 2004). Still, treatment-resistant depression, which typically refers to inadequate response to at least one antidepressant trial of adequate doses and duration, affects up to 50%– 60% of patients (Fava, 2003). Given this background, there is a pressing need to develop conceptually novel treatments to obtain a therapeutic response in a higher proportion of patients. Importantly, exposure to antidepressant drugs and other treatments, including electroconvulsive seizures, alters gene expression patterns in corticolimbic circuitry, including frontal cortex and hippocampus (Manji et al., 1999, Coyle and Duman, 2003, Yamada et al., 2005). Given that covalent histone modifications, including acetylation, play a key role for chromatin function and transcriptional regulation (Verdone et al., 2005), it is likely that differential regulation of histone acetylation contributes to these treatment-induced changes in gene expression. Indeed, in rodents, alterations in hippocampal gene expression in response to controlled seizures are associated with highly dynamic changes in histone acetylation in chromatin surrounding the promoter sequences of genes regulating transcription and neurotrophin signaling (Huang et al., 2002, Tsankova et al., 2004). Furthermore, a recent study showed that deacetylation of hippocampal histones blocks the ability of the

tricyclic antidepressant imipramine to reverse depression-like behavior in mice exposed to chronic psychosocial stress (Tsankova et al., 2006b).

On the basis of these recent findings, the aim of this preclinical study was to further explore the antidepressant potential of drug-induced changes in histone acetylation. Specifically, for anxiety and behavioral despair in mouse models, I tested the antidepressant potential of sodium butyrate (SB), a prototype member of an emerging class of drugs, histone deacetylase inhibitors (HDACi) (Davie, 2003). I hypothesized that systemic treatment with SB as single drug, or in combination with the SSRI, fluoxetine, would improve behavioral response in a mouse model of depression. Further, I proposed that this behavioral response would be observed at doses of SB that increase bulk histone acetylation levels, and would associate with changes in BDNF transcription in the hippocampus and frontal cortex, two brain regions previously implicated in depression and treatment-associated changes in transcription. Both in acute and chronic paradigms, I compared the antidepressant-like effects of SB with those of the selective serotonin reuptake inhibitor (SSRI) fluoxetine or a combination of both drugs. The purpose of this dual drug-treatment design was test if SB treatment in combination with the clinical antidepressant, fluoxetine, would result in a greater therapeutic response compared to single drug treatment – an established treatment strategy (Zisook et al., 2006). I report, for the first time, that chronic treatment with SB, given as single drug or in combination with fluoxetine, is superior to single drug fluoxetine in improving behavioral despair. When injected systemically, SB induced a short-lasting, transient acetylation of histones in frontal cortex and hippocampus, in conjunction with dynamic

changes in expression of the brain-derived neurotrophic factor (BDNF), a model gene frequently implicated in behavioral and pharmacological models for depression (Duman, 2004b). These novel findings warrant further investigations into the antidepressant potential of HDACi or SSRI and HDACi dual drug regimens.

Materials and Methods

Animals

All experiments were conducted with adult male and female C57BL/6J inbred mice (age 9–22 weeks). Animals were housed in groups of 2–4/cage with food and water ad libitum. Animals were purchased directly from the Jackson Laboratory (Bar Harbor, Maine), housed under 12-hour light/dark cycle, and allowed to acclimate to new housing for at least 5–7 days before experimental manipulation. All experimental procedures were approved by the Institutional Animal Care and Use Committee of the University of Massachusetts.

Drugs

For all molecular and behavioral assays, data from drug-treated animals were compared with saline-treated cage-mate control subjects of the same gender. The following treatments were included in this study: 1) high-dose SB (1.2 g/kg); 2) low-dose SB (.2 g/kg); 3) fluoxetine (10 mg/kg) with or without SB (.6 mg/kg). Control animals were treated with saline injections. Treatments were administered as acute, single dose (IP), or chronically, by IP injections once daily for 27–28 days (**Figure 2-1**). Drugs were dissolved in saline as vehicle; SB, or N-butyric acid sodium salt (Sigma-Aldrich, St Louis, Missouri) and fluoxetine hydrochloric acid (Mallinckrodt, Hazelwood, Missouri)

and were prepared fresh each day. For this study, SB was chosen for its effects on histone acetylation and fluoxetine was chosen as a prototype SSRI. To examine whether fluoxetine per se affects histone acetylation, I measured hippocampal H3 acetylation 30 min and 2 hours after acute fluoxetine treatment. H3 acetylation, selected as a well characterized, representative histone modification, revealed that in both groups, differences to saline-treated control subjects were 5% and not significant (data not shown).

Behavioral Testing

All animals were brought to the testing room at least 30 min before the start of each behavioral test and remained in the same room throughout the test. Tests were conducted during the light cycle between 7:30 AM and 2:30 PM. Behavioral tests were conducted every other day with a day of rest between each test while drug treatment continued as previously mentioned. Depending on drug, dose, and test, 12–36 animals/experiment were used, with a matched number of saline-treated control subjects. In the chronic paradigm, each behavioral test was conducted 23 hours after the previous drug injection. Tests were applied in the following sequence (**Figure 2-1**): 1) light-dark box (LD), 2) open field, 3) tail suspension (TST), and 4) forced swim test (FST). In the acute paradigm, only one test was applied, the TST, 30 min after the injections.

LD Exploration. Mice were introduced to a box (15x15x23 cm) consisting of one brightly lit open chamber connected by a small hole (4.5 cm) to a darkened, enclosed second chamber. Mice were placed into the lit compartment, and the time to the first transition, number of transitions between chambers, and time spent in each chamber were

manually recorded for 5 min after the first transition, with a 10-min maximum time (Crawley, 1999).

Open Field Exploration. Animals were placed in a 108x49x49 cm open field constructed of black Plexiglas with a transparent front pane and an object mounted on the rear wall during a 30-min test session. Spontaneous behavior was recorded with a video tracking system (Ethovision, Noldus, Wageningen, The Netherlands). The following variables were measured: 1) average speed and 2) time spent in field's central region or perimeter (thigmotaxis zone).

TST. Mice were suspended by securing a paper clip to the tail by wrapping adhesive tape around the tail, .75 cm from the tip; the clip then hung from a mounted hook 50 cm from the tabletop. Tail climbing was observed in only 3 of 209 animals, and data of these mice were removed from this test. The time to the first freeze (latency) and time spent immobile during a 6-min testing period were recorded in real time or by treatment-blind review of videotaped testing. No difference was found between real-time ratings and videotape-based ratings.

FST. Mice were placed into a 4-L Pyrex beaker (13 cm diameter, 24 cm height) filled with 22°C water, 17 cm deep. Latency to first freeze and time spent immobile during a 6-min testing period were measured. Immobility was defined according to criteria described (Schramm et al., 2001). In addition, data were analyzed for the last 4 min of the test separately. As in the 6-min analysis, no significant differences between treatment and control groups were found (data not shown).

Biochemical Analysis

Tissue Extraction. Mice were killed by cervical dislocation/ decapitation and whole brain was removed and processed immediately or snap-frozen on dry ice. Hippocampus was dissected bilaterally from coronal slices positioned between Bregma -1.46 mm and -2.92 mm. Frontal cortex, which is defined here as the anterior cingulate cortex, or areas CG1 and CG2 of Paxinos and Franklin (Paxinos and Franklin, 2001b) and immediate surroundings were collected from Bregma 1.34 mm to .02 mm. To compare sodium butyrate-induced histone acetylation in central nervous system (CNS) with tissue not affected by the blood-brain barrier, liver samples were collected from the same animals and processed in parallel to CNS tissue samples.

Western Blotting. Hippocampal and liver tissue were homogenized in Laemmli buffer, then incubated at 37°C for 10 min and centrifuged at 13,500 *g* at 4°C; the supernatant was denatured at 95°C for 5 min, then electrophoresed on a 10%–20% linear gradient Tris-HCl gel (Bio-Rad, Hercules, California) and transferred to polyvinylidene difluoride (PVDF) membrane (.2 m pore size; Bio-Rad). Immunostainings were performed with anti acetyl-histone H3 antibody (Upstate, #06-599; Lake Placid, New York) and, for loading control, anti-histone H4 antibody (Upstate, #07-108). Immunoreactivity was detected with peroxidase-conjugated secondary antibody (donkey anti-rabbit IgG; Amersham, Piscataway, New Jersey) in conjunction with chemiluminesence-based film autoradiography (Super Signal West Dura Extend Reagent; Pierce, Rockford, Illinois). For quantification, Quantity One (Biorad) software was used.

Real Time Reverse Transcription Polymerase Chain Reaction. From each animal, total hippocampal and frontal cortex RNA was extracted with the trizol-based

RNeasy Lipid Tissue mini kit (QIAGEN, Valencia, California). Amplification reactions were performed in triplicate, with the ABI PRISM 7500 Real Time polymerase chain reaction (PCR) System (Applied Biosystems, Foster City, California) in conjunction with the One-Step reverse transcription (RT)-PCR kit (Applied Biosystems), SYBR green as a reference dye, and the following cycling protocol: 48°C, 30 min; 95°C, 10 min; followed by 45 cycles of 95°C 15 sec, 60°C 1 min. The BDNF primers were designed to amplify a 117–base pair (bp) fragment from the BDNF coding sequence within exon VIII (Liu et al., 2006). The BDNF primer sequences: forward, gcgcccatgaaagaagtaaa; reverse, tcgtcagacctctcgaacct. A 133-bp fragment from mouse 18S ribosomal RNA (rRNA) was amplified in parallel reactions for normalization. The 18S rRNA primer sequences: forward, catggccgttcttagttggt; reverse, gaacgccacttgtccctcta. Quantification and normalization procedures were previously described (Stadler et al., 2005). Negative control assays included: 1) water only template, 2) RNA extracts from Nestin-Cre /BDNF1lox/1lox conditional null mutant mice (Rios et al., 2006), and 3) RNA extracts (from wildtype mice) not treated with reverse-transcriptase. No detectable amplification product was found for assays 1 and 3. For melting and amplification curves, see Supplement 2-1.

Enzyme-Linked ImmunoSorbent Assay. The BDNF Sandwich enzyme-linked immunosorbent assay (ELISA) kit (Chemicon, Temecula, California) was used to assay protein levels from whole hippocampus. The BDNF levels measured were approximately 50–150 pg/mg tissue, which is consistent with previous studies (Branchi et al., 2006).

Statistical Analysis. For each treatment group, mean value and SE were calculated, and

intra-group outliers (maximum 1/group) were removed by Grubb's test: .05 significance level. The remaining data were compared with one-way analysis of variance (ANOVA), and the Tukey-Kramer or Least-Significant Differences tests were used for post hoc comparisons.

Results

Systemic administration of sodium butyrate induces a transient increase in histone acetylation in brain and liver

Butyrate inhibits the activity of most HDAC subtypes, except class II HDAC 6 and HDAC10 and all class III HDACs (Davie, 2003). Previous studies showed that peripheral administration of SB upregulates overall levels of histone acetylation in brain chromatin, but dose-response and temporal course of this effect remain unclear (Ferrante et al., 2003, Dong et al., 2005). Therefore, we injected mice with 1.2 g/kg SB, a dose that ameliorates the neurological phenotype in a mouse model for Huntington's disease (Ferrante et al., 2003) and then determined, by immunoblotting, levels of histone H3 acetylation in brain and liver at various timepoints (5-120 min and 24hrs) post-injection. In liver, an organ not affected by the blood-brain barrier, a rapid, 35% increase in overall H3 acetylation was observed during the first 30 min after injection when compared to saline-treated animals [$F_{30\text{min}}(1,9) = 6.65$, $p<0.03$] (**Fig.2-2A**). However, within 60 minutes, H3 acetylation levels in liver returned to baseline, and were followed by a small but significant decrease that lasted for at least 24 hours when compared to saline treated animals [$F_{24\text{hrs}}(1,8) = 10.66$, $p<0.01$] (**Fig. 2-2A**). Similarly, H3 acetylation levels in

hippocampus peaked within 30 minutes, and then returned to baseline within 1 hour after SB injection when compared to saline treated animals [$F_{30min}(6,34) = 1.15$, $p<0.03$] (**Fig. 2-2B**). These kinetics remained unchanged even after 3 weeks of daily treatments (data not shown) and are consistent with the minute-scale half-life of the drug in humans (Miller et al., 1987). Furthermore, a SB dose of 0.4 g/kg or greater was required in order to induce a significant increase in levels of hippocampal H3 acetylation in comparison to saline-treated control animals [$F_{0.4g/kg}(1,8) = 6.63$, $p<0.03$; $F_{1.2g/kg}(1,8) = 5.3$, $p<0.05$] (**Fig. 2-2C**). To confirm that SB-induced acetylation is not limited to H3, we measured H4 acetylation in hippocampal extracts (**Fig. 2-2D**). There was a significant, 3-fold increase in hippocampal H4 acetylation 30 min after SB injection in comparison to saline-treated animals [$F_{1.2g/kg}(1,8) = 26.03$, $p < 0.001$]. To confirm that SB-induced acetylation affects corticolimbic regions other than hippocampus, we measured levels of H3 acetylation in tissue extracts from frontal cortex (**Fig. 2-2D**). There was a significant, 1.6-fold increase in frontal H3 acetylation 30 min after SB injection when compared to saline-treated control mice [$F_{1.2g/kg}(1,18) = 8.95$, $p < 0.01$].

Chronic administration of SB, given as daily injection for up to 28 days, was tolerated at low (0.2 g/kg), intermediate (0.6g/kg) and high (1.2 g/kg) doses, and no drug-related changes in weight were observed during this treatment period (data not shown). These findings are consistent with previous reports which showed that mice tolerate daily SB doses of 1.2 – 1.5 g/kg without apparent signs of toxicity (Ferrante et al., 2003, Ying et al., 2005). In addition, we observed that mice injected with SB show, independent of dose, a brief period of hypoactivity within the first 5 minutes post injection, and resumed

normal activity levels within 30 minutes post injection (data not shown). This finding is consistent with earlier studies conducted in cats (Matsuzaki et al., 1964).

Sodium butyrate exerts antidepressant-like effects in a behavioral despair paradigm

To examine the antidepressant potential of SB, mice were treated for a period of 4 weeks with daily injections of either high (1.2 g/kg) or low (0.2 g/kg) dose SB or saline as control, while subjected in the 4th week to a battery of four tests to measure anxiety-related behavior (light-dark box and open field test) and behavioral despair (tail suspension and Porsolt's forced-swim test). To rule out acute drug or injection procedure-related effects, each behavioral test was conducted 23 hours after the preceding injection. Significant treatment effects in the behavioral despair paradigms were found only in the group of animals treated with high dose SB when compared to their saline-treated control cohort (**Fig. 2-3A**). In the tail suspension test (TST), high dose SB animals showed a 25% increase in latency to the first freeze [F (1,64) = 9.49, p<0.003] and a 19% reduction in total freeze time, in comparison to saline-treated controls [F (1,64) = 6.59, p<0.013]. There were no significant differences between treatment groups and saline-treated control groups in the open field test (**Fig. 2-3B**) or forced swim test (data not shown). For the three parameters measured in the light-dark box experiment, the latency to the first cross into the dark compartment was differentially affected by high and low dose SB in comparison to respective saline-treated control groups [$F_{SB\text{-}H}$(1,65) = 4.408, p<0.04; $F_{SB\text{-}L}$(1,42) = 6.17, p<0.017] , while total crossings and total time spent in the dark were not significantly altered from saline-treated controls (**Fig. 2-3C**).

Polypharmacy, i.e. co-administration of two or more antidepressants, may result in a better therapeutic response, in comparison to single-drug regimens (Zisook et al., 2006). Therefore, we wanted to find out if co-treatment of SB with fluoxetine is superior to monotherapy with that SSRI. Mice were treated for a period of 4 weeks with daily injections of (i) an intermediate (0.6 g/kg) SB dose plus 10 mg/kg of fluoxetine, (ii) fluoxetine alone 10 mg/kg, or (iii) saline, and then subjected to the same behavioral test pattern as described above. Animals receiving both drugs showed approximately a 20% increase in latency to first freeze and a 26% decrease in total freeze time, in comparison to saline-treated controls. These changes were significant [$F_{SB+Fluox}(2,64) = 4.61, 5.51$, $p<0.01, 0.004$](**Fig. 2-4A**). In contrast, behavioral despair measures in animals receiving fluoxetine as single drug were not significantly changed from saline-treated controls (**Fig. 2-4A**). Furthermore, there were no significant differences between drug- and saline-treated animals in the light-dark box test (**Fig. 2-4C**) and forced swim test (data not shown). In the open field test, animals treated with fluoxetine, with or without SB, showed a significant, 20-22% significant increase in thigmotaxis [$F_{Fluox+/-SB}(2,59) = 8.83$; $p<0.001, 0.005$] (**Fig. 2-4B**).

Next, we wanted to find out if a single dose of SB, fluoxetine, or a combination thereof alters behavioral despair in mice. For this acute experiment, the same doses were administered that improved TST performance in the chronic paradigm. Thus, mice received either (i) SB (1.2 g/kg), or (ii) SB (0.6 g/kg) in combination with fluoxetine (10 mg/kg), or (iii) fluoxetine (10 mg/kg) as a single dose, or (iv) saline as control. All animals were subjected to the TST 30 min after drug injection. Animals receiving dual

treatment (SB/fluoxetine) showed the most robust changes in the acute paradigm, as evidenced by a 40% increase in latency to first freeze and a 34% decrease in total freeze time, in comparison to saline-treated animals (**Fig. 2-5A**). These differences were significant [$F_{SB+Fluox}(2,33) = 5.53, 6.41, p<0.008, 0.012$]. Furthermore, animals that received fluoxetine showed a similar improvement in total freeze time, but less robust changes in latency to first freeze (**Fig. 2-5A**). In contrast, after acute treatment with SB as single drug, animals showed an increase in total freeze time [$F(1,18) = 8.81, p<0.008$] (**Fig. 2-5B**).

Finally, we wanted to find out if the context of four separate behavioral tests (**Fig. 2-1**) was a factor in the significant improvement in TST performance after chronic SB treatment (**Fig. 2-2A**). Therefore, we repeated the chronic treatment paradigm for SB (1.2 g/kg) and saline as control in a separate group of mice, which were subjected the to the TST without prior exposure to other behavioral tests. In this group of animals, SB- and saline-treated animals did not show significant differences in TST measures [latency to first freeze (sec) treatment, mean ± S.E.: SB, 117.3 ± 9.2; saline, 121.2 ± 7.3; total freeze time (sec): SB, 112.7 ± 14.3; saline, 93.0 ± 5.9].

Bdnf expression in hippocampus and frontal cortex

Among the molecules considered relevant for the pharmacology of depression, brain-derived neurotrophic factor, BDNF, is by far the most studied (Tardito et al., 2006). While there is robust upregulation of BDNF in hippocampus after repeated electroconvulsive seizures (ECS) (Nibuya et al., 1995, Altar et al., 2003, Dias et al.,

2003, Tsankova et al., 2004), expression changes after fluoxetine treatment were less consistent (reviewed in (Tardito et al., 2006). Furthermore, the ECS-mediated increase in BDNF expression is not limited to the hippocampus but includes other corticolimbic brain regions such as the frontal cortex (Isackson et al., 1991, Nibuya et al., 1995).

To determine if the observed improvement in the TST scores are associated with changes in hippocampal or frontal BDNF expression, we measured levels of BDNF mRNA and protein at various time points (30 min, 120 min and 4-6 hrs) after drug injection (**Table 2-1**). As outlined above, there were 4 treatment conditions associated with improved immobility scores, i.e. an antidepressant-like behavioral response: acute fluoxetine with or without SB, chronic SB with or without fluoxetine, and saline as control. Three of these four treatment groups (acute fluoxetine with or without SB and chronic SB with fluoxetine) showed a transient upregulation of BDNF mRNA levels of 50% or more in the frontal cortex (**Table 2-1**). In two treatment groups, these changes reached the level of significance in comparison to saline treated control cohorts: acute fluoxetine [$F_{\text{Fluox}}(2,12) = 2.45$, $p<0.05$] and chronic SB plus fluoxetine [$F_{\text{Fluox+SB}}(2,13) = 88.04$, $p<0.01$] (**Table 2-1**).

In contrast to these treatment-induced increases in frontal BDNF, changes in the hippocampus were less consistent. There was a significant, 30-40% reduction in hippocampal BDNF mRNA within the first 30 min after fluoxetine injection, given alone or in combination with SB, in the chronic paradigm [$F_{\text{Fluox+/-SB}}(2,12) = 7.02$, $p<0.05, 0.01$] (**Table 2-1**). Notably, when administered as single drug, SB had neither in the acute nor in the chronic treatment paradigm any significant effects on hippocampal or frontal

BDNF levels (**Table 2-1**). These data suggest that increased BDNF expression in frontal cortex may be one of the molecular mechanisms that could contribute to antidepressant-like behavior after chronic co-treatment with SB plus fluoxetine, or after acute treatment with fluoxetine ± SB.

Discussion

We report that in mice, the HDACi sodium butyrate (SB), improves performance in a behavioral despair paradigm, the tail suspension test (TST). Notably, combined treatment with SB and the SSRI, fluoxetine, was superior to fluoxetine monotherapy both in the acute and chronic paradigm. In addition, mice that received SB as a single drug via daily injections over a period of 3 weeks showed a significant improvement in the TST, when applied within a battery of four tests designed to measure behavioral correlates of anxiety and despair. In contrast, chronic treatment with fluoxetine, when given as single drug, was ineffective in this setting. For the antidepressant actions of SB, doses sufficiently high to induce a global and transient hyperacetylation of frontal and hippocampal histones were required. Notably, three of four treatment paradigms resulting in an antidepressant-like behavioral response were associated with dynamic changes in BDNF transcript levels, including a transient, more than 50% increase in the frontal cortex.

Limitations of this study

Our study had several limitations. First, the significant improvement in TST scores after chronic treatment with SB was observed in mice that were subjected to the TST after completing the light-dark box and open field tests. When mice were subjected to the TST without the preceding tests, SB-treated animals did not show significant differences to controls. It is possible that by subjecting mice to the additional tests, the sensitivity of the animals to the antidepressant-like effects of SB in the TST was increased. Of interest in this context is the observation of (Tsankova et al., 2006b) that the antidepressant imipramine induced hippocampal histone hyperacetylation only in mice previously subjected to chronic social defeat stress, but not in non-stressed animals. This is quite analogous to humans, in which antidepressant drugs are only effective in depressed individuals, not normal people. In addition, other types of histone modifications, such as phosphorylation and methylation, may be required for antidepressant action (Tsankova et al., 2004, Tsankova et al., 2006b). Second, while in our study a significant drug response was observed in the TST, no changes were found in another test for behavioral despair, the forced swim test (FST), which was the 4th test applied in the chronic paradigm of the present study. This may, however, not be surprising given that C57BL/6J mice are less sensitive to fluoxetine in the FST, in comparison to other strains (Lucki et al., 2001). Third, comparatively high doses of SB were required to obtain antidepressant-like effects. This was not associated with apparent toxicity or side effects other than a brief period of sedation after injection, and has been used previously with success to treat chronic neurodegenerative disease in mice (Ferrante et al., 2003, Ying et al., 2005). Sedation after systemic SB injection was limited to the

first 30 min post injection, and therefore not a confound for the behavioral tests in the chronic paradigm, which were applied 23 hours after drug administration. However, the findings reported here should be viewed as preliminary, pending further investigations.

Co-treatment with SB and fluoxetine is superior to single drug regimen both in the acute and chronic paradigm

In most patients, the therapeutic effects of antidepressant drug treatment are not seen for weeks after initiation of treatment (Wong and Licinio, 2004). In mice, however, the efficacy of antidepressants in behavioral despair tests, including the TST and FST, are typically studied following an acute dose of drug (Porsolt et al., 1977a, Steru et al., 1987). Importantly, for drugs interfering with monoamine transporters and oxidases, these acute tests have good or excellent predictive validity, which is defined as the ability to predict therapeutic (antidepressant) efficacy in human subjects. Therefore, an acute paradigm was included in the present study. However, the predictive validity of any mouse model for a non-monoamine-based antidepressant remains unclear. Currently, this question cannot be addressed because all drugs approved to treat depression are monoamine-based (Berton and Nestler, 2006). To reproduce the requirement for prolonged drug action in humans, we included, in addition to the single dose paradigm, a chronic treatment paradigm. Importantly, C57BL/6J mice, which is the inbred strain of the present study, exhibit decreased immobility in the TST both after acute *and* chronic treatment with the tricyclic antidepressant, amitriptyline (Caldarone et al., 2003). Therefore, the C57BL/6J inbred strain is suited to examine antidepressant candidate

drugs both in acute and chronic paradigms. Notably, in the present study, the only treatment that resulted in improved TST scores both acutely and chronically was the dual drug regimen of SB and fluoxetine. In contrast, antidepressant-like effects of fluoxetine monotherapy were limited to the acute setting, and, conversely, SB monotherapy was only effective when administered chronically. Based on these findings in mice, we hypothesize that combined administration of an SSRI, together with a class I/II HDACi, could be promising new approach in the pharmacotherapy of depression.

HDACi show therapeutic effects in a range of neuropsychiatric disorders

There is increasing evidence for a role of histone acetylation in the neurobiology and pharmacology of mood disorders (Zarate et al., 2006). Notably, the anti-convulsant and mood-stabilizing sodium valproate (SV), which is structurally related to SB, upregulates histone acetylation in CNS neurons (Tremolizzo et al., 2002, Yildirim et al., 2003, Dong et al., 2005). Strong mechanistic evidence for a role of histone modifications in depression was provided by a recent study in mice showing that hippocampal mRNA levels for the histone deacetylase, *Hdac5*, are downregulated after chronic treatment with the tricyclic antidepressant imipramine and furthermore, forced overexpression of *Hdac5* antagonizes imipramine's antidepressant action (Tsankova et al., 2006b). Based on their homology to yeast HDACs, mammalian HDACs are commonly divided into three classes (HDAC I, II and III). Class I HDACs are homologues of the yeast *Rpd3* gene and class II HDACs, including *Hdac5*, are related to yeast *Hda1* (Marks et al., 2003, Thiagalingam et al., 2003). The class III HDACs, or "sirtuins", are related to yeast *Sir2*; they are

functionally distinct from class I/II HDACs and regulated by NAD+/NADPH (North et al., 2005). Drugs that act as HDAC inhibitors appear to block either class I/II HDACs or the sirtuins, but not both (Grozinger and Schreiber, 2002).

Intriguingly, there is increasing evidence that class I/II HDACi ameliorate neurological symptoms across a wide range of neuropsychiatric disease models, in addition to the antidepressant action reported here. For example, chronic neurodegeneration associated with Huntington's disease, dentato-rubral-pallidoluysian atrophy (DRPLA) and other polyglutamine repeat disorders is slowed or halted in rodents treated daily with SB and other class I/II HDACi (Ferrante et al., 2003, Hockly et al., 2003, Minamiyama et al., 2004, Gardian et al., 2005, Ying et al., 2005). Furthermore, neuroprotective actions of HDACi were also reported in animal models of amyotrophic lateral sclerosis, or motor neuron disease (Ryu et al., 2005), and Parkinson's disease (Gardian et al., 2004). Finally, hippocampal learning and memory is improved after systemic treatment with class I/II HDACi (Alarcon et al., 2004, Korzus et al., 2004, Levenson et al., 2004). Given that SB and other class I/II HDACi interfere with the balance between acetylation and deacetylation not only of HDACs, but also transcription factors and other molecules (Davie, 2003), multiple molecular mechanisms may underlie these neuroprotective and neurotrophic drug effects. Among these, cAMP-response-element binding protein (CREB)-mediated transcription is a likely candidate. First, in hippocampus, CREB appears to be a crucial mediator of antidepressant effects (Carlezon et al., 2005, Tardito et al., 2006). Second, decreased gene dosage or expression of an inhibitory mutant form of CREB-binding protein (CBP), a histone acetyltransferase and

co-activator of transcription, impairs hippocampal long-term potentiation (LTP) and memory (Alarcon et al., 2004, Korzus et al., 2004, Wood et al., 2005). Notably, these deficits are ameliorated by treatment with class I/II HDACi (Alarcon et al., 2004, Korzus et al., 2004). Notably, SB and several other of the above-mentioned class I/II HDACi are effective at comparatively high doses (g/kg); therefore it will be interesting to explore the neuroprotective and behavioral potential of newer, more potent compounds such as MS-275 (Simonini et al., 2006).

Three of four treatments associated with an antidepressant-like response are accompanied by a transient upregulation of BDNF expression in frontal cortex

In this study, three of four treatment conditions associated with an antidepressant-like response (acute fluoxetine with or without SB, and chronic SB plus fluoxetine) were accompanied by an upregulation of BDNF levels in cortico-limbic portions of mouse frontal cortex. This would suggest that increased BDNF supply in that brain region is important for treatment response. This hypothesis is in agreement with postmortem studies reporting decreased levels of frontal and hippocampal BDNF in depression and suicide victims (Dwivedi et al., 2003). Furthermore, electroconvulsive seizures induce expression of neurotrophic factors, including BDNF, in rodent frontal cortex (Isackson et al., 1991, Nibuya et al., 1995, Angelucci et al., 2002). Finally, cellular signaling pathways downstream of BDNF are dynamically modulated in frontal cortex after treatment with mood-stabilizers (Einat et al., 2003).

In contrast to the observed increase in frontal BDNF expression, changes in the hippocampus were somewhat less consistent across treatment groups. There was a transient *decrease* in hippocampal BDNF mRNA after chronic fluoxetine (with or without SB) treatment. Among the hippocampal genes regulated in the context of antidepressant treatment, the nerve growth factor, *Bdnf*, is the one which has been most intensely examined (Tardito et al., 2006). However, there are conflicting results with regard to hippocampal BDNF mRNA or protein levels after fluoxetine treatment: Three studies found an increase (Nibuya et al., 1996, Coppell et al., 2003, De Foubert et al., 2004) while a fourth study reported a decrease (Miro et al., 2002). In addition, three studies found no changes in BDNF transcript or protein levels (Altar et al., 2003, Dias et al., 2003, Vinet et al., 2004). Furthermore, it has been shown that CREB-deficient mutant mice lack antidepressant-induced changes in BDNF expression, but maintain normal drug responses in behavioral despair paradigms (Conti et al., 2002). It should be emphasized that our findings, and the above-mentioned studies, do not exclude the possibility that hippocampal *Bdnf* and other CREB-regulated genes play an important role for antidepressant-like drug action in rodents. First, serotonergic neurotransmission is altered in hippocampus and other brain regions of *Bdnf*-deficient mutant mice (Lyons et al., 1999, Rios et al., 2006). Second, ablation of *Bdnf* in forebrain (including hippocampus) results in an attenuated behavioral response to antidepressant drug treatment (Monteggia et al., 2004). Third, central administration of BDNF improves behavioral despair in the rat (Hoshaw et al., 2005). Therefore, BDNF plays an essential role in at least some antidepressant paradigms. However, further studies will be necessary to determine

additional brain regions in which changes in BDNF levels are meaningful the context of antidepressant drug treatment. To this end, it should be mentioned that BDNF exerts differential effects on antidepressant-like behavior, depending on the brain region involved. For example, local BDNF infusion into the vicinity of the midbrain serotonergic raphe nuclei exerts an antidepressant-like effect (Siuciak et al., 1997), while BDNF applied pharmacologically to the dopaminergic ventral tegmental area (VTA) has a prodepressant-like effect (Eisch et al., 2003). Conversely, genetic ablation of *Bdnf* in the VTA area results in antidepressant-like behavior (Berton et al., 2006).

Conclusion and further directions

There is increasing evidence that transcriptional changes, particularly of plasticity associated genes, are mediated by chromatin remodeling mechanisms including dynamic changes in covalent histone modifications (Tsankova et al., 2004, Tsankova et al., 2006b) or DNA methylation (Weaver et al., 2004, Weaver et al., 2005) and play an important role in the pathophysiology and treatment of depression. Here, I report, in support of part of my hypothesis, that the at a dose that increased bulk histone acetylation, treatment with the HDACi, SB, improves behavioral despair in mice. It is remarkable that SB-mediated antidepressant action was apparent one day (23 hrs) after the preceding dose, notwithstanding that SB-mediated acetylation of brain histones had returned to baseline levels within the first hour post-injection. This finding raises the question as to which molecular mechanisms contribute to the observed long-term behavioral changes after SB treatment.

Finally, it should be noted that, in support of my hypothesis, combined treatment with a hyperacetylating dose of SB in combination with fluoxetine was, in terms of antidepressant-like effects, superior to fluoxetine alone. This treatment was further in support of my hypothesis as it was associated with increased BDNF transcript in the frontal cortex of mice (albeit transiently) when compared to saline treated controls. Thus, the combination of a broad-acting, or brain region-selective (Simonini et al., 2006) HDACi together with an SSRI may eventually be a promising novel antidepressant treatment strategy that warrants further exploration in experimental animal models.

Acknowledgements

The authors would like to thank Yann Mineur for help and advice regarding the behavioral studies, and Anouch Matevossian and Yin Guo for technical help. This study was supported by a grant from the NIMH (MH074114).

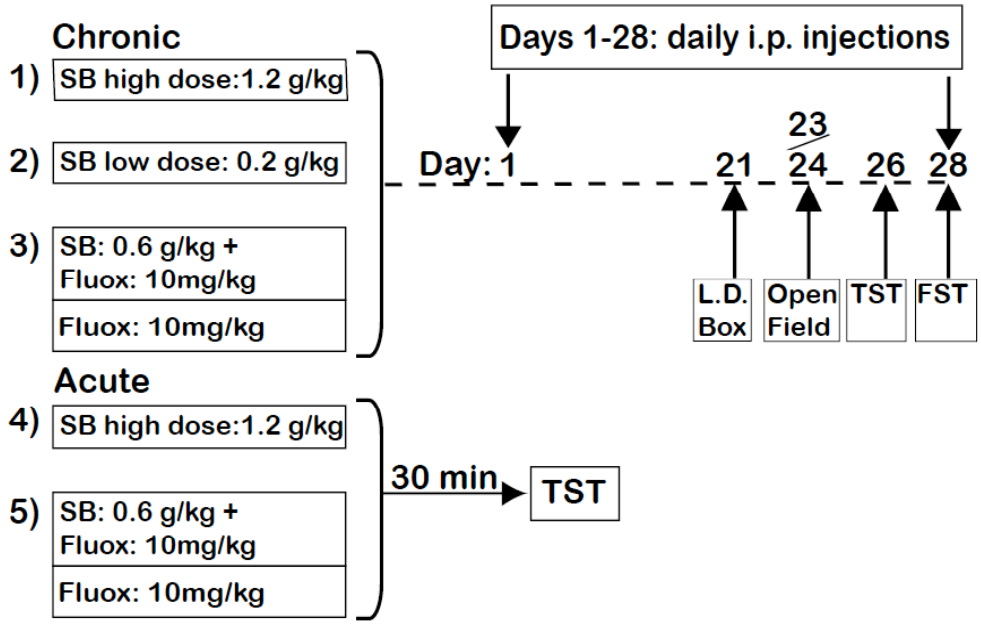

Fig. 2-1: Drug treatments and timeline.

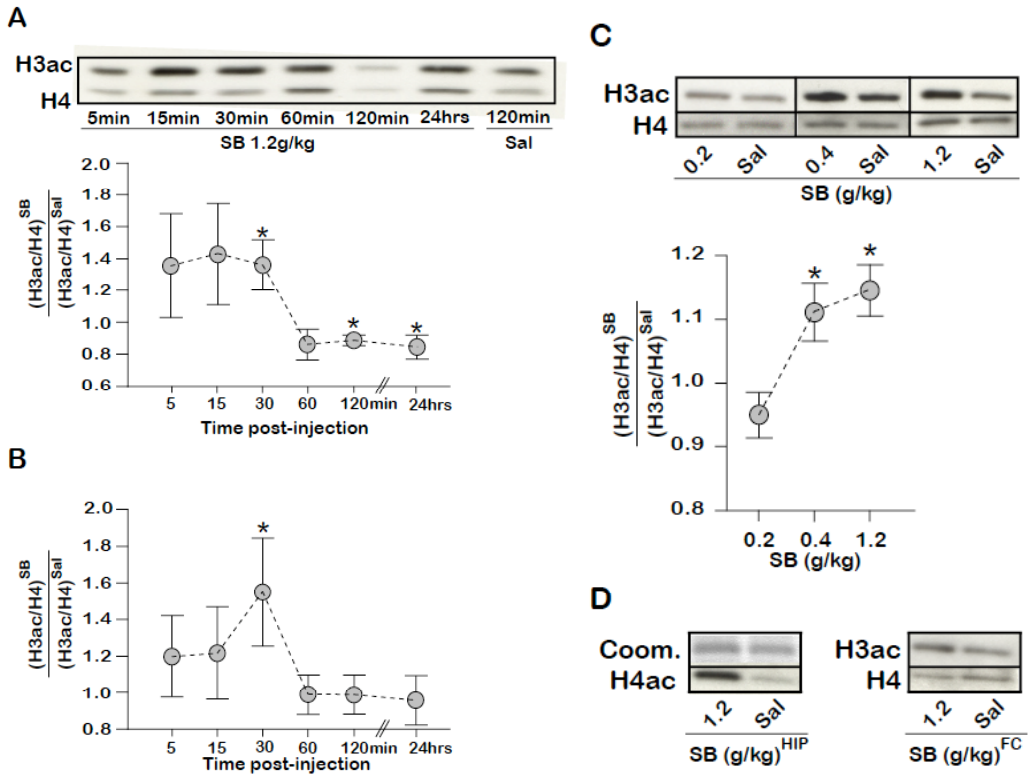

Fig. 2-2: SB injection (i.p.) induces transient histone hyperacetylation in bulk chromatin from liver and hippocampus.
(*A) Top:* Representative immunoblot of liver protein extract from SB and saline (Sal) treated animals, labeled with anti-acetyl H3 (upper band) and, for loading control, anti-H4 antibody (lower band) *Bottom:* Line graph showing temporal course of H3 acetylation in liver, after a single i.p. dose of 1.2g/kg SB (N= 5-7 / time point and treatment group). Data (mean +/- S.E.) are expressed relative to saline-treated controls, after normalization to histone H4. Notice increased levels of H3 acetylation within the first 30min after drug injection, followed by return to, or slightly below baseline levels thereafter. (*B)* Kinetics of hippocampal H3 acetylation from the same animals shown in (A). Notice that drug-induced H3 acetylation peaks at 30min, and returns to baseline at 60min post-injection. (*C) Top*: Representative hippocampal immunoblots from animals treated with 0.2, 0.4, or 1.2g/kg SB or saline. Acetylated H3 (upper band), modification-independent H4 for loading control (lower band). *Bottom*: Line graph showing dose-dependent increase in hippocampal H3 acetylation. Notice significant increase in H3 acetylation at the two highest doses (0.4 and 1.2g/kg). *(D)* Histone immunoblots 30 min after sodium butyrate injection; (Left) hippocampus, showing acetylated H4 and Coomassie blue as loading control and (Right) frontal cortex showing acetylated H3 and total H4 immunoreactivity for loading control. (A-C) N=5/ dose/timepoint, * $p < 0.05$; compared to saline-treated animals.

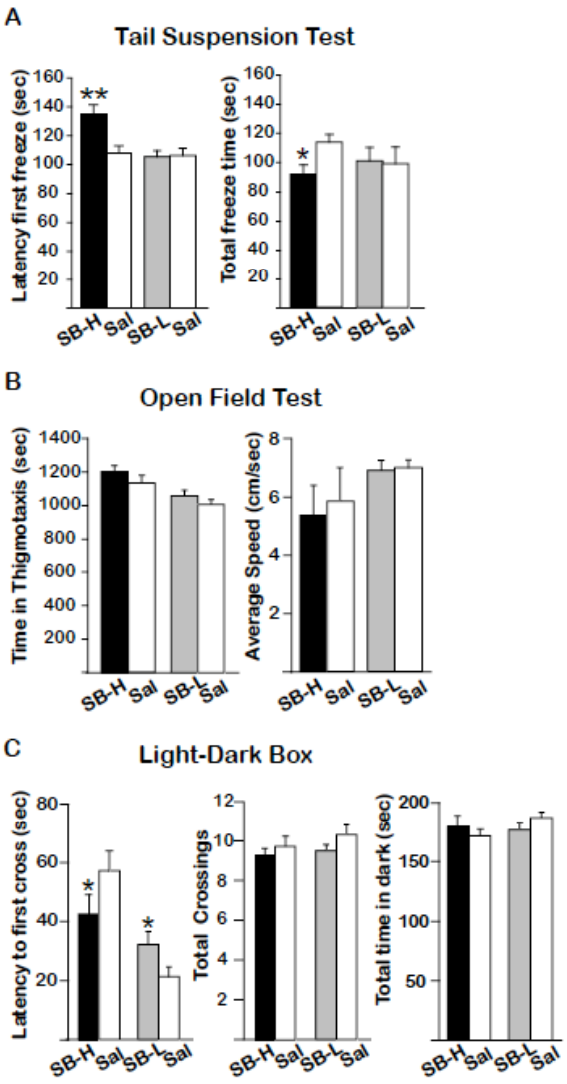

Fig 2-3: Behavioral measures of anxiety and despair after chronic treatment with SB. (A-C) Bar graphs summarizing results from a battery of four tests (see **Fig. 1**) in animals treated with SB high dose (SB-H; 1.2 g/kg; black bars) or low dose (SB-L; 0.2 g/kg; gray bars) or saline-treated controls (white bars). Data are represented as mean +/- S.E. *(A)* Tail suspension test (TST), left graph: latency to first cross; right: total freeze time. Notice significant decrease in immobility scores in high dose (SB-H) SB group; N = 32-34/treatment group, * (**) $p<0.05$ (0.01), ANOVA, post hoc Tukey. (B) Open field test, left graph: time in thigmotaxis zone (sec); right: average speed (cm/sec). *(C)* Light-dark (LD) box, graphs (left to right) show latency to first cross, total crossings and total time in dark side. Notice lack of significant changes in forced swim and open field, and no consistent effect in LD test.

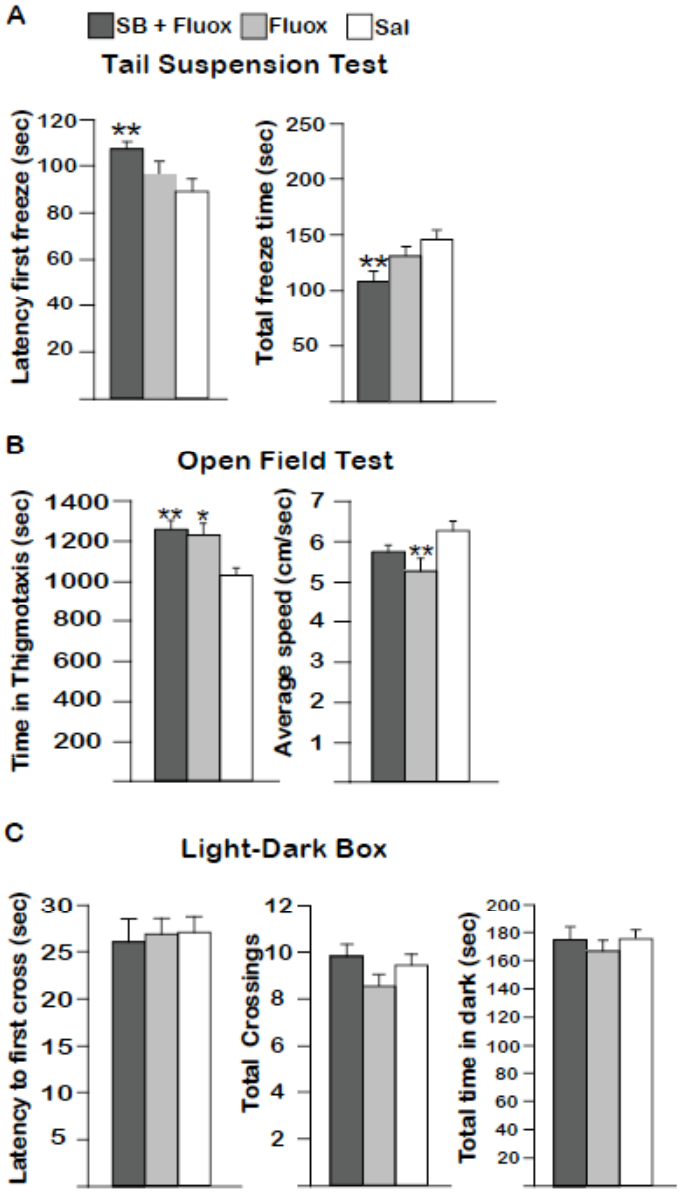

Fig 2-4: Chronic co-treatment with SB and fluoxetine decreases immobility in the TST. (A-C) Bar graphs summarizing results from battery of four tests (see **Fig. 1**) in animals treated with (i) SB (0.6g/kg) plus fluoxetine (10 mg/kg) (dark gray bars) or (ii) with 10 mg/kg fluoxetine as single drug (light gray bars) or (iii) saline (white bars). Data are represented as mean +/- S.E. *(A)* Tail suspension test (TST), left (right) graph shows latency to first cross (total freeze time). Notice significant decrease in immobility scores in group treated with SB plus fluoxetine. *(B)* Panel B as in **Fig. 3**. *(C)* Light-dark (LD) box, graphs (left to right) show latency to first cross, total crossings and total time in dark side. Notice lack of significant changes in LD (*C*), and no consistent anti-anxiety effect by open field test (*B*). N = 18-24/treatment group, * (**) $p<0.05$ (0. 01), ANOVA, *post hoc* Tukey.

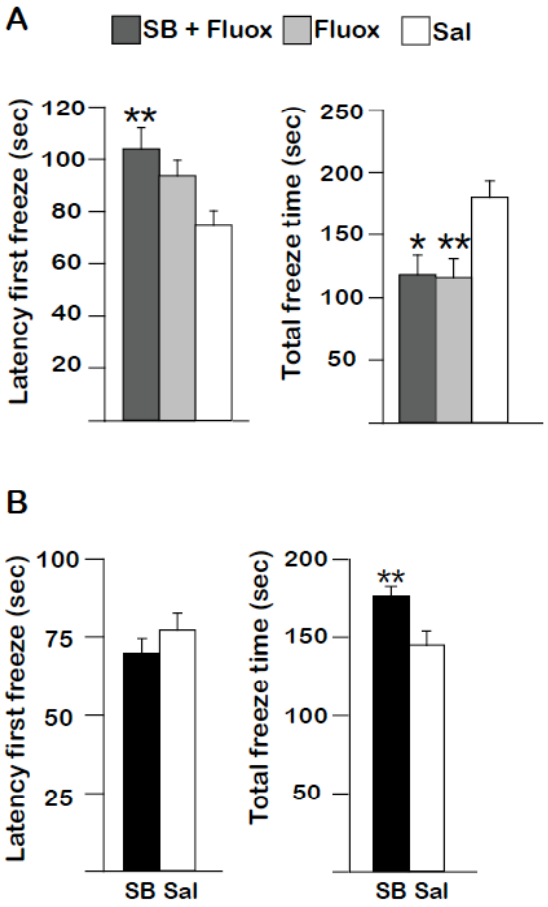

Fig 2-5: Behavioral despair measures after acute treatment with SB and/or fluoxetine. (A,B) Bar graphs summarizing data (mean +/- S.E.) from TST 30 min after acute injection (i.p.) of *(A)* (i) SB (0.6 g/kg) plus fluoxetine (10 mg/kg) (dark gray bar), (ii) fluoxetine 10 mg/kg as single drug (light gray bar) or saline as control (white bar), and *(B)* SB (1.2 g/kg) as single drug (striped bar), in comparison to saline. Notice robust decrease in immobility scores in animals co-treated with SB and fluoxetine *(A)*. N = 10-12/treatment group, * (**) $p<0.05$ (0. 01), ANOVA with *post hoc* Tukey.

Table 1. Changes in BDNF expression after SB and Fluoxetine treatment

Time post-injection	Brain region	SB (1.2g/kg)		SB (0.6g/kg) + Fluox. (10mg/kg)		Fluox. (10mg/kg)	
		Acute	Chronic	Acute	Chronic	Acute	Chronic
30min	HIP	1.14± 0.19	1.03± 0.13	1.33± 0.22	**0.60±0.08***	0.86± 0.11	**0.69±0.08***
	FC	1.23± 0.32	0.81± 0.26	1.65± 0.40	0.50± 0.25	**2.10±0.29***	0.75± 0.40
120min	HIP	0.74± 0.14	1.1± 0.08		0.96± 0.04		1.11± 0.10
	FC	1.17± 0.17	0.68± 0.19		**1.61±0.66****		0.93± 0.51
4-6hrs	HIP		1.00± 0.13		0.93± 0.12[E]		1.03± 0.09[E]
	FC		1.27± 0.41		0.8± 0.25		0.96± 0.48

Table 2-1: Levels of hippocampal BDNF after acute and chronic treatment with SB and/or fluoxetine.

Data (mean ± S.E.) show fold-changes in comparison to saline-treated animals, after normalization to 18S ribosomal RNA in hippocampus (HIP) and frontal cortex (FC). Notice significant increase in frontal BDNF mRNA levels 30 min after acute fluoxetine and 120 min after chronic co-treatment with fluoxetine + SB. Notice further the significant decrease in HIP after chronic treatment with fluoxetine ± SB. E= ELISA. * (**) $p < 0.05$ (0.01).

Supplemental 2-1: Schroeder et. al, *Antidepressant Action of Sodium Butyrate*

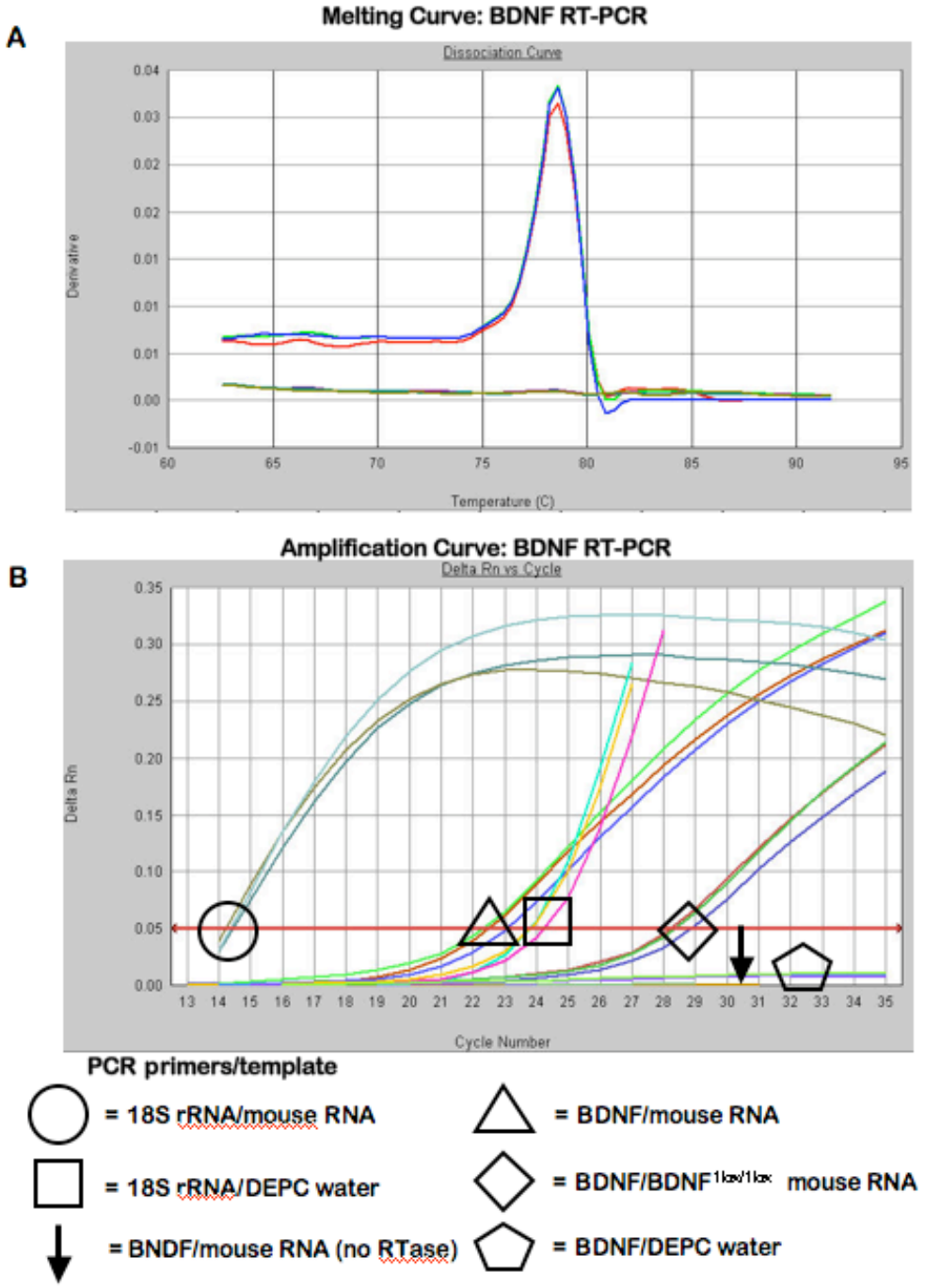

Supplemental Fig. 2-1: A. BDNF qRT-PCR melting curve control. Single peak suggests single amplicon, particularly in comparison to water template (no derivative peak). B. BDNF qRT-PCR amplification plot, with primers/template combinations indicated in key; illustrates very low contamination of reagents with nuclear material (pentagon, arrow) and accurate results (tight clustering of data within other shapes).

CHAPTER III:

Drug-induced Activation of Dopamine D_1-Receptor Signaling and Inhibition of Class I/II Histone Deacetylase Induces Chromatin Remodeling in Reward Circuitry and Modulates Cocaine-Related Behaviors

The work presented in this chapter is reproduced from a study by Schroeder et al., published in *Neuropsychopharmacology* (Schroeder et al., 2008).

This work was conducted under the direction of Dr. Schahram Akbarian, and it is with gratitude to him and the other authors that I reproduce these data for the purposes of this dissertation with minor changes in style and text. My contributions to this work consisted of leading treatment and preparation of brain samples for all (non-HPLC) mouse biochemical experiments, western immunoblotting of *in vivo* samples, immunohistochemistry, and assisting with ChIP and qPCR execution (Fig.3-2, 3-3, and 3-4A-C, and Supplemental Fig. 3-1, 3-2 and 3-4). In the preparation of the manuscript, prepared together with Dr. Akbarian, I was responsible for preparation of all figures, figure legends and statistics, as well as major contributions to the Results, Materials and Methods sections in addition to providing feedback on other sections. Krista Penta contributed the mouse behavioral testing. Anouch Matevossian contributed by assisting greatly in the ChIP and qPCR experiments. Dr. Sara Jones contributed by conducting HPLC experiments. Dr. Christine Konradi contributed by conducting *in vitro* immunoblotting experiments. Dr. Andrew Tapper led design of the behavioral testing and assisted in statistical analysis.

ABSTRACT

Chromatin remodeling, including histone modification, is involved in stimulant-induced gene expression and addiction behavior. However, to date, the impact of HDAC activity on an animal's behavior response to stimulant drug has been assessed following repeated administration to cocaine – a drug known to affect multiple neurotransmitter systems. To further explore the role of dopamine D_1 receptor signaling, we measured cocaine-related locomotor activity and place preference in mice pre-treated for a period of 10 days with the D_1-agonist SKF82958 and/or the histone deacetylase inhibitor (HDACi), sodium butyrate. Co-treatment with D_1-agonist and HDACi significantly enhanced cocaine-induced locomotor activity and place preference, in comparison to single drug regimens. However, butyrate-mediated reward effects were transient and only apparent within 2 days after the last HDACi treatment. These behavioral changes were associated with histone modification changes in striatum and ventral midbrain: (1) a generalized increase in H3 phospho-acetylation in striatal neurons was dependent on activation of D_1 receptors and (2) H3 de-acetylation at promoter sequences of *tyrosine hydroxylase* (*Th*) and *brain-derived neurotrophic factor* (*Bdnf*) in ventral midbrain, together with up-regulation of the corresponding gene transcripts after co-treatment with D_1-agonist and HDACi. Collectively, these findings imply that D_1-receptor-regulated histone (phospho)acetylation and gene expression in reward circuitry is differentially regulated in a region-specific manner. Given that the combination of D_1-agonist and HDACi enhances cocaine-related sensitization and reward, the therapeutic benefits of D_1-receptor

antagonists and histone acetyl-transferase inhibitors (HATi) warrants further investigation in experimental models of stimulant abuse.

INTRODUCTION

To date, the molecular mechanisms that underlie cocaine and other stimulant addiction become increasingly clear but current pharmacological treatment options remain surprisingly limited. Therefore, it will be important to further elucidate the molecular pharmacology of cocaine addiction in pre-clinical models. Among the various drug-based interventions that modulate the animal's response to cocaine are two radically different classes of compounds – dopamine D1 receptor agonists and histone protein deacetylase inhibitors (HDACi). Notably, D1 agonist drugs elicit reward functions, including reinstatement of cocaine-related addiction behavior (Self and Stein, 1992, Graham et al., 2007) and the importance of D1-mediated signaling for the neurobiology of stimulant abuse is established by various genetic and pharmacological approaches (Hummel and Unterwald, 2002). Importantly, the neurochemical and behavioral adaptations in response to stimulant or D1 agonist exposure are thought to result, at least in part, from changes in gene expression affecting dopaminergic circuitry, including ventral midbrain and the striatum and other major target zones within the forebrain. Recently, it was recognized that among these cocaine-sensitive transcriptional mechanisms, histone acetylation and other histone modifications are of particular importance; for example, pharmacological inhibition or genetic ablation of class I/II histone deacetylases enhances cocaine-related behavioral sensitization and reward (Kumar et al., 2005, Renthal et al., 2007). Conversely, striatal overexpression of histone deacetylase (HDAC) or genetic ablation of

histone acetyl-transferases, including *Cbp*, attenuates the animal's response to cocaine (Kumar et al., 2005, Levine et al., 2005).

However, it is not known whether or not these two reward-enhancing drug types – D_1 receptor agonists and HDAC inhibitors operate synergistically or independently. Therefore, it was the goal of this study to understand how drug-induced changes in D1-receptor signaling and histone deacetylase activity modulate the animal's behavioral and molecular responses to cocaine. Specifically, I hypothesized that sensitization of the dopaminergic system by combined treatment of SB with the dopamine D_1-receptor agonist, SKF82958 (SKF), would enhance an animal's behavioral response to subsequent cocaine challenge. I also proposed that SB+SKF combination treatment would be associated with changes in transcription of tyrosine hydroxylase and BDNF in addition to chromatin modification changes in the promoter regions of these genes. We applied, in C57Bl/6J mice, two cocaine-related behavioral assays – locomotor sensitization and place preference. The molecular studies were conducted on ventral midbrain at the level of the substantia nigra/ventral tegmental area (SN/VTA) and striatum (including but not limited to the nucleus accumbens)(Winder et al., 2002, Kalivas and Volkow, 2005) – two key regions of the brain's reward circuitry. Specifically, we examined drug-induced changes in nucleosome core histone H3 and H4 acetylation and phospho-acetylation, two types of modifications previously linked to changes in dopaminergic signaling (Li et al., 2004, Brami-Cherrier et al., 2005, Kumar et al., 2005, Levine et al., 2005, Santini et al., 2007).

Our results indicate that combined D1 receptor activation and HDAC inhibition was associated with a heterogeneous set of region-specific histone modification mechanisms, including a generalized histone phospho-acetylation response in striatal neurons and histone deacetylation in SN/VTA chromatin at promoters of tyrosine hydroxylase (Th) and brain-derived neurotrophic factor (Bdnf) – two genes with a key role for drug-induced plasticity(Self et al., 2004, Corominas et al., 2007). However, changes in cocaine-related behaviors after previous exposure to D_1 agonist with or without HDACi co-treatment were complex, because the two different types of drugs exerted a synergistic effect in some but not all behavioral assays. These differences were, at least in part, explained by the observation that butyrate-mediated reward effects were transient and only apparent within 2 days after the last HDACi treatment.

Methods and Materials

Drugs

SB, or N-Butyric Acid sodium salt, and SKF, or Chloro-APB Hydrobromide (±)-SKF-82958 hydrobromide, or cocaine (Sigma-Aldrich) were dissolved in saline and prepared fresh each day. For this study, SKF was chosen as a full D_1-like agonist and SB was chosen as a class I/II HDAC inhibitor. Other drugs included in this study were the PKA inhibitor N-[2-(p-bromocinnamylamino)ethyl]-5-isoquinolinesulfonamide dihydrochloride, (H89) and the NMDA receptor antagonist [(+)MK 801 hydrogen maleate] (MK-801), both dissolved in DMSO.

Animals

All experimental procedures were approved by the Institutional Animal Care and Use Committee of the University of Massachusetts. For all experiments with the D_1 receptor agonist SKF82958, male C57BL/6J mice, age 9-15 weeks, were used. Animals were purchased directly from the Jackson Laboratory, Bar Harbor (Maine), and housed in groups of 2-4 per cage with food and water *ad libitum* under 12-hour light/dark cycle. For behavioral experiments, mice received i.p. injections with SB (100mg/kg or 25 mg/kg) or saline followed 15 min later by SKF (0.25mg/kg) or saline once daily for 10 days. For the remaining experiments, mice received i.p. injections with SKF (1 mg/kg) or saline as vehicle, with or without concomitant SB (200mg/kg or 25 mg/kg), as single dose or once daily for 2-10 days.

For tissue extraction, animals were sacrificed by cervical dislocation/decapitation and whole brain was removed and processed immediately or snap-frozen on dry ice. Striatum was dissected unilaterally from coronal slices positioned between Bregma 1.18mm and –0.46mm; Ventral midbrain was dissected from coronal slices positioned between Bregma -2.80mm and –3.80mm and ventral to the dorsal 3rd ventricle; the dissected blocks of tissue thus included the full rostro-caudal and dorso-ventral extent of the substantia nigra and the ventral tegmental area (SN/VTA) (Paxinos and Franklin, 2001a).

Behavioral Testing

Tests were conducted during the light cycle between 7:30am and 2:30pm. Depending on the drug and test, 8-10 animals per experiment were used, with a matched number of saline-treated control subjects.

Locomotor activity. Animals were placed in clean, 19.1x29.2x12.7cm shoebox-style cages (Allentown, Inc., Allentown, NJ) and locomotor activity measured continuously for 190 min (from t = 0 min to t = 190 min) using a photobeam activity system (San Diego Instruments, San Diego, CA). All mice were placed in activity cages and allowed to habituate for 75 minutes prior to any injection. To assay the effects of SB and SKF pretreatment on cocaine-induced locomotion, mice were first introduced to the test and injected with saline at t = 90 min to record basal activity (day zero). The next day, a 10-day pretreatment period was initiated with daily i.p. injections of: *i,* Sal+SKF; *ii,* SB+SKF; *iii,* SB+Sal; or *iv,* Sal+Sal, each at t = 75 min and t = 90 min, respectively. During pretreatment, activity was measured on days 1, 2, 5, 7 and 10. On day 11, animals were placed in activity cages, saline injected at t = 75 min followed by cocaine (15mg/kg) at t = 90 min, and activity measured for 190 min total.

Conditioned Place Preference.

The conditioned place preference (CPP) test apparatus consisted of a rectangular cage with overall inside dimensions of 46.5 x 12.7 x 12.7cm (med-associates, St. Albans, VT). This included a center neutral gray compartment, 7.2cm long, and a hinged clear polycarbonate lid for loading the test animal. The adjacent conditioning compartments

measured 16.8 cm long. One compartment was black with a stainless steel grid rod floor and the other white with a square stainless steel mesh floor in order to make the context of each chamber as different as possible for counterbalancing drug-independent place preference. Chambers were equipped with photobeams to measure activity and time spent in each chamber. Guillotine doors separated the chambers and could be fixed in the closed or opened position. The apparatus was placed in a sound attenuation cubicle.

Two cocaine-related CPP paradigms were used in the present study, with the main difference being the timeline of SKF and SB treatments:

Paradigm 1: Preceding CPP testing, all animals were treated for 10 days with daily injections of: Sal+SKF or SB+SKF or Sal+Sal as described above. Then, CPP was tested in three stages over a 6-day period. In the first stage, each mouse was placed in the central compartment and allowed free access to all chambers. The time spent in each chamber was then recorded over a 20 min period. During the second stage, i.p. injections of cocaine (5mg/kg) were paired with one of the conditioning chambers and saline injections paired with the other. Each mouse received cocaine injections and was placed in the isolated cocaine-conditioning chamber on day 3 and 5; each mouse received saline injections and was placed in the saline chamber on day 2 and 4. Each training trial lasted 20 min. During stage 3, the testing phase, each mouse was once again given free access to all chambers for 20 min. The time spent in each chamber during stage 1 (baseline) was subtracted from the time spent in each chamber during stage 3. A preference toward the cocaine-associated chamber compared to baseline is a measure of the reward behavior associated with cocaine. Control mice received saline in both chambers. Mice that

exhibited an initial bias for the white or black chamber received cocaine in the least-preferred chamber.

Paradigm 2: In contrast to paradigm 1, no pre-treatment were administered and animals were subjected to the first (baseline, day 1) and second stage (saline, days 2 and 4; cocaine, days 3 and 5) of CPP training as described above. In addition, on days 1, 2 and 4, animals received within one hour after the training session SKF ± SB at the same doses described above.

Cell culture studies

Primary striatal cultures were prepared as described previously, with minor modifications (Konradi et al., 1996, Rajadhyaksha et al., 1998). Striata from 18-d-old Sprague Dawley rat fetuses were dissected and resuspended in defined medium [50% F12/DMEM and 50% DMEM (Gibco-Invitrogen, Grand Island, NY) with the following supplements per liter of medium: 4 gm of dextrose, 1X B27, 10 ml of penicillin-streptomycin liquid (Gibco-Invitrogen), and 25 mM HEPES]. Cells were resuspended in defined medium to 1.2x 10^6 cells/ml and plated in 12-well plates (Costar, Cambridge, MA) at 2 x10^6 cells/well. Plates were pretreated with 1 ml of a 1:500-diluted sterile solution of polyethylenimine in water for 18 hr, washed twice with sterile water, coated with 2.5% serum-containing PBS solution for at least 4 hr, and aspirated just before plating. All experiments were performed in triplicate with cells 6 d in culture and repeated at least once in an independent dissection. As determined by HPLC analysis, glutamate levels in the medium on the day of the experiments ranged from 1 to 5 μM. The neuron to astroglia ratio was below 25:1, as established by immunocytochemical staining with the

glial fibrillary acid protein (Dako, Carpinteria, CA) and counterstaining with 1% cresyl violet. All drugs used for the in vitro experiments were purchased from Sigma. At two different time points prior to harvest – 3 hours and 30 minutes – cells were treated with one of the following drugs (treatment #1): (1.1) vehicle (10 uL DMSO); (1.2) the PKA inhibitor N-[2-(p-bromocinnamylamino)ethyl]-5-isoquinolinesulfonamide dihydrochloride, (H89), 20 μM; (1.3) the NMDA receptor antagonist [(+)MK 801 hydrogen maleate] (MK-801), 2 μM. Three hours before harvest, cells were treated with one of the following drugs (treatment #2): (2.1) vehicle (10 μL water); (2.2) Sodium butyrate (10μM to 10mM); (2.3) SKF82958 (50 μM).

Western blotting

Striatal tissue was homogenized in Laemmli buffer, then incubated at 37°C for 10min, centrifuged at 13,500*g* at 4°C; the supernatant was denatured at 95°C for 5min, then electrophoresed on a 10-20% linear gradient Tris-HCl gel (Bio-Rad) and transferred to PVDF membrane (0.2uM pore size, Bio-Rad). Immunolabelings were performed with anti-phospho (Ser10)-acetyl (Lys14)-histone H3 antibody (#07-081), anti-phospho (Ser10)-histone H3 antibody (#05-598); anti-acetyl-histone H3 antibody (#06-599), and recognizing total histone H4 as loading control, the anti-histone H4 antibody (#07-108), all from Upstate, Lake Placid, NY. Additional blots were probed with anti-tyrosine hydroxylase (#T-2928), Sigma-Aldrich, St. Louis, MO and anti-phospho (Ser31)-tyrosine hydroxylase (#36-9900), Zymed Laboratories-Invitrogen. Immunoreactivity was detected using peroxidase-conjugated secondary antibody (donkey anti-rabbit IgG or sheep anti-mouse, Amersham) in conjunction with chemiluminesence-based film

autoradiography (Super Signal West Dura Extend Reagent, Pierce). For quantification, Quantity One software was used (Biorad).

Immunohistochemistry

Coronal sections (14 μm) were cut from blocks containing striatum and collected in ice-cold PBS for free-floating immunohistochemistry. Sections were blocked in 0.3% Triton X-100/± 2% goat serum/0.1M sodium phosphate (pH 7.4). Sections were next incubated in 0.3% Triton X-100 / 0.1 M sodium phosphate buffer and the anti-phospho (ser10) - acetyl (Lys9)-histone H3 antibody (1:500, #ab4272, Abcam, Cambridge, MA) together with the monoclonal anti-NeuN antibody (1:300, #MAB377, Chemicon, Temecula, CA) overnight at 4°C, washed, then incubated with Texas-Red-conjugated horse anti-mouse antiserum and FITC-conjugated goat anti-rabbit antiserum (1:200, Vector) for 60 min at RT, washed, slide-mounted, dried, counterstained with 4,6,-diamidino-2-phenylindole dihydrochloride (DAPI) and coverslipped with Vectashield (Vector). Sections were examined with a Zeiss Axiovert microscope and digitized images were obtained with OpenLab software (Improvision, Lexington, MA).

Quantitative RT-PCR

From each animal, total RNA from striatum or ventral midbrain was extracted using the trizol-based RNeasy Lipid Tissue mini kit (QIAGEN). Amplification reactions were performed in triplicate, using the ABI PRISM 7500 Real Time PCR System (Applied Biosystems) in conjunction with the One-Step RT-PCR kit (Applied Biosystems), SYBR green as a reference dye and the following cycling protocol: 48°C, 30min; 95°C, 10min; followed by 45 cycles of 95°C 15s, 60°C 1min. Primer sequences were designed to

amplify 90-150bp fragments from respective gene coding regions: *Tyrosine Hydroxylase (Th)* primer sequences (94bp product): forward, *attggaggctgtggtattcg*; reverse, *cgagacagtgaggagggttt*. *Bdnf* primer sequences (118bp product), forward *gcgcccatgaaagaagtaaa*, reverse *tcgtcagacctctcgaacct*. *C-fos* primer sequences (147bp product), forward, *atccttggagccagtcaaga*; reverse, *gcatagaaggaaccggacag*. β_2 microglobulin (*B2m*) primer sequences (98bp product), forward, *tggtgcttgtctcactgacc*; reverse, tatgttcggcttcccattct. A 133bp fragment from mouse *18S* rRNA was amplified in parallel reactions for normalization. *18S* rRNA primer sequences: forward, *catggccgttcttagttggt*; reverse, *gaacgccacttgtccctcta.* For additional information on PCR primers and products, see Supplemental Table. Quantification and normalization procedures were previously described (Stadler et al., 2005).

Chromatin Immunoprecipitation and Quantitative PCR

Ventral midbrain tissue (30mg, pooled from 2-3mice) was homogenized and digested with micrococcal nuclease for further application to native chromatin immunoprecipitation (ChIP) with anti-acetyl-histone H3 (Upstate #06-599) or anti-acetyl-histone H4 (Upstate #06-598) antibodies or the control antibody against total histone H4, anti- H4 (Upstate #07-108) and anti-H3 (Abcam Ab1791-100) followed by quantitative-PCR (qPCR) as previously described (Huang et al., 2006). Primers were selected upstream of respective gene transcription start sites (TSS), with product sizes in the range of 75-125bp in order to amplify from mononucleosomal DNA (147bp). Three primers were designed to amplify sequences proximal to the tyrosine hydroxylase promoter region: *Th-a,* forward, *ttgaagacacagcctgcaac*; reverse, *ggggaggtcagaagacccta,* (70bp

product, -652bp from TSS = 150085865; NC_000073.5); *Th-b*, forward, *acggaggcctctctcgtc*; reverse, *gtcccccacctcctacctc*; (103bp product, -91bp from TSS = 150085865; NC_000073.5); and *Th-c*, forward, *ctggggtatccacccattta*; reverse, *gccgtctcagagcaggatac* (113bp product, +48bp from TSS = 150085865; NC_000073.5). Three primers were designed to amplify sequences from the non-coding BDNF promoter regions pI, pIII, and pIV: pI, (106bp product, forward, *tggagacccttagtcatggtg*; reverse, *gcctctctgagccagttacg*; pIII, 129bp product, forward, *aatgtgcagtggggaaagag*; reverse, *ggcagggataccgagagaat*; pIV, 114bp product, forward, *aaatggagcttctcgctgaa*, reverse, *agtctttggtggccgatatg*). Primers were designed for the housekeeping gene β_2 microglobulin, *B2m*, forward, *gggaaagtccctttgtaacct*, reverse, *gcgcgcgctcttatatagtt* (112bp product, -57bp from TSS = 121973475; NC_000068.6). For additional information on PCR primers and products, see Supplemental Table.

Statistical Analysis

Biochemical data (immunoblots, quantitative PCR) from experiments with two groups were compared using Student's T-test. For experiments with three or more groups, comparisons were made with one-way ANOVA and the Tukey-Kramer or Least-Significant Differences tests for *post hoc* comparison (SYSTAT). Significance in all behavior experiments was determined by one- or two-way ANOVA followed by post-hoc analysis (Tukey test unless otherwise stated).

Results

Systemic Pretreatment with D_1-agonist and HDACi Enhances Cocaine-induced locomotor activity and reward

We first examined whether cocaine-induced locomotion is affected by previous exposure to the D_1/D_5 agonist, SKF82958. The drug was administered once daily (0.25 mg/kg i.p.) for 10 days and 24 hours after the last dose, animals received a single dose of cocaine (15 mg/kg i.p.). Comparison of locomotor activity of mice pre-treated for 1-10 days with SKF±SB (2-way ANOVA) revealed significant main effects due to treatment [$F_{SB+SKF\ vs\ Sal+SKF}(1,70) = 10.1$, $p<0.01$] and time [$F_{SB+SKF\ vs\ Sal+SKF}(4,70) = 13.3$, $p<0.001$, but no significant interactive effect between treatment and time [$F_{SB+SKF\ vs\ Sal+SKF}(4,70) = 0.962$, $p=0.434$] (**Fig. 3-1A).** Furthermore, in comparison to animals pre-treated with saline, exposure to D1-agonist resulted in a more than 2-fold increase in cocaine-induced locomotion (**Fig. 3-1B**), which is in agreement with previous studies (Pierce et al., 1996, De Vries et al., 1998, Sorg et al., 2004). Importantly, this cocaine-related locomotor sensitization was even further enhanced – up to 5-fold when compared to saline controls - in animals pre-treated for 10 days with D_1 agonist plus SB (100 mg/kg) (**Fig. 3-1B**). The cocaine-induced activity in the group co-treated with 100 mg/kg SB+SKF was also significantly increased compared to mice pretreated with SKF as single drug **(Fig 3-1C)** [$F_{SB+SKF\ vs\ Sal+SKF}(3,28) = 33.39$, $p < 0.001$]. Notably, 100 mg/kg SB administered as single drug was indistinguishable from saline (**Fig. 3-1B,C**). Furthermore, SB+SKF co-treatment with a lower dose of SB (25mg/kg) was indistinguishable from the SKF single drug regimen (**Fig. 3-1C**). We conclude that pre-treatment with D_1 agonist and the

HDACi, SB, results in a synergistic and dose-dependent locomotor activity effect of a subsequent dose of cocaine administered 24 hours later.

Next, we wanted to examine whether or not previous exposure to D_1 agonist and HDACi results in sustained (long-term) changes in cocaine-related reward behavior. To examine this, we treated three groups of mice for 10 days either with (i) saline or (ii) SKF 82958 (0.25 mg/kg), (iii) SKF plus SB (100 mg/kg). Then, animals were subjected for a 6-day period to a place preference paradigm (CPP, paradigm 1, see Methods) to distinguish the rewarding effects of cocaine (5 mg/kg) from saline (see Methods for details). On the 6^{th} and final CPP day, animals that had been pre-treated with SKF showed a significant increase in preference for the cocaine chamber (**Fig. 3-1D**), which is in good agreement with a recent report in rats (Graham et al., 2007). However, in this paradigm, co-treatment with SB was not more effective than single drug SKF (**Fig. 3-1D**), and therefore we conclude that exposure to the D_1 agonist but not the HDACi induced a sustained change in behavioral plasticity as it pertains to cocaine-related preference behavior.

The above CPP results suggest that repeated exposure to D_1 agonist, but not SB induces sustained changes in reward circuitry that lasted at least 6 days. Next, we wanted to find out whether or not SB enhances cocaine reward of animals that receive a much shorter course of SKF treatments. Therefore, in CPP paradigm 2, no pre-treatment with SKF or SB was administered, and instead these drugs were administered during the training period and cocaine reward was evaluated 48 hours after the last dose of SKF ± SB (see Methods). Indeed, in paradigm 2, mice treated with SKF+SB showed significant

cocaine-related place preference. This effect was not seen in animals that received single drug SKF (**Fig. 3-1E**). We conclude that exposure to SB enhances cocaine-related reward of D_1-agonist within a shorter time frame.

Exposure to D_1 agonist and HDACi is associated with increased gene expression in ventral midbrain and histone modfication at selected promoter sequences

To find out whether the increased cocaine-related locomotion in animals pre-treated with SKF82958 and SB is associated with changes in gene transcription in ventral midbrain and striatum as key structures of the reward pathway, we assayed mRNA levels for (i) tyrosine hydroxylase (TH) (Belin et al., 2007) the rate limiting enzyme in catecholamine biosynthesis, (ii) brain-derived neurotrophic factor (BDNF), a nerve growth factor molecule thought to play an important role in the neurobiology of cocaine addiction (Guillin et al., 2001, Hall et al., 2003, Graham et al., 2007), (iii) c-fos, a prototype early response gene and (iv) β2-microglobulin, a "housekeeping gene", as a control. For each gene (i) – (iv), transcript levels were determined by qRT-PCR and normalized to *18S* rRNA levels which differed less than 5 – 10% between groups, with no consistent effect by treatment.

Notably, animals that received 10 daily doses of SKF + 100 mg/kg SB (i.e., the treatment associated with the highest degree of locomotion upon subsequent exposure to cocaine, see **Fig. 1B,C**) showed significantly higher levels of *Th* and *Bdnf* mRNA levels in ventral midbrain, in comparison to SKF+Sal treated animals **[**$F(3,15)_{SB+SKF\ vs\ Sal+SKF} = 9.586_{TH}$, $p<0.03$; $= 8.891_{BDNF}$, $p<0.04$] (**Fig 3-2A).** In contrast, ventral midbrain *B2m*

mRNA levels, and all striatal transcripts were indistinguishable between animals that received SB or Sal as co-treatment together with SKF (**Fig. 3-2A**). We conclude that the locomotor-activating effects of the HDACi, SB, are associated with transcriptional changes in ventral midbrain.

Next, we wanted to examine if the increases in ventral midbrain *Th* and *Bdnf* mRNA levels in the SKF+SB treated animals are associated with changes in histone modification events at the corresponding promoters. Importantly, transcriptional profiling by microarray consistently revealed that after treatment with class I/II HDACi, a nearly equal number of genes show *decreased* or increased expression (Mariadason et al., 2000, Nusinzon and Horvath, 2005, Chen and Cepko, 2007). Furthermore, it is possible that – in addition to their established function in transcriptional repressor complexes (Butler and Bates, 2006) HDAC activity is necessary to maintain transcriptional activity at selected genomic loci (Dehm et al., 2004). These novel findings suggest that both increased, or decreased histone acetylation in a promoter chromatin environment could potentially be associated with increased gene expression levels. Therefore, we monitored histone H3 acetylation levels at *Th, Bdnf,* and *B2m* gene promoters. Immunoprecipitation of ventral midbrain prepared by micrococcal nuclease digestion showed that one out of three sites within close proximity to the *Th* transcription start site (**Fig. 3-2B, a-c**) had a significant *decrease* in H3 acetylation in 1mg/kg SKF + 200 mg/kg SB treated animals compared to saline controls. The H3 acetylation changes after co-treatment with SKF and the higher SB dose were specific because H4 acetylation at this portion of the Th promoter was unchanged (Suppl. Figure 1). This particular finding may not be too surprising given that

differential regulation of H3 and H4 acetylation has been noted before both in cell lines (Rada-Iglesias et al., 2007) and brain tissue (Kumar et al., 2005, Chwang et al., 2007). Moreover, SB-induced H3 acetylation changes were dose dependent, because co-treatments with 1 mg/kg SKF + 25 mg/kg SB did not result in significant histone acetylation changes at the Th promoter (Suppl. Figure 3-2).

Furthermore, we measured histone H3 acetylation in chromatin surrounding *Bdnf* - a gene with complex transcriptional regulation, multiple promoters and non-coding exons (Timmusk et al., 1993). For example, increased *Bdnf* expression after antidepressant treatment involves exon I (Russo-Neustadt et al., 2000, Dias et al., 2003). Moreover, dramatic increases in exon III and IV expression were observed in an animal model for social stress (Tsankova et al., 2006a). Given this background, we determined H3 acetylation at the *Bdnf* for each promoter of the non-coding exons I, III and IV. Chromatin from ventral midbrain of SB+SKF-treated mice showed, in comparison to saline treated controls, no changes in H3 acetylation at *Bdnf* promoters PI and PIII (**Fig. 3-2B**). However, ventral midbrain chromatin from the SKF + SB treated animals showed a significant down-regulation of H3 acetylation at *Bdnf* promoter IV at the higher SB dose of 200 mg/kg **(Fig. 3-2B)** but not after 25mg/kg SB (Suppl. Figure 3-2). Furthermore, changes in H4 acetylation were more variable (Suppl. Figure 3-1). Furthermore, there were no significant acetylation changes at the *B2m* promoter **(Fig. 3-2B)**. Taken together, our result show that in ventral midbrain, up-regulated expression of *Th* and *Bdnf* in response to D_1 agonist and HDACi co-treatment is associated with histone H3 deacetylation events of selected portions of the corresponding gene promoters. Given

that our immunoprecipitation assays were performed on mononucleosomal chromatin preparations from ventral midbrain (see Methods), we wanted to find out whether a decrease in nucleosomal densities underlies the observed histone hypoacetylation at selected sequences of the *Th* and *Bdnf* promoters in the SB+SKF treated animals. We therefore conducted ventral midbrain ChIP with an antibody recognizing total H4 or an antibody raised against the C-terminus of histone H3; however SKF+SB treated animals showed, in 5 out of 6 experiments, an *increase* in nucleosomal densities at the Th promoter sequence "a" (see also Fig. 2B) and similar changes at Bdnf promoter IV, in comparison to saline-treated controls (data not shown). Therefore, the observed decrease in histone acetylation - which was approximately 0.5-fold for *Th* and *Bdnf* (**Fig. 3-2B**) - cannot be explained in terms of dispersion or decrease in nucleosome density.

Co-treatment with D_1 agonist and HDACi is associated with a transient up-regulation of Th protein in striatum

To find out whether the observed changes in gene expression and histone acetylation at the Th promoter in ventral midbrain occur in conjunction with alterations in TH protein levels, we assayed TH protein levels, including its phospho-activated form, phospho-Ser^{31}-TH (Moy and Tsai, 2004). Animals were sacrificed 30 min after acute or chronic treatment (see Methods), which corresponds to the time (post-injection) at which changes in locomotor activity were observed. We assayed two brain regions, the SN/VTA and striatum including nucleus accumbens and caudate-putamen, a cocaine-sensitive target for dopaminergic fibers (Graybiel et al., 1990, Winder et al., 2002). In the striatum,

significant changes were limited to the group of animals treated with SB + SKF, which showed a 2-fold increase in TH immunoreactivity when compared to saline-treated controls (**Fig 3-3A**, [$F_{SB+SKF\ vs\ Sal+Sal}$ (3,32) = 2.936, $p < 0.01$]). In contrast, animals treated with single drug SKF or SB did not show significant changes (**Fig. 3-3A**). Likewise, significant changes in striatal phospho-Ser^{31}-TH were limited to the group of SKF+SB treated animals, which showed a 30% increase compared to animals treated with single drugs. These changes were significant [$F_{SB+SKF\ vs\ SKF+Sal\ or\ SB+Sal}$ (3,32) = 2.312, $p < 0.040$] (data not shown). In contrast to the significant up-regulation of striatal TH immunoreactivity in the SKF+SB treated animals, levels of TH protein in ventral midbrain remained unaffected (**Fig. 3-3B**). Furthermore, the observed increase in striatal TH after SKF+SB was transient because it was apparent at 30 min (**Fig. 3-3A**) but not 6 days (**Fig. 3-3C**) after the last of 10 daily treatments. We conclude that repeated exposure to D_1-agonist and HDACi is associated with a transient increase in striatal TH protein. Furthermore, we assayed the concentration of dopamine and its metabolite, DOPAC, by HPLC and no significant differences between treatment groups were observed (Suppl. Figure 3). This would suggest that an increase in striatal TH (including phospho-TH) is not necessarily reflected by a net change in dopamine tissue levels.

Activation of D1-signaling is linked to a nucleosomal response in striatum

Based on the findings of the present study, repeated treatment with SKF+SB selectively induces gene expression changes and histone modification in ventral midbrain, and this occurs in conjunction with an increase in locomotor activity upon a subsequent dose of cocaine (**Fig. 3-1, B-C**). However, repeated exposure to the D_1 agonist SKF –

administered with or without the HDACi, SB – results in a sustained change in behavioral plasticity because it was linked to enhanced cocaine reward 6 days after the last dose of SKF (**Fig. 3-1D**). As a first step towards understanding these phenomena, we wanted to identify a chromatin-remodeling mechanisms linked to D_1-signaling. Notably, previous studies reported D_1- agonist or stress induced changes in hippocampal histone phosphorylation and phospho-acetylation (Crosio et al., 2003, Chandramohan et al., 2007) and D_2-like antagonist –induced changes in striatal histone phospho-acetylation (Li et al., 2004). Importantly, the kinetics of this generalized H3 phosphorylation and phospho-acetylation bears resemblance to the induction pattern of immediate-early-genes (IEGs) and has been discussed as a "nucleosomal response" in response to receptor activation and other stimuli (Thomson et al., 1999).

To examine the *in vivo* kinetics of striatal H3 phospho-acetylation (phospho-serine 10, acetyl-lysine 14, H3pS10acK14) – a dual histone modification enriched in neuronal nuclei (**Fig. 3-4A**) – in response to D_1-receptor activation, we treated mice either with a single dose, or by repeated, daily injections (2 and 10 days) of SKF, with or without SB, and measured striatal H3pS10acK14 levels 30-120 min after the last dose. Levels of H3pS10acK14 showed a more than 2.5-fold increase after acute administration of SKF82958, and returned to baseline within 120 min after treatment (**Fig. 3-4B,C**; $\mathbf{[F_{SKF\ 30min\ vs\ Sal}(2,13) = 17.954, p < 0.001]}$. These changes were specific for the dual modification, H3pS10acK14, because levels of the single modification, H3pS10, remained unchanged after SKF82958 treatment (**Fig. 3-4B**). Similar changes were observed after repeated exposure for 10 – but not 2 – days of SKF when administered

either as single drug or in combination with SB (**Fig. 3-4B,C**). In contrast, single drug SB was indistinguishable from saline (**Fig. 3-4B,C**). The transient resistance of the histone modification machinery to further induction by SKF82958 in the two day treatment paradigm (**Fig. 3-4B,C**) was not due to tolerance, as striatal activation of the prototype early response gene, *c-fos*, was robust at all time points examined (Suppl. Fig. 3-4).

To confirm the role of D_1-receptors for these dynamic changes in H3S10pK14ac for a second rodent species, and in order to test if functional brain circuitry is required, we used dissociated rat striatal neuronal cultures that lack midbrain and cortical pre-synaptic inputs. Treatment of striatal cultures with the D1-agonist, SKF82958 (25 – 50 μM), induced a significant 1.4 – 2.0 -fold increase in H3pS10acK14 within 30 min (not shown) and peaked at 3 hours (**Fig. 3-4D, F; *, p<0.05**). These changes were specific, because levels of global H3 acetylation remained unaffected in cultures treated with SKF single drug (**Fig. 3-4E**). In contrast, addition of >100 μM SB to the cell culture medium resulted in significant increases in H3 acetylation and phosphoacetylation (**Fig. 3-4D, E**).

Finally, given that dopamine-regulated gene expression in striatal neurons involves cyclic AMP and NMDA receptor pathways (Konradi et al., 1996), we examined the effects of NMDA receptor blockade (MK-801, 2μM) and inhibition of cAMP-dependent protein kinase A (H89, 20 μM). Indeed, pre-treatment with MK-801 or H89 prevented or attenuated the up-regulation of H3pS10acK14 after D_1-agonist treatment (**Fig. 3-4F**). Taken together, both studies *in vitro* and *in vivo* demonstrate that activation of dopamine D_1 receptors up-regulates bulk chromatin levels of H3pS10acK14 in the

nuclei of striatal neurons. Furthermore, D_1-regulated striatal H3 phospho-acetylation was, at least *in vivo*, not modulated by concomitant treatment with the HDACi, SB.

DISCUSSION

Several recent studies identified chromatin remodeling in the striatum - including the regulation of histone acetylation - as an important regulator of stimulant-related plasticity and addiction behavior (Kumar et al., 2005, Levine et al., 2005, Kalda et al., 2007, Renthal et al., 2007). The present study extends the findings of these earlier studies in two ways - first, by demonstrating that histone modification contributes to drug-induced changes in gene expression in other parts of the reward circuitry, including the ventral midbrain at the level of SN/VTA. Secondly, this report underscores the link between D_1-dopamine receptor signaling and chromatin modification mechanisms, by showing that treatment with D_1- agonist (i) is associated with increased sensitization and reward behavior upon subsequent exposure to cocaine (ii) induces a generalized, but short-lasting, nucleosomal response – as defined by the phospho-acetylation of histone H3 in bulk chromatin (Thomson et al., 1999) – and (iii) regulates under certain conditions, including drug-induced inhibition of class I/II HDAC, histone acetylation and gene expression in ventral midbrain chromatin.

Our study faces several limitations, including the broad molecular action of SB – a drug considered a prototype for inhibition of class I/II HDACs but which also interferes with the de-acetylation of transcription factors, high-mobility group and other non-

histones proteins important for chromatin function (Davie, 2003). Therefore, the histone deacetylase-containing complex mediating unexpected histone de-acetylation at ventral midbrain *Bdnf* and *Th* promoters after co-treatment with D_1-agonist and SB, in conjunction with an up-regulation of corresponding mRNAs - both shown in the present study - remains to be identified. In any case, given that Bdnf has trophic actions on midbrain dopaminergic neurons (Dluzen et al., 2001, Baker et al., 2005) , the observed increase in Bdnf expression may relate, directly or indirectly, to the rise in Th mRNA (ventral midbrain) and protein (striatum) in SKF/SB treated animals. Notably, expression of Bdnf is dynamically regulated in stress-related models (Lippmann et al., 2007) (and references therein)(Berton et al., 2006, Pu et al., 2006). It will be interesting to determine if D_1-agonist and HDACi co-treatments affect expression of GDNF and other growth factors important for ventral midbrain and dopaminergic neuron function (Chen et al., 2006). Notably, recent studies showed that the mood stabilizer, sodium valproate, a short-chain fatty acid structurally similar to sodium butyrate, induces Bdnf expression and promoter-associated histone acetylation in prefrontal cortex (Fukumoto et al., 2001, Bredy et al., 2007). Furthermore, both butyrate and valproate positively regulate a number of intracellular effectors of Bdnf signaling, including extra-cellular signal related kinases (ERK) pathways and the Ca2+/cAMP dependent transcription factor CREB which in turn up-regulate Th expression (Shah et al., 2006, Shaltiel et al., 2007). It is possible that transient increases in neurotrophin supply - including those of Bdnf - evoke further adaptations in a subset of dopaminergic or other neurons, which then underlie the observed changes in cocaine-related behaviors. This scenario would also explain

important differences in the timing of the various, drug-induced adaptations, which is another limitation of the present study: While the dynamic changes in striatal H3 phospho-acetylation, and *Th* and *Bdnf* expression in ventral midbrain were measured within minutes or the first hours after drug treatment, behavioral outcomes were monitored up to six days after the last treatments with D_1-agonist and HDACi.

Remarkably, the up-regulation of striatal histone H3 phospho-acetylation after activation of D_1-signaling (present study) or blockade of D_2-like signaling (Li et al., 2004) is readily apparent on immunoblots from tissue homogenates or extracts, indicating that this is a "nucleosomal response" (Thomson et al., 1999) that includes -- but is not limited to – *c-fos*, *c-jun* and other immediate early gene promoters (Thomson et al., 1999, Li et al., 2004). In this context, it is noteworthy that D_1-agonist-induced H3 phospho-acetylation in striatal neurons is completely blocked by the PKA inhibitor, H89 (**Fig. 3-4F**). Furthermore, H89 inhibits the nucleosomal response in fibroblasts, via functional inactivation of mitogen- and stress-activated protein kinase 1 (MSK1) (Thomson et al., 1999). Notably, recent reports attributed to MSK1 a key regulatory role for hippocampal and striatal histone acetylation and phosphorylation (Brami-Cherrier et al., 2005, Chwang et al., 2007).

The present paper reports that in animals co-treated with D_1-agonist and class I/II HDACi, cocaine-induced reward behavior is enhanced. It is therefore tempting to speculate that the opposite strategy, i.e. treatment with D1-antagonist and a histone acetyl-transferase inhibitor (HATi), could perhaps prevent, or attenuate, some of the behaviors associated with cocaine reward. Evidence from clinical trials suggest that

administration of D1-antagonist drugs to active users may be ineffective or even counterproductive (Haney et al., 2001), albeit reduction of cocaine-induced euphoria and stimulation had also been reported (Romach et al., 1999). However, there is evidence from animal studies that D_1-antagonism may prevent relapse (Alleweireldt et al., 2002, Anderson et al., 2003, Sanchez et al., 2003). From the viewpoint of translational medicine, it will therefore be of considerable interest to explore whether or not co-treatment of animals with histone modifying drugs, including HATi or HDACi, alters reinstatement or relapse of cocaine-related behaviors. Finally, it will be important to evaluate how chromatin-modifying drugs would affect the developing brain which may be particularly vulnerable to stimulant drugs (Schmauss, 2000, Crandall et al., 2004).

ACKNOWLEDGEMENTS

This work was supported by a grant from the National Institutes of Drug Abuse (NIDA) to S.A. (R01 DA017660).

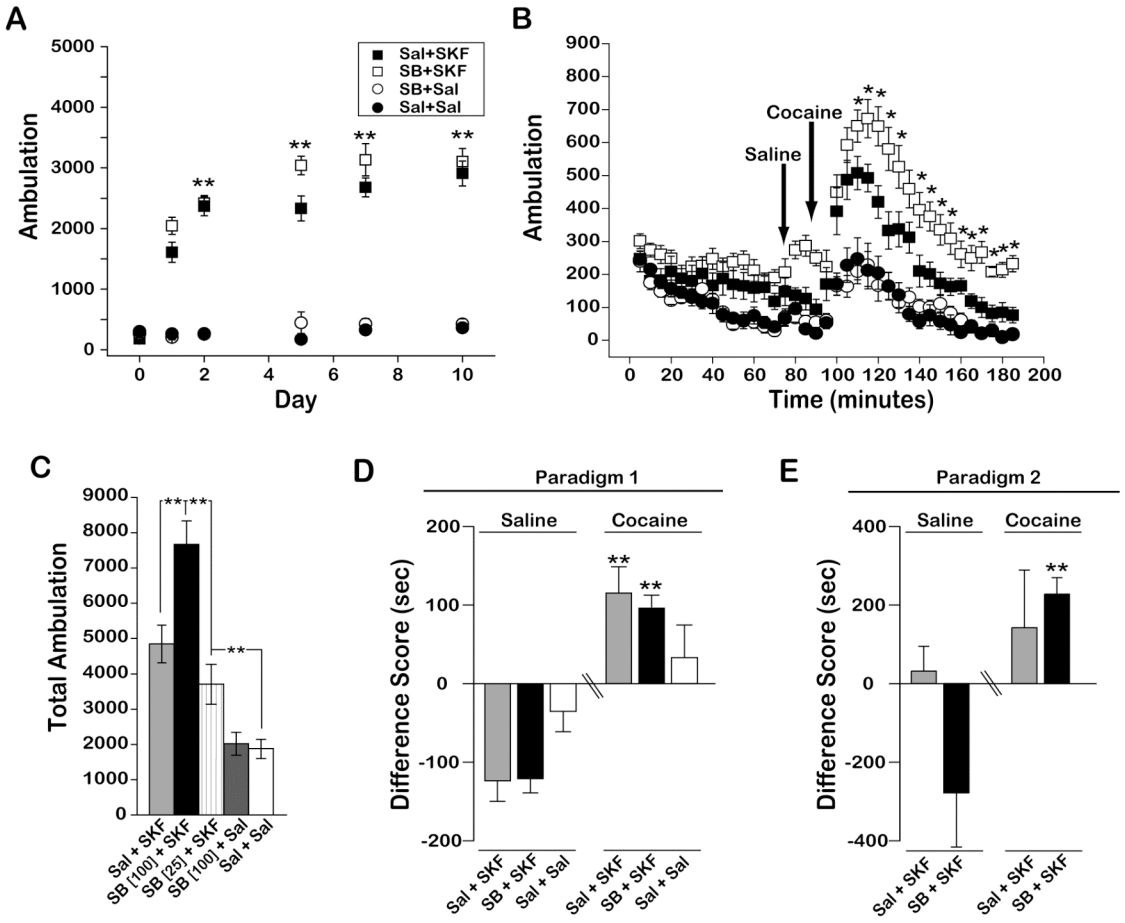
A
Ambulation
Day
Sal+SKF
SB+SKF
SB+Sal
Sal+Sal
B
Ambulation
Time (minutes)
Cocaine
Saline
C
Total Ambulation
Sal + SKF
SB [100] + SKF
SB [25] + SKF
SB [100] + Sal
Sal + Sal
D
Paradigm 1
Saline
Cocaine
Difference Score (sec)
Sal + SKF
SB + SKF
Sal + Sal
E
Paradigm 2
Saline
Cocaine
Difference Score (sec)
Sal + SKF
SB + SKF

Figure 3-1.

Fig. 3-1. Changes in cocaine-induced behavior after pre-treatment with D_1-agonist and HDACi. (**A**) Locomotor activity during pre-treatment; Sal followed by SKF (filled square); SB followed by SKF (open square); SB followed by Sal (open circle) and Sal followed by Sal (filled circle). Data show locomotor activity for the first 60 min following second drug (mean ± S.E.M., N = 8-10 animals/group). Notice that locomotor activity was significantly increased in mice treated with SKF±SB when comparing activity on day 1 with days 2, 5, 7, or 10 (**, $p<0.001$) **(B)** Locomotor activity before and after a single dose of cocaine Animals were placed in activity cages 24 hours after the last pre-treatment (see A) and behavior was recorded for t = 190 min total (x-axis). Saline injected at t = 75min and cocaine (15 mg/kg) at t = 90 min as indicated by arrows. Notice that animals pre-treated with HDACi plus D_1-agonist (SB+SKF; open squares) show a significant increase in cocaine-induced ambulation when compared to group pre-treated with D_1-agonist only (Sal+SKF, filled circles) (mean ± S.E.M., N = 8-10 animals/group). **(C)** Total ambulation after cocaine (see also B). Notice that pre-treatment with 100 mg/kg SB+SKF, but not 25 mg/kg SB+SKF, is associated with a significant, 4-fold increase in cocaine-induced ambulation, and pre-treatment with SKF (Sal+SKF) with a 2.5-fold increase, when compared to mice pre-treated with saline only (Sal+Sal). **(D, E)** Conditioned place preference (D = paradigm 1, E = paradigm 2, see Methods), expressed as difference in time spent in cocaine - or saline-associated chamber before and after exposure (y-axis). Notice (**D**) enhanced place preference in animals pre-treated with Sal+SKF is similar to group treated with SB+SKF, when compared to mice pretreated with saline (Sal + Sal). Notice (**E**) significant cocaine-related place preference in group treated with SB+SKF, as compared to single drug SKF. *, $p < 0.05$; **, $p < 0.01$; n=8-10/group, all data shown as mean ± S.E.M.

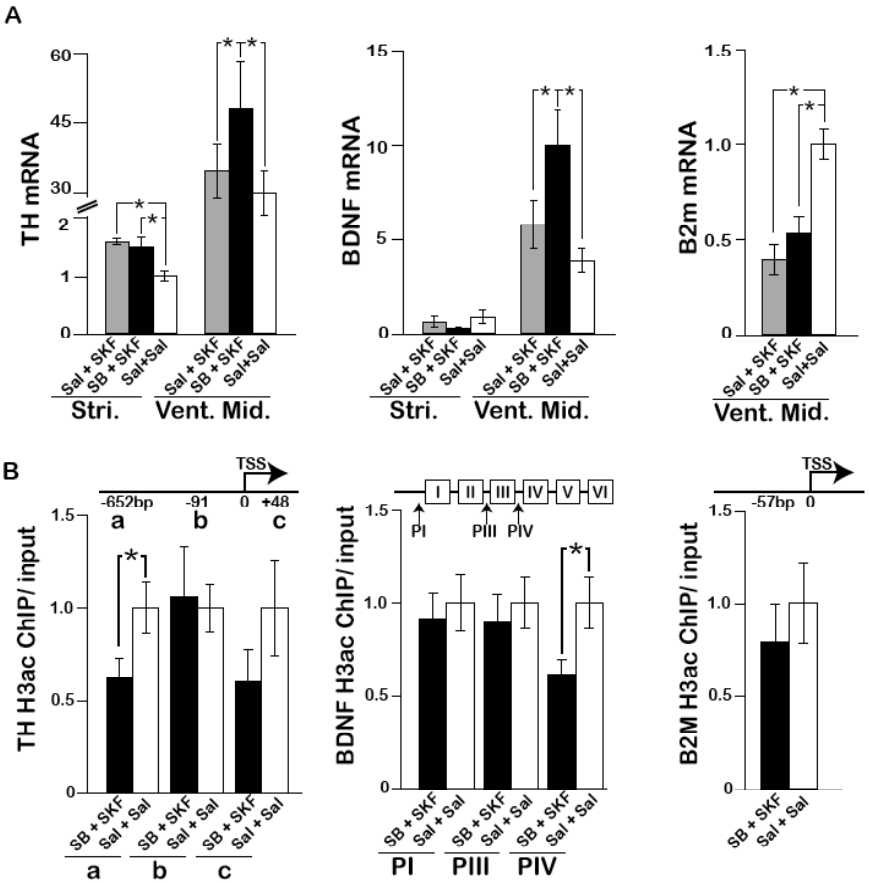

Fig. 3-2: Treatment with D_1 agonist and HDACi is associated with increased gene expression in ventral midbrain and histone modification at selected promoter sequences **(A)** mRNA levels for *Th, Bdnf*, and *B2m* from striatum (Stri.) and ventral midbrain (Vent. Mid.) of animals treated for 10 days with Sal+SKF or SB+SKF or SB+Sal or Sal+Sal and sacrificed 30min after last injection. Data from qRT-PCR expressed as mean ± S.E.M. after normalization to *18S* rRNA. Notice that ventral midbrain of animals treated with SB+SKF shows significant increases in *Th, Bdnf* transcripts compared to Sal+SKF and Sal+Sal. In contrast, ventral midbrain *B2m* levels were significantly decreased in SKF+/-SB mice. N=5/group/brain region, *, $p<0.05$; **, $p<0.01$. **(B)** Top, schematic presentation of positioning of primer pairs used for ChIP studies at *Th, Bdnf* and *B2m* promoters (left graph: *Th* promoter, a-c; middle graph: *Bdnf*, promoter I, III, IV; and right graph, *B2m*) for amplification of mono-nucleosomal DNA. TSS = transcription start site. Bar graphs showing levels of H3 acetylation at promoter sequences from ventral midbrain of mice after 10 daily treatment with SB+SKF (black bars) or Sal+Sal (white bars) as indicated. Animals were sacrificed 30 min after last treatment. Data shown as chip-to-input ratios (mean ± S.E.M., N = 5-10 /group). Notice a significant *decrease* in histone acetylation at *Th* promoter sequence "a" and *Bdnf* promoter IV following SB+SKF treatment. (*, $p<0.05$).

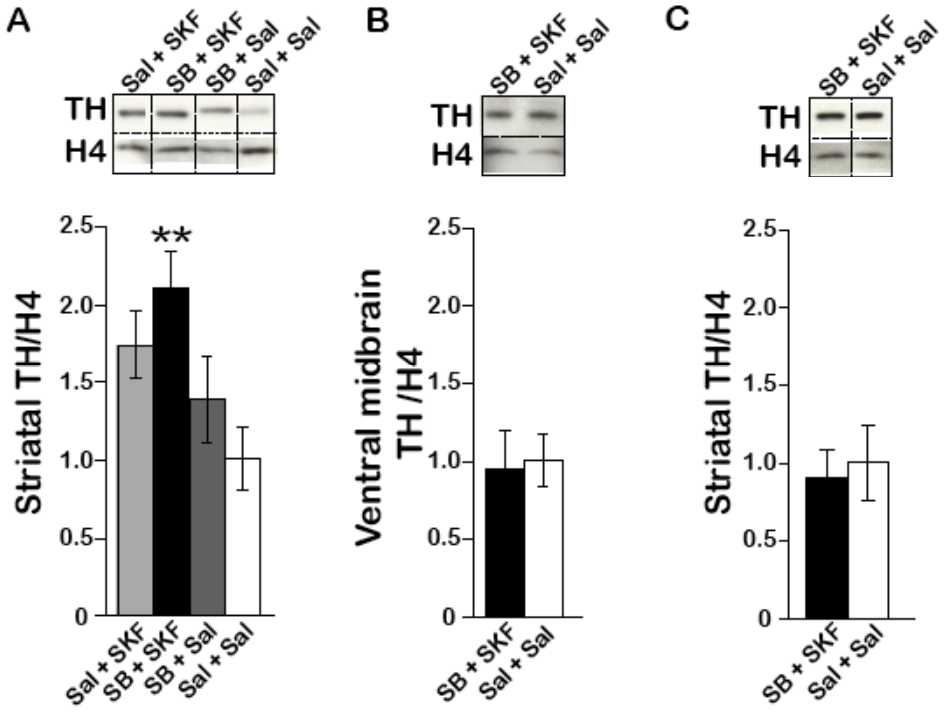

Fig. 3-3: A transient increase in striatal TH after exposure to D_1-agonist and HDACi. (**A**) Top: Representative immunoblots from striatum of animals treated for 10 days with Sal+SKF or SB+SKF or SB+Sal or Sal+Sal and sacrificed 30min after last injection. Blots were labeled with anti-TH (upper band) and anti-histone H4 as loading control (lower band). Bottom: Bar graph showing densitometric quantification of striatal immunoblots (mean ± S.E.M., N = 6-10/group). Notice significant, 2-fold increase in TH protein levels in animals treated with SB+SKF compared to saline-treated controls. **(B)** TH immunoblots from ventral midbrain of animals treated with SB+SKF and Sal+Sal (same groups as shown in A) reveal no significant differences. **(C)** Striatal TH immunoblots from mice subjected to CPP (see also Fig. 1D), animals were sacrificed 6 days after last injection of SB+SKF and 24 hours after last dose of cocaine. There is no significant difference between mice pre-treated with SB +SKF as compared to pre-treatment with Sal+Sal (N = 3/group). ** $p < 0.01$.

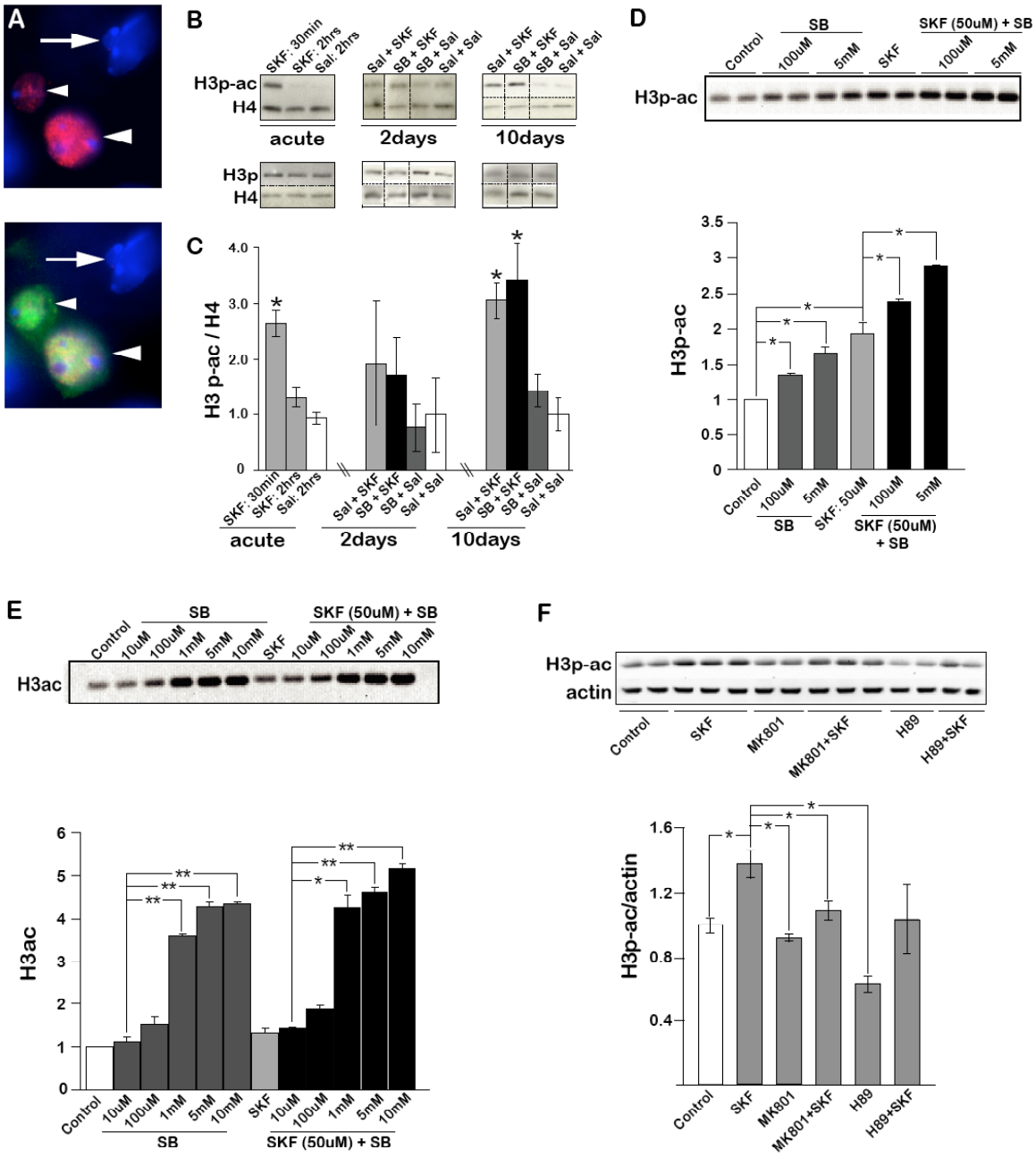
A
B
H3p-ac
H4
SKF: 30min
SKF: 2hrs
Sal: 2hrs
Sal + SKF
SB + SKF
SB + Sal
Sal + Sal
acute
2days
10days
H3p
H4
C
H3 p-ac / H4
D
Control
SB
SKF (50uM) + SB
100uM
5mM
SKF
H3p-ac
E
10uM
1mM
10mM
H3ac
F
actin
MK801
MK801+SKF
H89
H89+SKF
H3p-ac/actin

Figure 3-4.

Figure 3-4. D_1-receptor signaling regulates H3 phospho-acetylation in striatal neurons. **(A)** Digitized images from striatal section processed for H3p-ac (red, upper panel), and NeuN (green, lower panel) immunofluorescence, with DAPI counterstain (blue). Notice robust H3p-ac signal in NeuN-positive cells (arrowheads) but absent in non-neuronal (NeuN negative) cell (arrow). Images taken at 10 x 63 magnification. **(B, C)** Histone immunoblots and densitometric quantifications from striatum of mice treated with SB and SKF as single drug or co-treatments as indicated. Blots in (**B**) labeled with H3p-ac (upper panels) and H3p (lower panels), each with H4 as loading control. Notice robust increase in striatal H3 phospho-acetylation both after acute and 10 days of treatment of SKF with or without SB. Animals were sacrificed 30 min after last treatment. Bar graphs in (**C**) show densitometric quantifications (mean ± SE) of striatal H3p-ac (N = 3-5/group) with comparison to saline-treated control. **(D, E)** Immunoblot (top) and densitometric quantification (bottom) from cultured striatal neurons showing changes in (**D**) H3p-ac and (**E**) H3ac after 3 hours of treatment with SB and/or SKF. Notice (**D**) significant increase in H3p-ac after 3 hours treatment with SB or SKF, with the highest levels in cultures co-treated with SB+SKF. In contrast, (**E**) up-regulation of H3ac is mediated by SB but not SKF. (**F**) H3p-ac immunoblots (top) and densitometric quantifications (bottom) from cultured striatal neurons treated with D_1-agonist (SKF) and/or the NMDA receptor antagonist MK801 and the PKA antagonist H89 as indicated. Notice attenuated response to D1-agonist in the presence of MK801 or H89. A-F (*, $p<0.05$; **, $p<0.01$).

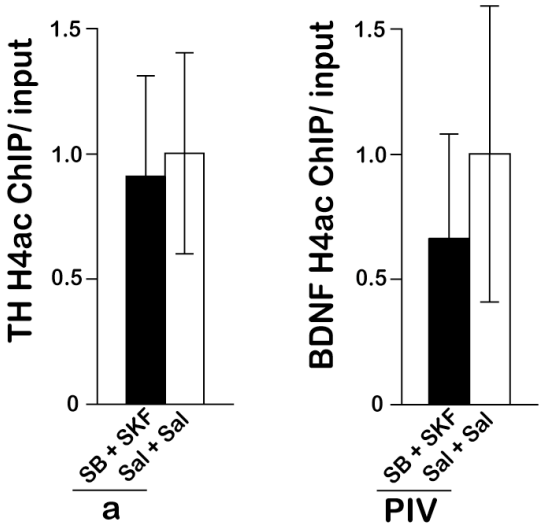

Supplemental Figure 3-1: *Histone H4 acetylation at Th and BDNF gene promoters.* Bar graphs showing levels of H4 acetylation at promoter sequences Th 'a' and Bdnf PIV (see Fig. 2B in main manuscript) from ventral midbrain of mice after 10 daily treatments with SB+SKF (black bars) or Sal+Sal (white bars) as indicated. Animals were sacrificed 30 min after last treatment. Data shown as chip-to-input ratios (mean ± S.E.M., N = 5 /group).

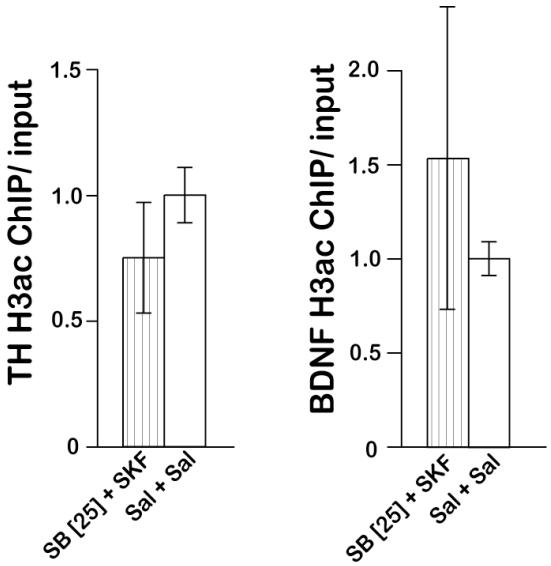

Supplemental Figure 3-2: Histone H3 acetylation at Th and BDNF gene promoters. Bar graphs showing levels of H3 acetylation (expressed at ChIP-to-input) at promoter sequences Th 'a' and BDNF PIV (see Fig. 2B in main manuscript) from ventral midbrain of mice after 10 daily treatments with SB (25mg/kg) + SKF (1mg/kg) (striped bars) or Saline+Saline (Sal+Sal) (white bars) as indicated. Animals were sacrificed 30min after the last treatment (mean ± S.E.M., N=4/group).

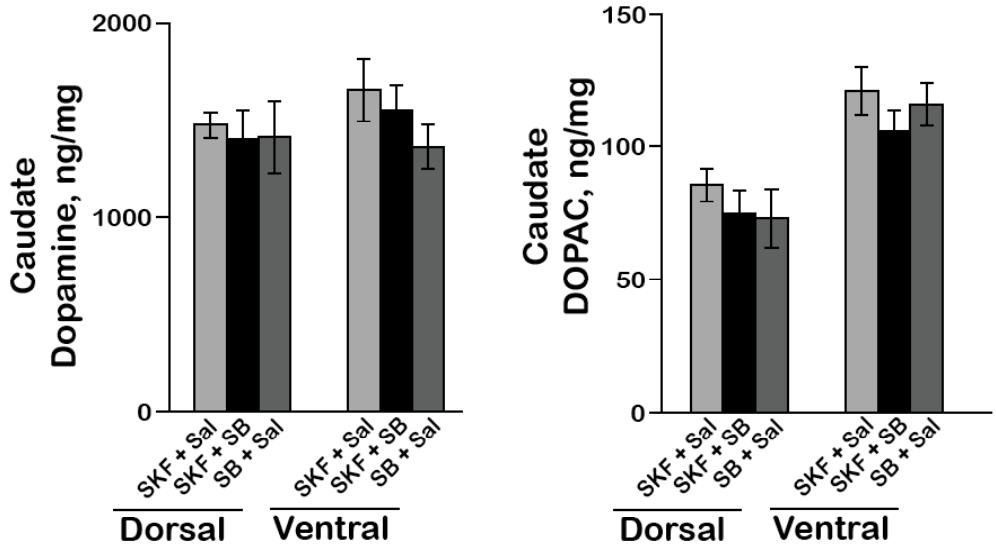

Supplemental Figure 3-3: Steady-state dopamine and DOPAC levels from caudate of mice, determined by HPLC.

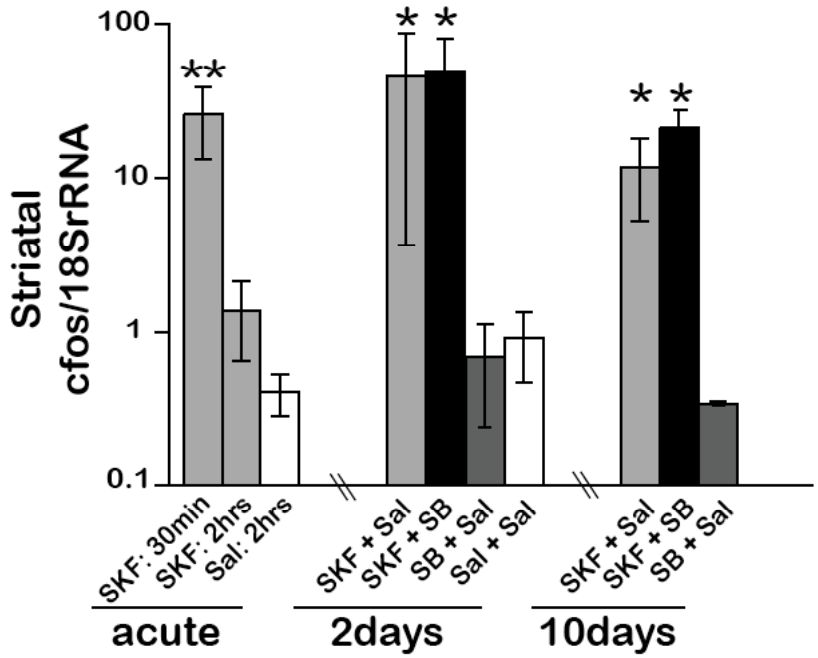

Supplemental Figure 3-4: Striatal c-fos expression in mice, determined by QRT-PCR.

CHAPTER IV:

Imaging Cocaine-Sensitive Brain Areas Responsive to Chromatin Modifying Drugs

The work presented in this chapter is reproduced from a manuscript, currently under revision, by Febo et al. This work was conducted under the collaborative direction of Drs. Marcelo Febo, Schahram Akbarian and Craig Ferris and it is with gratitude that I reproduce these data for the purposes of this dissertation with minor changes in style and text. My contribution to this work was the experimental execution, data quantification, and statistical analysis of the Western blots (Fig. 1). Drs. Febo and Ferris contributed by conducting all BOLD imaging, behavioral studies and associated statististical analyses. The manuscript was prepared by Dr. Febo with contributions from Drs. Akbarian and Ferris; I contributed a portion of the Materials and Methods section.

Abstract

Inhibitors of histone deacetylases (HDACi) and acetyltransferases (HATi) facilitate or impede gene expression in response to drugs of abuse by regulating chromatin packaging. Here we tested whether the HDACi sodium butyrate (SB) and the HATi curcumin influence changes in brain activation during the initial stage of repeated cocaine administration. Four groups of rats were challenged with cocaine during functional magnetic resonance imaging (fMRI), (*i*) those given cocaine for the first time, (*ii*) those receiving cocaine for two days and rats pretreated on each of the two days with either (*iii*) SB or (*iv*) curcumin 30 min prior to cocaine. Pretreatment with SB increased cocaine-induced activity in selected regions, including the anterior thalamus, the hippocampus at the level of the dentate gyrus and CA3, portions of the amygdala, septum, and somatosensory cortex. Curcumin pretreatment, on the other hand, trended towards an opposite outcome; reducing brain activation in these regions in comparison to SB. Our results underscore a potential role for histone-modifying drugs in modulating cocaine-induced brain responses and the neuroadaptive changes occurring during the initial phases of repeated exposure. Given the known roles of the above brain regions in learning, memory, motivation and social recognition, it is possible that chromatin remodeling contributes to reinforcing cocaine-associated memories.

Introduction

Psychostimulants and other classes of drugs induce the expression of a variety of early response genes. For example, the genes *c-fos*, *c-jun*, *fosB, junB*, *zif268* are all elevated in neurons of the dorsal and ventral striatum of the rat by a single injection of cocaine or amphetamine (Hope et al., 1992, Moratalla et al., 1993, Berke et al., 1998). Protein products orchestrated by these genes are presumed to be part of a systematic adaptation to the drug (Moratalla et al., 1993), which ultimately determines subsequent neuronal and behavioral responses (Canales and Graybiel, 2000). With chronic cocaine exposure, the pattern of genes expressed is modified (Hope et al., 1994, Moratalla et al., 1996), (Moratalla et al., 1996) an event that may underlie several neurophysiological consequences such as alterations in overall electrical excitability of neurons (Yao et al., 2004, Dong et al., 2006), alterations in receptor-signal transduction mechanisms (Gainetdinov et al., 2003), behavioral changes (Hyman, 1999) and further long-term gene expression changes (McClung and Nestler, 2003). Knowledge of the molecular steps regulating cocaine-induced genes, particularly during the initial stages of drug administration may be essential for targeted treatments for addiction.

A variety of covalent histone modifications, including acetylation, play a key role for chromatin function and transcriptional regulation (Verdone et al., 2005) and are therefore likely to be play an important role for cocaine-regulated gene expression and plasticity. Indeed, acute and chronic exposure to cocaine induces dynamic changes in acetylation, phosphorylation and methylation of histones and other chromatin associated

proteins in striatum (Brami-Cherrier et al., 2005, Kumar et al., 2005, Levine et al., 2005) and prefrontal cortex (Black et al., 2006b, Cassel et al., 2006). Furthermore, alterations of striatal histone acetylation levels by histone deacetylase (HDAC) inhibitor drugs or virus-mediated gene delivery strongly affect cocaine-regulated gene expression and behaviors (Kumar et al., 2005). Conversely, mice with haploinsufficiency for the transcriptional regulator and histone acetyl-transferase (HAT), cAMP-response element binding protein (CBP) show an attenuated neurochemical and behavioral response to the stimulant (Levine et al., 2005).

On the basis of these recent findings, the aim of this preclinical study was to further explore the effects of chromatin modifying drugs on the brain's reward and addiction circuitry. Specifically, we examined if drug-induced inhibition of two functionally opposing classes of enzymes – HDACs and HATs – modulate the animal's response during the initial stages of cocaine-induced changes in brain function. We used blood-oxygen-level-dependent (BOLD) fMRI to measure the acute and repeated neural response to cocaine in the presence of sodium butyrate (SB), a prototype member of class I/II histone deacetylase inhibitor drugs (Davie, 2003) or curcumin, a curry spice extract of *Curcuma longa* acting as CBP-specific HAT inhibitor (Balasubramanyam et al., 2004). We report, for the first time, that both SB and curcumin were able to modulate the BOLD response to cocaine upon re-exposure, albeit in distinct directions. The HDAC inhibitor, SB, enhanced cocaine-induced BOLD activity in specific brain regions, whereas the HAT inhibitor curcumin demonstrated an overall opposite action. Interestingly, our findings

point away from the mesocorticolimbic system for these changes in cocaine sensitivity and towards brain areas commonly associated with learning and memory functions.

Materials and Methods

Animals

Adult Long Evans male rats were purchased from Charles River Laboratories (Charles River, MA). Rats were housed in pairs in a temperature and humidity controlled room and maintained on a 12L:12D light-dark cycle, with lights off at 1900 hr. Water and Purina rat chow were provided *ad libitum.* Animals were acquired and cared for in accordance with the guidelines published in the Guide for the Care and Use of Laboratory Animals (National Institutes of Health Publications No. 85-23, Revised 1985) and adhere to the National Institutes of Health and the American Association for Laboratory Animal Science guidelines. The Institutional Animal Care and Use Committee at the University of Massachusetts Medical School approved the protocols used in this study.

Drug preparation and administration

Cocaine hydrochloride, sodium butyrate acetate (SB) and curcumin extract were all purchased from Sigma-Aldrich Co. (St. Louis, MO). Cocaine and SB were dissolved in 0.9% sterile saline solution. Cocaine was prepared fresh at a dose of 15 mg kg^{-1} and sodium butyrate at 200 mg kg^{-1} and both were injected i.p. at a volume of 0.1 cc 100 g^{-1}. The SB and cocaine administration protocol used in the present study was partly based on the one used by Kumar et al (Kumar et al., 2005). According to their results, pretreatment of rats with 100 mg kg^{-1} SB 15-min before cocaine on two days leads to a heightened cocaine-induced locomotor response on the second day (Kumar et al., 2005). For imaging experiments, cocaine was injected intracerebroventricularly (ICV) during

functional scan acquisition at a concentration of 20 μg in 10 μL artificial cerebrospinal fluid (aCSF contained, in mM: 145 NaCl, 2.7 KCl, 10 $MgCl_2$, 12 $CaCl_2$, 20 $Na_2HPO_4 \bullet 7H_20$, pH 7.4). Curcumin was prepared in 80% dimethylsulfoxide (DMSO) at a dose of 30 mg kg^{-1} and injected i.p. at a volume of 0.25 cc 100 g^{-1}. This dose was chosen because a lower dose of orally administered curcumin (10 mg/kg, p.o., in peanut oil) given 60 min before testing was shown to cause behavioral alterations (reduced immobility) and increase serotonin, norepinephrine and dopamine in the frontal cortex and hippocampus of mice (Xu et al., 2005). Changes in global histone acetylation levels after exposure to SB or curcurmin were monitored in neuronal cultures from embryonic rat forebrain. As expected, histones became hyperacetylated after SB (5-10 mmol) but hypoacetylated after curcurmin (1-5 μmol), in comparison to vehicle (**Fig. 4-1**).

Four groups of rats were challenged with cocaine during functional imaging, those given cocaine for the first time (group *i*, 1 day saline-cocaine), those receiving cocaine for 2 days (group *ii,* 2 day saline-cocaine) and rats pretreated on each of the two cocaine treatment days with SB (group *iii*, 2 day SB-cocaine) or curcumin 30 min prior to cocaine (group *iv,* 2 day curcumin-cocaine). For the latter two groups, rats were given an i.p. injection of a histone modifying drug and following 30 minutes they were given an i.p. injection of cocaine (15 mg kg^{-1}). On day 2, rats were imaged for their response to cocaine after pretreatment with vehicle or one of the two histone modifying drugs. They were injected and then placed under 2-3% isoflurane anesthesia in preparation for fMRI (see below). Following 30 minutes, all rats were challenged with intra-cerebroventricular (ICV) cocaine during functional scanning. This route of injection and dose of cocaine is

reported to enhance dopamine neurotransmission and increase blood-oxygen-level-dependent (BOLD) signal in the mesocorticolimbic system without the cardiovascular or respiratory complications caused by systemic administration of cocaine (Febo et al., 2004). Injections were made via a plastic 300-μL syringe connected at the end of the ICV cannula tubing. Cannula placement was verified prior to cocaine imaging with a short anatomical MR scan. Only animals with correct placement were included in the study.

Functional magnetic resonance imaging

All imaging experiments were done in fully awake, unanesthetized male rats. Anesthesia (2-3%isoflurane) was used only during the rat setup preceding the experiments (see above). Functional MRI experiments were carried out using a multi-concentric dual-coil small animal restrainer (Insight NeuroImaging Systems, Worcester, MA). All rats were acclimated to the restrainer and the imaging protocol at least a week before functional imaging (King et al., 2005). To reduce discomfort from ear and nose bars during both acclimation and imaging experiments, a topical anesthetic (10% lidocaine cream) was applied to skin and soft tissue in the ear canal and over the bridge of the nose. Immediately prior to imaging studies, rats were anesthetized with 2-3 % isoflurane, the skull surface was exposed and the landmark suture Bregma located. Lidocaine cream was applied around the incision area. A 26-gauge cannula of polyethylene tubing (PE-10: inner diameter 0.28 mm, outer diameter 0.61 mm) was lowered into the lateral cerebral

ventricle (1 mm caudal to Bregma, 2 mm lateral to the mid-sagittal sinus, and 4 mm ventral to dura) and secured to the skull with surgical glue.

Magnetic resonance imaging was conducted in a Bruker Biospec 4.7-T/40-cm horizontal magnet (Oxford Instrument, Oxford, U.K.) equipped with a Biospec Bruker console (Bruker, Billerica, MA U.S.A) and a 20-G/cm magnetic field gradient insert (inner diameter = 12 cm, 120-μs rise time). A high-resolution anatomical scan used for overlays and multi-subject alignment was collected for 6 minutes using a fast spin echo (RARE) pulse sequence (effective echo time = 48 msec, repetition time = 2500 msec, field of view = 30 mm, 14 slices, 1.2 mm slice thickness, 256^2 data matrix for an in-plane resolution of 117 μm^2, echo train length = 16, 6 averages). Functional imaging was performed with a T2-weighted multi-slice fast spin echo pulse sequence with the following parameters: effective echo time = 53.2 msec, repetition time = 2108 msec, 64^2 data matrix for an in-plane resolution of 468 μm^2, echo train length = 16, echo spacing = 7 msec. Except for the lower in-plane resolution, the geometrical setup of the functional scans exactly matched the anatomical scans for each subject. A single acquisition of all 14 slices took 8.4 sec. A total of 110 brain images were collected for 15 minutes. Cocaine was administered following the initial 35 repetitions (4.9 minutes), which corresponded to the pre-cocaine baseline acquisition.

Assessment of cerebrovascular reactivity

In order to test whether the histone modifying drugs themselves might affect cerebrovascular reactivity and consequently affect the BOLD response to cocaine, a

separate group of rats were challenged with a 10% CO_2 pulse during functional scanning (Cohen et al., 2002, Sicard et al., 2003). The release of carbon dioxide from metabolically active neuronal tissue triggers dilation of vascular smooth muscle allowing the influx of oxygenated blood. Therefore, despite the absence of a neuronal-driving stimulus, cerebral blood flow and BOLD-weighted intensity increase in the presence of hypercapnia ('mock' BOLD activation). Functional imaging was performed using the same pulse sequence parameters described above, with the exception that the total acquisition time was 8-min (56 repetitions), with two alternating pulses of 10% CO_2 given at 1-min blocks (7 reps each) between three 2-min baselines (14 reps each). Animals were given an i.p. injection of either saline vehicle (n = 5), 80% DMSO vehicle (n = 6), 200 mg kg^{-1} SB (n = 5) or 30 mg kg^{-1} curcumin (n = 5) during setup, 30 min prior to functional imaging.

Cell cultures

Cells were prepared from forebrain of E14.5 SASCO SD rat embryos (Charles River). Live cells were plated out at 1.2-1.4x10^6 cells per 100-mm poly-l-lysine coated dishes pre-coated with 15ug/ml poly-l-ornithine (Sigma) and 1ug/ml fibonectin (R&D systems), treated daily with10ug basic fibroblast growth factor 2 (FGF2 - R&D systems) and maintained at 37°C, 5% CO_2 and grown in media composed of: DMEM/F12 + 1% N2 supplement + 1% pen/strep + 0.2% Glutamax + 0.01% Glutamine + 0.34% Glucose (45% solution, Sigma).

At DIV5, cells were passaged and plated at 0.8-1.0 x10^6 cells per pre-coated plate and expanded as above for a further 3-4 days (expansion approx 300%). Cells were

passaged again, plated at 1.1-1.4 x10^6, and after 1-2 days, FGF2 was removed. Cells were then washed once with media and resuspended in FGF2-free media with or without sodium butyrate (5mM, EMD Chemicals, Inc, dissolved in media.) or curcumin (1μM, Sigma-Aldrich, dissolved in 100% Ethanol). 48 hours later, SB-containing cultures/controls were harvested and media from curcumin-containing cultures/controls was replaced with fresh FGF2-free media with or without curcumin (1μM) and maintained for an additional 48 hours before harvest. Cells were harvested by aspirating media, rinsing/aspirating briefly with PBS, and snap freezing on dry ice.

Western Blotting

Frozen rat cells were thawed at 25°C for ~1 min, scraped from culture plates with Laemmli homogenization buffer, then incubated at 37°C for 10 min and centrifuged at 4°C, 13,500 *g*. The supernatant was denatured at 95°C for 5 min, then electrophoresed on a 10-20% linear gradient Tris-HCl gel (Bio-Rad) and transferred to polyvinylidene difluoride (PVDF) membrane (0.2μm pore size, Bio-Rad). Immunostainings were performed with anti-acetyl histone H3 antibody (Chemicon/Upstate #06-599) and, as loading control, anti-histone H4 antibody (Chemicon/Upstate, #07-108). Immunoreactivity was detected with peroxidase-conjugated secondary antibody (donkey anti-rabbit IgG; Amersham) in conjunction with chemiluminesence-based film autoradiography (Super-Signal West Dura Extend Reagent, Pierce). For quantification, Quantity One software (Bio-Rad) was used.

Behavior testing

Automated measurements of acute (1 day) and chronic (5 day) locomotor activity were taken using an open field box coupled to a digital camera-computer software system that quantified rat movement (in cm). The open field box (dimensions in cm: 51 X 51 X 24) contained black walls and floor to contrast the rat against its background. Testing was done between 0700 to 1100 hrs under dim lighting. The tracking software (Noldus, MA) divided the cage into 4 equally spaced quadrants and tracked rat movement based on color-contrast. For our studies, 4 groups of rats (n = 8) were tested during 10 min after pretreatment with vehicle or chromatin-modifying drugs and then again 10 mins after treatment with cocaine. The groups were saline-cocaine, DMSO-cocaine, SB-cocaine and curcumin-cocaine. On the first day of testing, rats were given an injection of vehicle or chromatin drug and placed into the open field box for 10 mins (same doses and volumes as described in drug preparation section above). Thirty mins after the first injection, rats were administered an i.p. injection of 15 mg kg^{-1} cocaine and placed into the open field box once again for 10 more mins. This procedure was repeated on a 5^{th} day of testing (rats were injected in their homecages on days 2 to 4 following the same drug dosing and sequence). Statistical analysis using a Kruskall-Wallis ANOVA by ranks ($p < 0.05$) was performed on the data. The dependent variables were rat movement (in cm) during pretreatment and cocaine administration. The independent or grouping variable was pretreatment (Sal, DMSO, Curc or SB).

Statistical analysis

Each functional MRI scan was first inspected for excess motion by estimating the standard deviation from the image center-of-mass on the Stimulate software (Strupp, 1996). Animals showing an average displacement exceeding 25% of the total inplane (X-Y) voxel resolution (>120 μm out of 468 μm) or more than 25% displacement in the slice (Z) direction (>300 μm out of 1200 μm slice thickness) were excluded. Time series movies were also generated in order to qualitatively confirm the presence of motion (eg, continuous timecourse spikes, up-down head movements). Low frequency drift is also a common problem in time series fMRI studies and contributes to signal variability. Instability in temperature regulation with high performance gradients is one source of the problem; however, physiological noise and head motion are also considered to be contributing factors to drift (Turner, 1997). The occurrence of false positive voxels is a concern particularly in the simple off-on activation paradigm used in these studies comparing the average baseline signal for a given voxel to its average post-stimulation signal. To control for this issue, awake rats (n = 4) were exposed to an 18 min long imaging protocol mimicking that described above for the fMRI studies. A 6 min long high resolution anatomical scan was followed 2 min later by a 10 min long fMRI time series. During the fMRI time series there was no stimulus presentation. The change in MR signal over the 10 min period mimicking the fMRI study without the presentation of a stimulus did not differ by more that 2% for any of the four animals studied (see **Supplemental Fig. 4-1**). The data corroborate our previous work reporting a baseline variability in MR signal of approximately 2% in fully conscious animals imaged with an

INSL rodent restrainer system and dual coil RF electronics at 4.7T (Brevard et al., 2003, Febo et al., 2004, Ferris et al., 2005). The present data were acquired during 8 or 15-minute scans and statistical tests performed using the 1st 10-minute block of the time series. Scans with prestimulus baseline drifts over 2% were largely due to gradient heating from malfunctioning equipment. These scans were excluded from the study. Data from a total of 49 rats were originally collected. After applying exclusion criteria, the final N was 24 (6 animals per 4 conditions). Scans that passed the initial exclusion criteria were aligned to a 3D atlas of the rat brain.

Region-of-interest (ROI)-based statistical analysis was done using Medical Image Visualization and Analysis (MIVA) software (http://ccni.wpi.edu/cwbench/cwbench-tiles.jsp). Details of the alignment of scans to the rat brain atlas have been published elsewhere (Wu, 2003, Ferris et al., 2005). Each subject was registered to a fully segmented electronic rat brain atlas based on 2D textbook images (Paxinos, 1997, Swanson, 1999). The alignment process began by outlining the brain perimeters for each slice of the anatomy image sets. A marching cubes algorithm with automated linearization creates accurate 3D surface shells for each subject (Wu, 2003). This enhanced surface generation strategy eliminates the characteristic stair-stepped behavior of the marching cubes algorithms while simultaneously increasing the accuracy of the geometry representation. These anatomy shells are aligned to the atlas shell. The affined registration involved translation, rotation, and scaling in all 3 dimensions, independently. The matrices that transformed the subject's anatomy shells to the atlas space were used to embed each slice within the atlas. All transformed pixel locations of the anatomy images

were tagged with the segment atlas major and minor regions creating a fully segmented representation of each subject. The inverse transformation matrix $[T_i]^{-1}$ for each subject (*i*) was also calculated.

Statistical *t* tests were performed on each subject within their original coordinate system. The baseline period was 32 repetitions immediately preceding drug administration and the stimulation window was the 32 repetitions following ICV cocaine (4.5 minutes for each). Statistical *t* tests used a 95 % confidence level, two-tailed distribution, and heteroscedastic variance assumptions. In order to provide a conservative estimate of significance, a false-positive detection-controlling algorithm was introduced into the analysis (Genovese et al., 2002). This ensured that the false-positive detection rate was below our cutoff of 5 % (Ferris et al., 2005). Statistically significant pixels were assigned their percentage change values (stimulus mean minus control mean) and all other pixels were set to zero. Statistical composite maps were created.

The segmented atlas was cropped and rendered onto 14 slices of 256^2 resolution corresponding to the field of view of the subjects. The cropped atlas served as a segmented composite with coordinates for row, column and slice. A statistical composite was created for each group. A Bonferroni correction factor was used to maintain an overall uncertainty level of 5% for comparisons between groups. The individual analyses were summed within groups. The composite statistics were built using the inverse transformation matrices. Each composite pixel location (ie, row, column, slice), premultiplied by $[T_i]^{-1}$, mapped it within a subject voxel (*i*). A trilinear interpolation of the subject's voxel values (percent change) determined the statistical contribution of the

subject (*i*) to the composite location. The use of $[T_i]^{-1}$ ensured that the full volume set of the composite was populated with subject contributions. The average value from all subjects within the group determined the composite value. Due to the inability to align each subject at a pixel-level resolution, the composite BOLD response maps may result somewhat broader in their spatial coverage than in the individual maps. However, the subjects did align very well at a ROI-level resolution. The number of voxels per ROI and their corresponding average percent change values were statistically evaluated using a non-parametric Neuman-Keuls test ($p < 0.05$).

Results

Cocaine-stimulated brain activation: acute versus repeated (1 versus 2-day treatment)

The total volume of brain activation for each of the four experimental conditions can be viewed as 3D models (**Fig. 4-2**). These 3D volumes of activation are a composite of six subjects each and provide a visual representation comparing the difference in the number of activated voxels across experimental conditions. The volumes of activation shown are parsed into major brain regions, e.g. cortex, hippocampus, thalamus, amygdala (Fig. **4-3**). The cortex reveals similar activity across 1 and 2 Day saline/cocaine and 2 Day SB/cocaine however showed a dramatic decrease in the curcumin treated group. This visual observation is confirmed when the voxel numbers are compared between experimental groups as shown on the left column. The curcumin group has a significantly lower number of voxels activated with cocaine as compared to the SB group ($p<.01$). The hippocampus and the amygdala show the lowest number of activated voxels in the 2

Day saline/cocaine and curcumin groups versus the SB condition ($p<.05$). For the thalamus, the 1 Day saline/cocaine and 2 Day SB/cocaine groups had a significantly higher volume of activation than 2 Day saline/cocaine. In all major brain areas the highest median number of activated voxels occurs in the 2 Day SB/cocaine group.

BOLD activation maps, co-registered on 2-D, of coronal sections for each of the four experimental conditions are shown in **Fig. 4-4**. These activation maps from the four conditions are a composite of six subjects each, fully registered into a 3D rat MRI atlas and segmented for volumes of interest (VOI). An increase in significant BOLD signal intensity changes at least 2% above baseline are evident by the volume of colored shading (red-yellow) illustrates robust activation across much of the cortical mantle with 2 Day SB/cocaine. In comparison, the curcumin treated group revealed much less activation in motor (MO) and somatosensory (SSp) cortices. Further, the accumbens (ACB) revealed comparable activity across all experimental conditions. Interestingly, the dorsal thalamus in the area of anterior thalamic nuclei (AM) and medial dorsal thalamus (MD) showed evidence of high activity following 2 Day SB/cocaine treatment. Lastly, cocaine-induced activation in the cortical nuclei of the amygdala (COA) was observed following 2 Day SB/cocaine treatment, but not under the other conditions.

Brain areas showing a significant difference and opposite response in their BOLD signal between SB and curcumin treatments are listed in **Table 4-1** and include the somatosensory cortex, hippocampus, cortical nuclei of the amygdala, anterior thalamic nuclei, septum, periaqueductal gray and substantia nigra. These eight sites were identified from 93 brain areas by comparing the volume of activation (i.e. number of

voxels) between all four conditions using a non-parametric, Newman-Keuls test for multiple comparisons. Six of these eight sites are presented in **Fig. 4-5** showing bar graphs of their median (minimum – maximum) voxel number together with their change in BOLD signal over time following cocaine injection. In all cases, there was a greater change in BOLD signal over time to cocaine with SB than all other conditions. BOLD signal increases over the first 2-3 min following ICV cocaine and plateaus over the remaining 10 min post-stimulus scanning period.

Modulation of mesocorticolimbic BOLD response by cocaine and histone drug treatments

There was no appreciable difference in BOLD activation in the mesocorticolimbic system between treatment groups, including in the striatum and ventral midbrain (**Fig. 4-6**).

Histone modifying drugs and cerebrovascular reactivity

Summarized in **Fig. 4-7** are the data for the BOLD response to 10% CO_2 30 min after pretreatments with saline, DMSO or histone modifying drugs. At the present dose, SB did not have any significant effect on baseline BOLD contrast in comparison to its corresponding vehicle control (saline). This was observed for the number of activated voxels and percent BOLD signal change. Similarly, curcumin did not increase BOLD signal change in response to CO_2 in comparison to its vehicle control group (DMSO).

Interestingly, DMSO treated animals showed a greater number of activated voxels than saline pretreated animals ($p = 0.02$), suggesting that it might influence baseline cerebrovascular responsivity. Given that there is BOLD increase after curcumin exposure due to its vehicle, the observed modulation of the cocaine-related BOLD response in curcumin-treated animals could be underestimated and curcumin may even more strongly attenuate cocaine-responses than those observed in this study.

Histone modifying drugs on cocaine-stimulated locomotor activity

Rats given SB and cocaine showed a greater amount of movement within the open field cage than any other of the treatment groups (**Fig. 4-8b**). Statistical tests revealed a significant effect of SB treatment on day 1 but not on day 5 ($H_{3,30} = 9.6$ $p = 0.02$ for grouping variable). SB rats showed higher locomotor activity than saline pretreated ($p = 0.02$) and DMSO rats ($p = 0.01$). However, SB-treated rats were not significantly different from the curcumin group ($p = 0.06$). A similar trend, albeit not statistically significant, was observed between SB and curcumin rats on day 5 ($p = 0.06$). There were no significant differences in open field activity between the treatment groups tested before cocaine administration (**Fig. 4-8a**).

Discussion

These studies adopt the notion that addiction is a neuroadaptive response to repeated drug exposure and that the changes in brain neurobiology are a consequence of altered gene expression due to chromatin modifications, specifically histone acetylation. At the onset

we asked the question whether fMRI could be used to identify cocaine-sensitive areas responsive to drugs that interfere with enzymatic acetylation and deacetylation of histones. To this end we tested whether SB, a class I/II HDAC inhibitor, and curcumin a CBP/HAT inhibitor could affect cocaine-induced BOLD signal changes. Our experimental designed followed that published by Kumar and colleagues (Kumar et al., 2005) using a two day cocaine exposure with and without SB. They reported that pretreatment with SB leads to a sensitized locomotor response to cocaine that correlates with striatal histone H3 phosphoacetylation. Based on these findings we predicted SB would enhance cocaine-induced changes in BOLD signal. The corollary to this proposition predicts that curcumin would reduce cocaine-induced changes in BOLD signal. Using a 3D segmented MR atlas we screened 93 brain areas for significant and opposite BOLD signal changes to SB and curcumin and identified eight brain areas that met these critieria (**see Table 4-1**).

As predicted, SB increased BOLD signal in response to cocaine. This effect appeared to be generalized to most brain areas as shown in the 3D models depicting the volume of activation in the whole brain (**Fig. 4-2**) and major brain areas (**Figs. 4-3, 4-4**), however the mesocorticolimbic dopamine system and the striatum revealed surprisingly little difference in BOLD response compared to control rats (**Figs. 4-4, 4-5**). Presumably, cocaine-induced enhancement in BOLD signal is due to compensatory blood flow to metabolically active areas (Stein and Fuller, 1993, Luo et al., 2003, Febo et al., 2004). However, it could be argued that the generalized increase in BOLD signal may be unrelated to cocaine's psychostimulant properties; instead, systemic treatment with SB

caused an increase in cerebral arterial vascular responsivity. However, this is unlikely since CO_2 challenge causes a comparable change in signal intensity and activation profile as vehicle (**Fig. 4-6**). From these preliminary data, the mechanism of SB-enhanced brain activiation response to cocaine remains unclear. Given that SB interferes with the orderly de-acetylation of histones, transcription factors and other molecules (Davie, 2003), the drug could alter the normal chromatin response to repeated cocaine exposure, which at least at some gene loci is associated with suppressed transcription (Kumar et al., 2005). Indeed, the normal BOLD response to repeated cocaine exposure is reduced signal, suggesting the brain is less responsive to this psychostimulant (Febo et al., 2005). Taken together, these findings suggest the brain's initial response to repeated-cocaine exposure triggers a desensitization-like mechanism. By pretreating with SB, this normal desensitization response may be attenuated, resulting in an sustained BOLD signal despite repeated exposure to cocaine, as observed in the present study.

In contrast to SB's effects, curcumin pretreatment decreased the BOLD signal in response to cocaine (relative to SB/cocaine treated animals). However, similar to SB, curcumin appeared to affect most brain areas as shown in the 3D models depicting the volume of activation in the whole brain (**Fig. 4-2**) and major brain areas (**Fig. 4-3**), albeit again the mesocorticolimbic dopamine system and the striatum showed surprisingly little changes (**Figs. 4-4, 4-5**). It is unlikely that this blunted BOLD response to cocaine in the curcumin-treated animals is due to decreased vascular responsivity since CO_2 challenge causes a robust change in signal intensity and activation profile (**Fig. 4-6**). Indeed, the response to CO_2 following pretreatment with curcumin exceeds that observed with saline

vehicle or SB, suggesting that our study would, if anything, underestimate the true inhibition of cocaine-induced brain activation by curcumin. Curcumin targets CPB/p330 which acetylates histones and possibly other chromatin-associated proteins (Balasubramanyam et al., 2004). While curcumin has not yet been tested for its potential role in cocaine-induced behavioral sensitization, the present finding that curcumin pretreatment decreases BOLD signal to cocaine challenge would predict an inhibitory effect on cocaine's reinforcement and addiction behavior. Conversely, if one of the neural characteristics of cocaine sensitization in the rat is a reduced BOLD response with repeated cocaine exposure, then the opposite proposition may be made. In this case, curcumin, by reducing the BOLD response to cocaine may be accelerating the process of cocaine sensitization in the rat. Behavioral experiments should be able to determine this.

In agreement with our previous findings using fMRI in unanesthetized animals, we observed here that repeated cocaine administration resulted in reduced BOLD activation. As with our previous work, a present concern is that the neuroadaptations observed after 2 days of cocaine largely represent tolerance to the acute effects of cocaine and not sensitization per se. We find that there is an overall reduction in BOLD activation in the thalamus with 2 days of cocaine administration and across many brain areas after 7 days of cocaine (Febo et al., 2005). This 'tolerance-like' result is supported by past studies using other in vitro metabolic assays with cellular-level resolution (Hammer and Cooke, 1994). Moreover, Kumar and collegues showed that by day 2 of cocaine treatment at the dose used here produces a increased locomotor activity with subsequent exposure, a trait reflecting sensitization and not tolerance (Kumar et al.,

2005). Thus, reduced BOLD activation with repeated cocaine may be an underlying neural trait of sensitization in male rats, however further experiments will be needed to rule out the impact of decreases in inhibitory synaptic activity.

Many of the areas that show a cocaine-induced significant and opposite BOLD signal change in the presence of SB and curcumin play significant roles in learning, memory (CA3 and dentate gyrus of the hippocampus, anterior nucleus of the thalamus) and social recognition (central nucleus of the amygdala, septum), a finding that may provide evidence supporting a role for chromatin remodeling in cocaine-induced cognitive changes (Browman et al., 1998, Levenson et al., 2004). These same areas also form an integrated neural circuit. Lesions of the anterior thalamic nuclei disrupt recall of spatial (Mitchell et al., 2002) as well as nonspatial odorant memory (Wolff et al., 2006) and lead to reduced Fos-like expression ('hypoactivity') in the hippocampal formation (Jenkins et al., 2002). Rats trained on a fear-conditioning paradigm showed increased acetylation of H3 but not H4 histones on the CA1 subfield of the hippocampus (Levenson et al., 2004). Treatment with HDACi, including SB and trichostatin A enhanced the consolidation of conditioned freezing responses, long-term potentiation in CA1 pyramidal neurons of hippocampal slice preparations and other memory functions (Alarcon et al., 2004, Korzus et al., 2004, Levenson et al., 2004). Sodium butyrate also enhances cocaine sensitization and conditioned place preference (Kumar et al., 2005). A case can therefore be made that during the initial exposure to cocaine, chromatin alterations occur in specific brain circuitry to enhance associative learning and memory. However, this remains to be tested experimentally. With regards to the somatosensory

cortex it is unclear what the role of cocaine-associated chromatin modifications with this region may be, however it has been shown to have a significant degree of synaptic plasticity in response to cocaine administration in the rat (Drouin and Waterhouse, 2004) and in the case of the amygdala, to play an important role in social and olfactory memory (Ferguson et al., 2001, Keller et al., 2004).

At the onset of these studies we anticipated that the mesocorticolimbic dopaminergic system would be most affected by cocaine challenge in the face of SB and curcumin pretreatments. However, this was not the case, indeed there was a conspicuous absence of any distinct activation profile in the reward circuitry to chromatin modifying drugs as shown in **Fig 4-5**. Conventional wisdom points to these dopamine enriched regions as the initial targets for cocaine and its ensuing molecular alterations leading to addiction, however it may be that chromatin remodeling in the hippocampal formation and associated memory circuits play greater roles than originally anticipated. Indeed, electrical stimulation of the ventral subiculum at a specific frequency reinstates cocaine self-administration (Vorel et al., 2001) and inhibiting with lidocaine microinjections in this region reduced reinstated cocaine seeking behavior (Sun and Rebec, 2003). Excitatory synaptic projections from the ventral hippocampus to the ventral tegmental area regulate the release of dopamine in other areas of the brain such as the nucleus accumbens and medial prefrontal cortex (Legault et al., 2000). These physiological roles of the hippocampus in long-term responding to cocaine could arise from progressive alterations in nucleosome structure by chromatin modifications. However, the role of hippocampal subregions in cocaine-sensitization needs to be further explored.

It is important to mention several caveats of the present experimental design. First, in order to avoid the peripheral cardiovascular stimulating actions of cocaine we administered the drug at a low ICV dose whereas other studies such as Kumar et al. measured behavior in response to 15 mg/kg. The low dose and direct central administration of the drug may have resulted in less activation of regions of the brain classically involved in cocaine's mechanism of action. And it may have also resulted in an underestimation of SB and curcumin's effects on these regions (eg, the dorsal striatum, nucleus accumbens). As explained in previous studies, the chosen dose and route of administration minimizes the autonomic of cocaine during imaging. Another potential caveat was observed from the use of the 80% DMSO vehicle, which resulted in increased CO_2 stimulated BOLD signal changes. There are reports of 20% increases in cerebral blood flow with high doses of DMSO (Kassell et al., 1983) and increases in blood oxygen tension in ischemic skin tissue extracts (Myers and Donovan, 1975). These unbeknownst actions of DMSO may have contributed to elevation of the 'mock' BOLD response to CO_2.

However, the present results are important in that they are the first attempt to tie functional changes at the global nervous system level using functional MRI in rats to molecular and chromatin-related "epigenetic" level changes. Unexpectedly, brain areas commonly associated with learning, memory, motivation and social recognition showed the most robust brain activation changes in our paradigms. Therefore, it is possible that dopamine-regulated chromatin remodeling mechanisms, in addition to their effects on striatal gene expression (Li et al., 2004, Kumar et al., 2005), regulate cocaine-associated

plasticity in widespread brain regions. Furthermore, based on the present results, we predict that curcumin and other HAT inhibitors could emerge as a promising class of anti-substance abuse drugs that warrant further exploration in experimental animal models of addiction.

Acknowledgments: The authors wish to thank Ms. Tara L. Messenger-Stolberg and Ms. Jessica Shields for their excellent technical assistance throughout the course of the study. This work was supported by NIH National Institute on Drug Abuse grants to Craig F. Ferris (R01 DA13517), Marcelo Febo (R01 DA019946) and Schahram Akbarian (R01 DA017660).

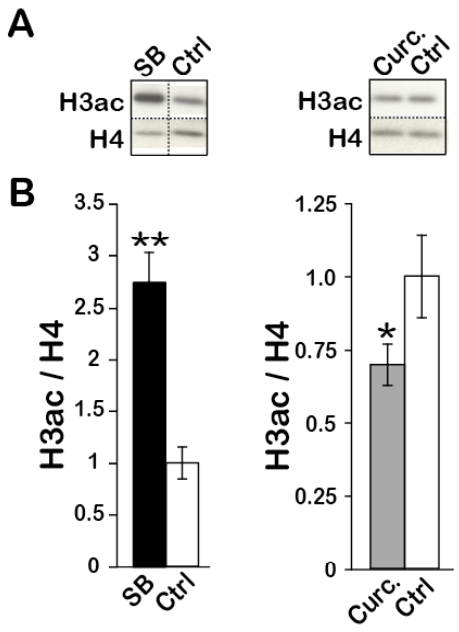

Figure 4-1. Histone H3 acetylation after HATi and HDACi treatment. (A) Immunoblots from neuronal cultures treated (left) with or without the HDAC inhibitor, sodium butyrate (SB, 5mM, 48hrs) or (right) with or without the HAT inhibitor, curcumin (Curc., 1uM, 4days). Membranes were probed with anti-acetyl-histone H3 (H3ac, upper panels) or anti-histone H4 as loading control (H4, lower panels). (B) Densitometric quantifications (mean +/- S.E.M.) of H3ac normalized to H4. Notice (left) SB-induced >2.5 fold increase in H3ac compared to untreated control cells. (n=3/group,**, $F(1,4)=30.83$, $p=0.005$, one-way ANOVA). Notice also that (right) curcumin treatment caused a decrease of H3ac to <75% of control group levels. (n=10/group, *, $F(1,18)=4.483$, $p=0.048$, one-way ANOVA).

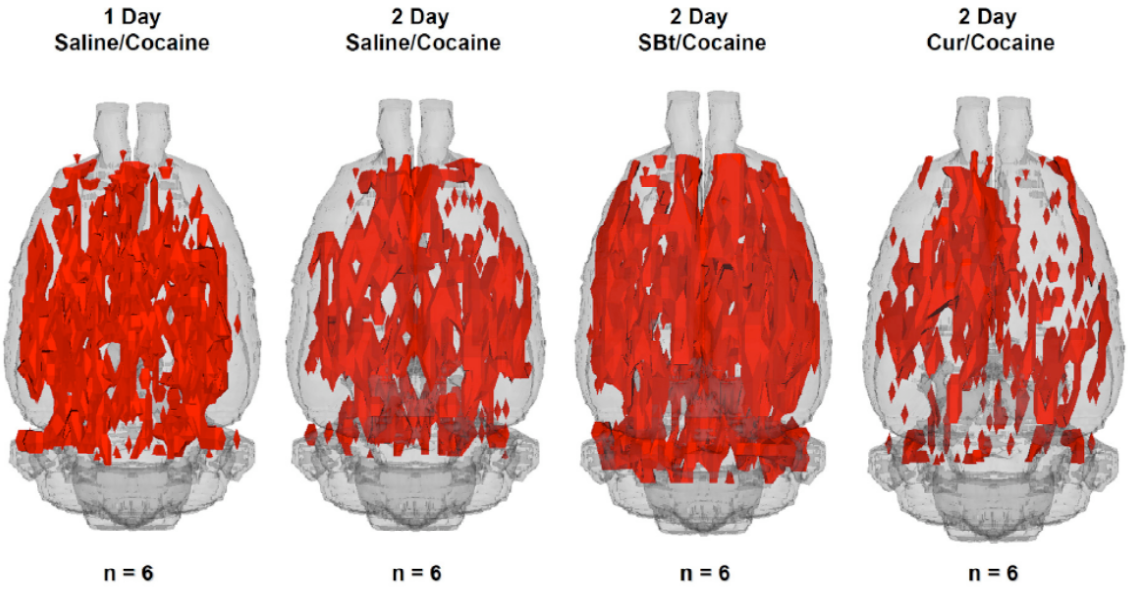

Figure 4-2. 3D maps highlighting the volume of brain activation for each of the conditions: 1 day cocaine treatment, 2 day cocaine, 2 day cocaine and sodium butyrate pretreatment (SB) or 2 day cocaine with curcmin (Curc) pretreatment.

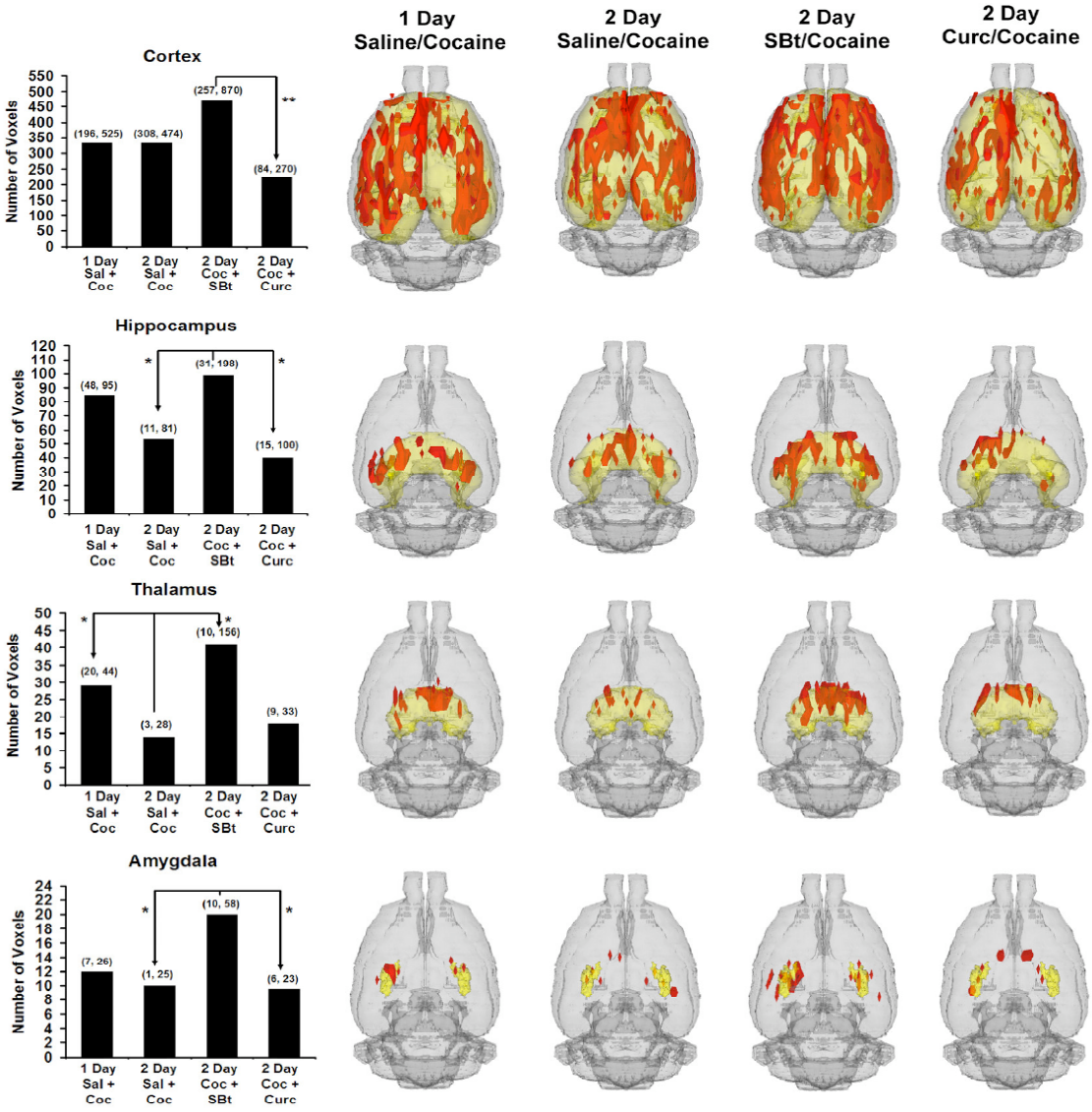

Figure 4-3. Number of voxels responsive to cocaine treatment for each condition. Treatment groups are: 1 or 2-day cocaine treatment and 2-day treatment in the presence of either SB or Curc. Three-dimensional atlas maps on the right present a pictorial view of the volume of activation per each region of interest presented in the bar graphs to the left. Hue indicates relative BOLD activity from yellow (low) to red (high). Data for voxel activations presented as median with minimum-maximum values in parenthesis over the corresponding bar graphs. Asterisks indicate significant differences for multiple comparisons using a non-parametric Neuman-Keuls test (*$p < 0.05$, **$p < 0.01$).

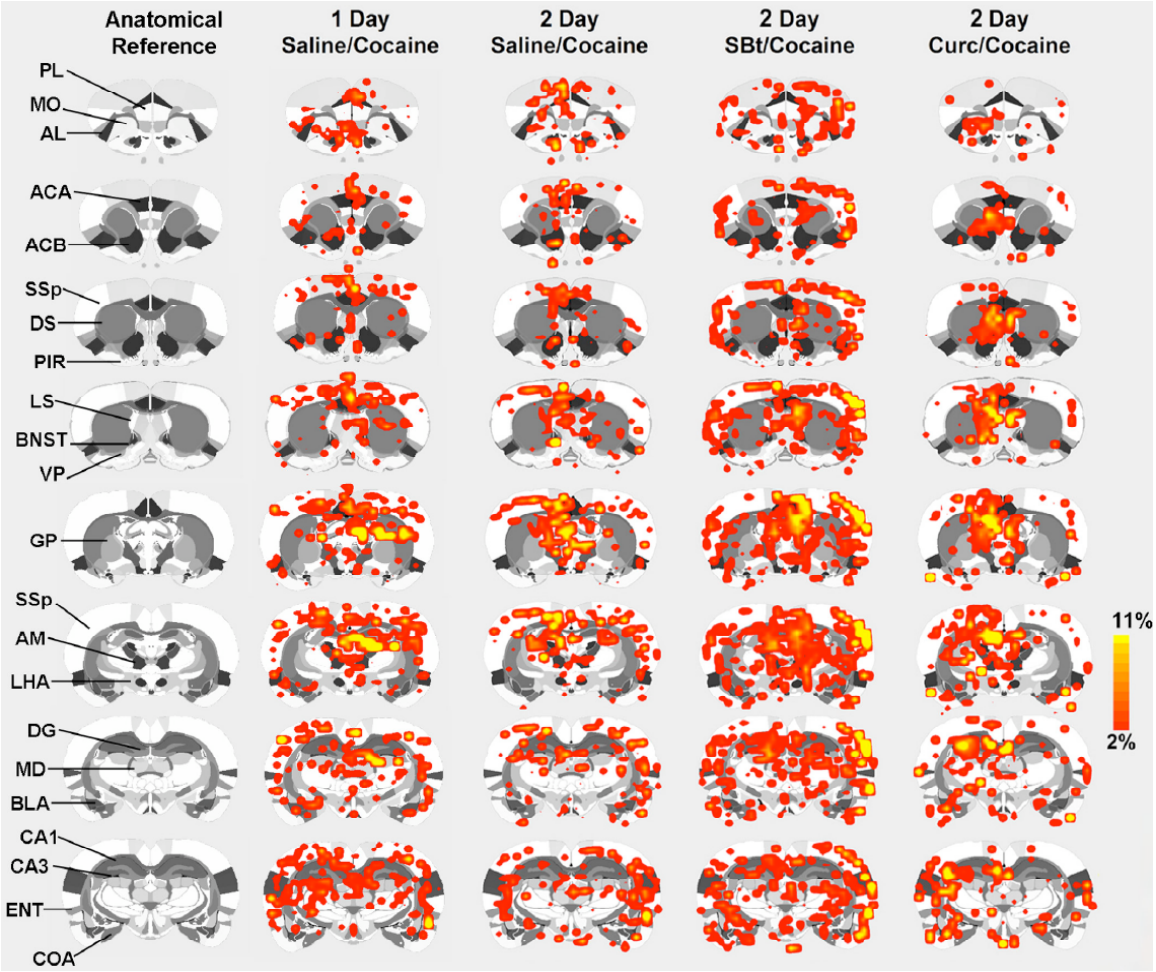

Figure 4-4. BOLD signal changes in response to cocaine in rats pretreated with vehicle or a histone-modifying drug. 2D rat atlas maps segmented into various regions of interest (abbreviated on the left). Colored areas correspond to brain regions that showed statistically significant increases in BOLD signal intensity with cocaine administration ($p < 0.05$, corrected for multiple *t*-tests). Scale bar hue on the right indicates percent increase in BOLD (thresholded between 2-11%). *Abbreviations:* PL, prelimbic area; MO, medial orbital area; AL, agranular insula; ACA, anterior cingulate; ACB, accumbens; SSp, somatosensory cortex; DS, dorsal striatum; PIR, piriform cortex; LS, lateral septum; BNST, bed nucleus of stria sterminalis; VP, ventral pallidum; GP, globus pallidus; AM, anteromedial thalamus; LHA, lateral hypothalamic area; DG, dentate gyrus; MD, mediodorsal thalamus; BLA, basolateral amygdala; CA1, CA3, subfields of the hippocampus; ENT, entorhinal cortex; COA, central amygdala.

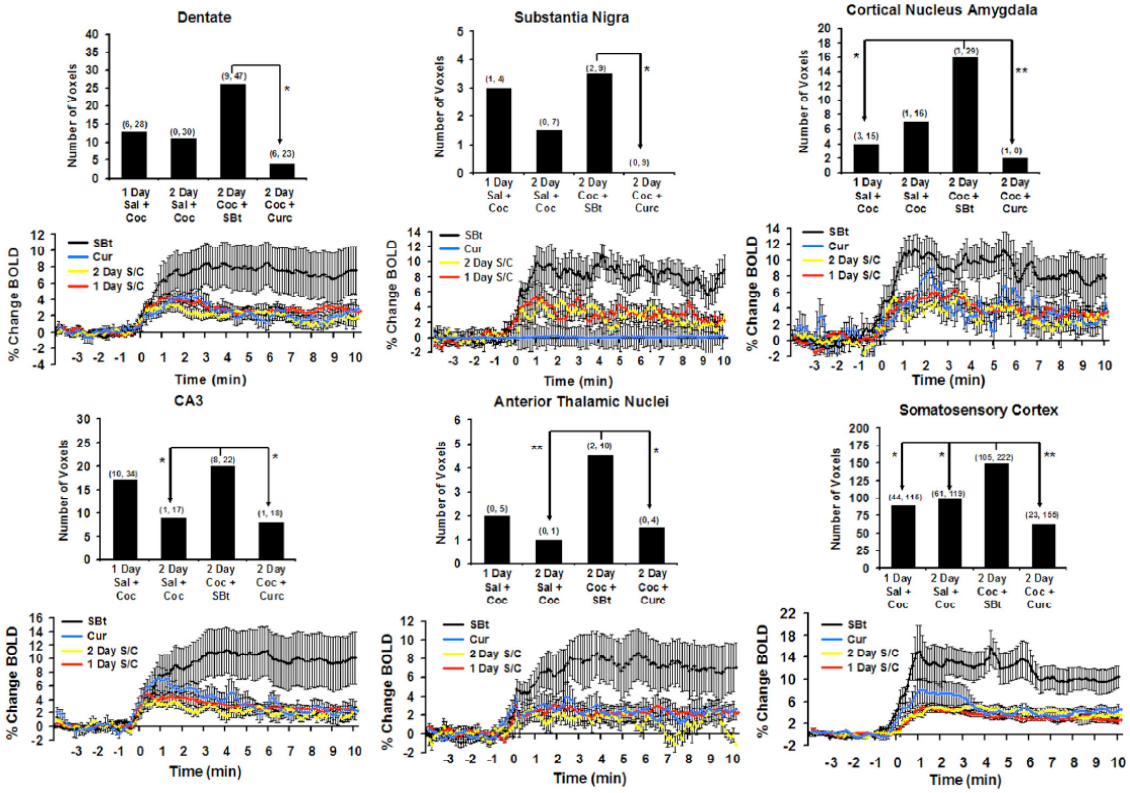

Figure 4-5. Number of voxels responsive to cocaine treatment and percent change in the BOLD signal over time for each condition. Treatment groups are: 1 or 2-day cocaine treatment and 2-day treatment in the presence of either SB or Curc. Data for voxel activations presented as median and minimum-maximum values in parenthesis. Timecourse plots for the activated voxels are shown under each corresponding bar graph. Cocaine was administered ICV at time 0. Asterisks indicate significant differences for multiple comparisons using a non-parametric Neuman-Keuls test (*$p < 0.05$, **$p < 0.01$). Data for percent changes over time presented as mean ± standard error of the mean.

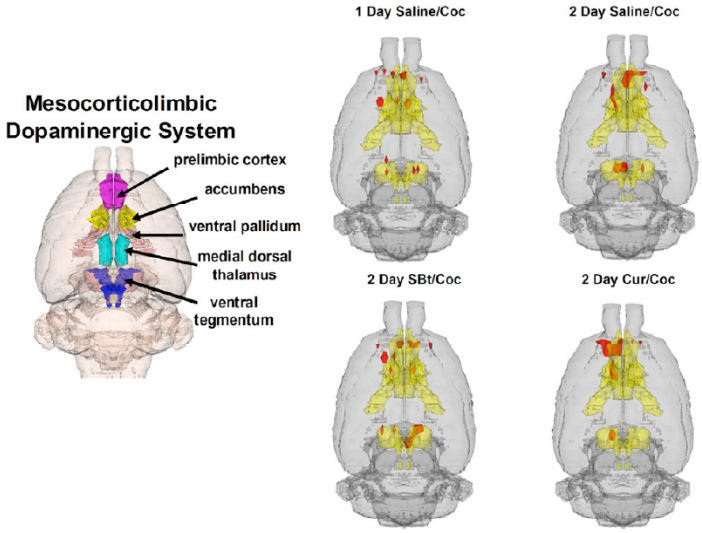

Figure 4-6. Three-dimensional atlas maps showing cocaine-induced voxel activations in the mesocorticolimbic system for treatment conditions as presented in figures 4-2 and 4-3.

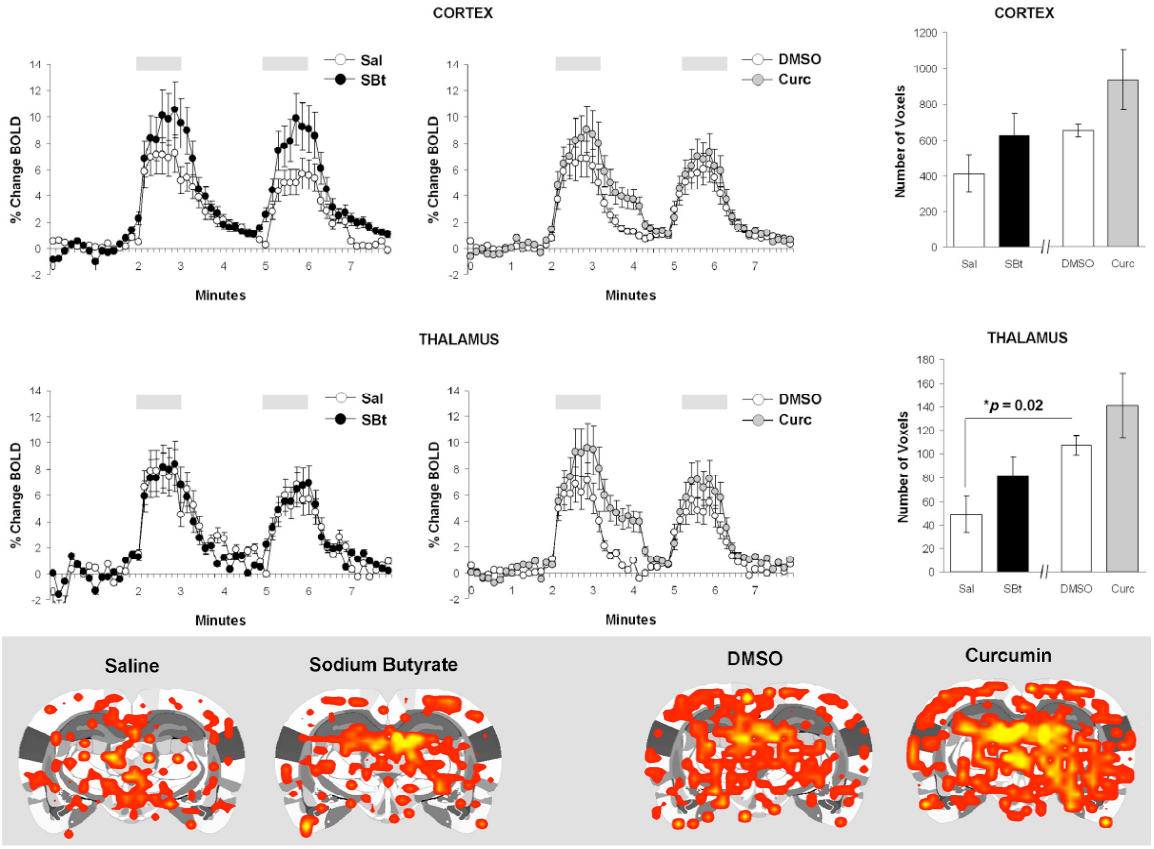

Figure 4-7. BOLD response to 10% carbon dioxide challenge in rats pretreated with saline, DMSO, sodium butyrate or curcumin 30 mins before functional imaging. Percent BOLD signal change (top left) or volume of activation (top right) are presented as mean ± standard error of the mean. Gray horizontal bars above timecourse plots denote the time when the CO_2 pulses were given. Below are 2D composite atlas maps showing global BOLD response to CO_2 for each condition. Asterisks indicate significant differences between vehicle groups for the number of activated voxels in the thalamus (*p = 0.2, *t*-test).

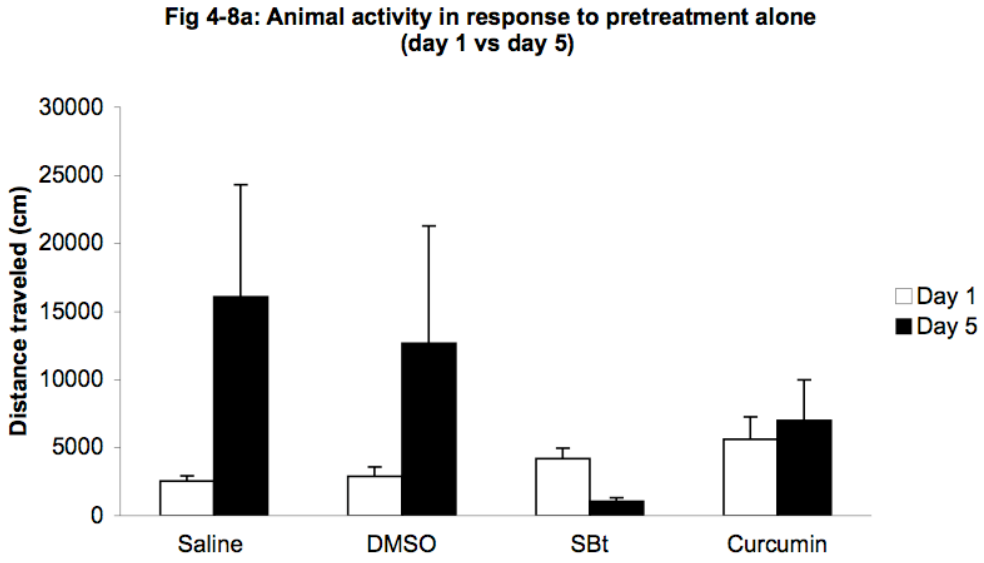

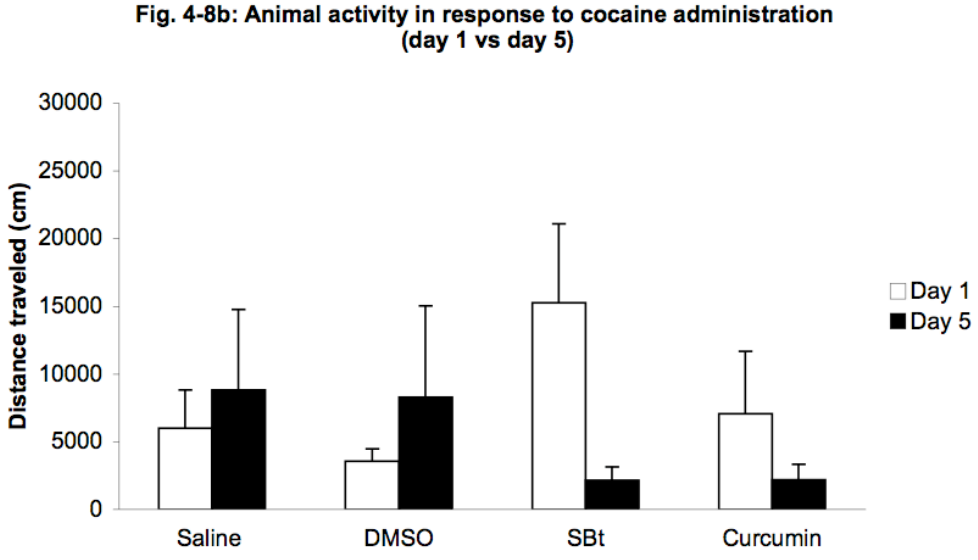

Figure 4-8. Open field locomotor activity during pretreatment with histone modifying drug or vehicle (A) and after cocaine administration (B). Measurements were taken during acute (day 1) treatment and following repeated administration (day 5). Asterisk denotes statistical differences ($p < 0.05$).

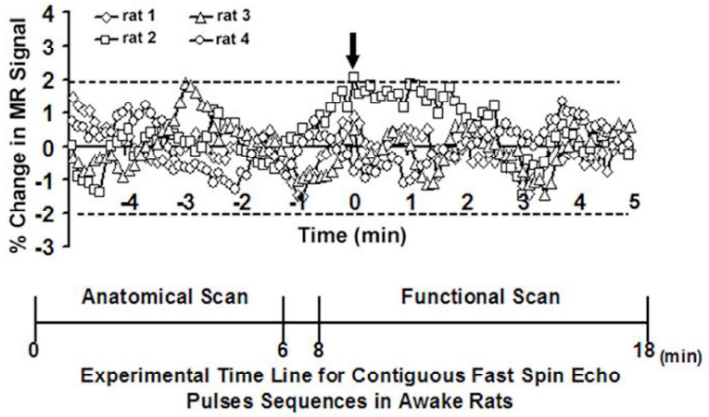

Supplemental Figure 4-1. Control imaging study to assess whether there are BOLD signal changes in the absence of any stimulus. The occurrence of false positive voxels is a concern particularly in the simple off-on activation paradigm used in these studies comparing the average baseline signal for a given voxel to its average post-stimulation signal. To control for this issue, awake rats (n = 4) were exposed to an 18 min long imaging protocol mimicking that described above for the fMRI studies. A 6 min long high resolution anatomical scan was followed 2 min later by a 10 min long fMRI time series. During the fMRI time series there was no stimulus presentation. Voxels were statistically compared before and after the arrow mark for signal intensity changes using a t-test (α=0.05, corrected for multiple comparisons). The change in MR signal over the 10 min period mimicking the fMRI study without the presentation of a stimulus did not differ by more that 2% for any of the four animals studied.

Volume of Interest	1 Day Saline/Coc	2 Day Saline/Coc	2 Day SB/Coc	2 Day Curc/Coc
somatosensory cortex	90 (44,115)*	98 (61,119)*	149 (105,222)	63 (23,151)**
CA3 hippocampus	17 (10,34)	9 (1,17)*	20 (8,22)	8 (1,18)*
dentate gyrus	13 (6,28)	11 (0,30)	26 (9,47)	3.5 (3,19)*
cortical nucl. amygdala	4 (3,15)*	7 (1,16)	15.5 (3,29)	2 (1,8)**
septum	8 (2,14)	6 (0,10)*	14.5 (7,23)	7.5 (3,12)*
periaqueductal gray	3 (1,12)	3 (0,8)	5 (0,21)	0.5 (0,7)*
anterior nucl. thalamus	2 (0,5)	1 (0,1)*	4.5 (0,3)	1.5 (0,4)*
substantia nigra	3 (1,4)	1.5 (0,7)	3.5 (2,9)	0 (0,9)*

Table 4-1. Activated voxels in regions of interest of rats treated with chromatin modifying drugs or vehicle prior to cocaine. Data representing voxel activations presented as median with minimum-maximum values in parenthesis. Asterisks indicate significant differences for multiple comparisons using a non-parametric Neuman-Keuls test (*$p < 0.05$, **$p < 0.01$). Specific comparisons between the treatment groups are shown in Figs. 4-3 and 4-5. Differences in septum and periaqueductal gray are in comparison to 2 Day SB/Coc.

CHAPTER V:

Comprehensive Discussion

Transcriptional components underlying the cause of depression, drug addiction and their therapies have been recognized for many years. Indeed, the success of these treatments, albeit limited, highlights the incredible, plastic nature of the cellular and molecular systems within the brain. However, given the high proportion of patients unresponsive to treatment, and the physical, emotional and financial strains associated with depression and substance abuse, there is a great need to develop effective, mechanism-based treatments.

Impact of Findings

This study provides evidence that systemic administration of chromatin modifying drugs dramatically alters an animal's response, on a behavioral and molecular level, to environmental- and stimulant drug-induced changes. Specifically, we have shown in three independent studies featuring antidepressant and stimulant drugs that co-administration with the class I/II HDACi, sodium butyrate, augments their effects in comparison to single-drug treatment.

In Chapter II, I wanted to test the effects of SB in an animal model of depression – that doses sufficient to induce bulk histone acetylation would be associated with an antidepressant-like behavioral and molecular response. This hypothesis included a proposal to address the cooperative effects of SB with the selective serotonin reuptake inhibitor, fluoxetine as combination therapy is an established clinical tool, particularly in cases of resistant forms of depression. Our work illustrated the potential for the HDACi,

sodium butyrate (SB), to augment the effects of the clinical antidepressant, fluoxetine, in an animal model of behavioral despair. Morever, these changes were associated with increases in acetylation of bulk chromatin and increased mRNA levels of brain derived neurotrophic factor (BDNF) in the frontal cortex. Given the implications of increased corticolimbic BDNF expression by the neurotrophic hypothesis, these data represent potential for a new direction in antidepressant therapies.

In Chapters III and IV, we provided evidence using a broad range of techniques that systemic administration of drugs known to affect histone modfication and transcription markedly affected cocaine response in rodents. Sensitization of the dopaminergic system by extended treatment with SB and the full D_1-agonist, SKF82958 (SB+SKF) resulted in a dramatic increase in stimulant and reward behavior in response to subsequent cocaine challenge. Moreover, combined administration of SB with SKF was associated with changes in chromatin modification and gene expression in ventral midbrain and striatum, key regions in dopaminergic transmission putatively involved in stimulant-induced reward (Chapter III). Further, imaging results presented in Chapter IV showed brain metabolic responses that were differentially regulated in paradigms combining treatment of cocaine with inhibitors of HDAC (sodium butyrate) or HAT (curcumin). Given that SB/stimulant co-administration resulted in activating effects on behavior and brain metabolic response across these two studies at brain regions involved in the reward circuitry (including striatum and hippocampus) and that activation of the BOLD signal by repeated cocaine treatment was attenuated with HATi co-treatment

provides exciting promise for the design of future studies addressing stimulant drug mechanism and treatment.

Alternative explanations

Together, this collective work supports our general hypothesis that histone modification has a role in the mechanisms underlying the actions of antidepressant and stimulant drugs. However, it is clear that sodium butyrate, albeit a non-specific HDACi, has pleiotropic effects whose mechanism in our experimental paradigms remains largely unclear. Indeed, recent evidence has shown that butyrate exerts its effects via three mechanims; i) inhibition of histone deacetylation, including related facilitation of higher-order chromatin structure ii) induction of *cis*- and *trans*-acting butyrate-dependent transcription factors for selected genes (via acetylation or physical interaction) and iii) regulating expression of genes involved in post-transcriptional mRNA stability (Parab et al., 2007). Moreover, the association of sodium butyrate with bidirectional changes in gene expression has been recently extended in a report showing rapid, dynamic effects on promoter-region histone acetylation *in vitro* (Rada-Iglesias et al., 2007).

Our results in Chapter II on the kinetics of *in vivo* sodium butyrate-induced histone hyperacetylation correspond with these *in vitro* results (Rada-Iglesias et al., 2007). We report that SB administration is sufficient to increase bulk levels of histone acetylation in mouse hippocampus and liver, with peak levels of acetylation reached 30min after injection, and returned to baseline at 60min post-injection (figure 2-2). This general increase in histone acetylation after less than 30min of SB treatment was recapitulated *in vitro* by Rada-Iglesias and colleagues, though interestingly, their data

also suggest that the profile of histone acetylation over 2-18hours is differentially regulated on a gene-specific basis (Rada-Iglesias et al., 2007). These comparisons should be considered carefully as the impact of histone tail modification is known to be dependent on the context in which the histone tail 'code' is read – specifically that critical factors for unique cellular 'interpretation' of the code may not be present in an *in vitro* system. Thus, future experiments would be needed to accurately determine the butyrate-induced acetylation kinetics of our plasticity associated genes of interest, including BDNF. These emerging data, particularly those illustrating the dynamic transcriptional effects following HDACi administration, may also help to explain why the antidepressant-like behaviroal responses we observed following HDACi treatment, both behavioral and molecular (Chapter II), could be similarly reported by a researchers administering the HATi, curcumin (Xu et al., 2005, Xu et al., 2006, Xu et al., 2007).

Moreover, the muliple mechanisms attributed to the action of sodium butyrate provide additional explanation for the effects we observed following *in vivo* treatment of sodium butyrate. As reported in chapter III, we observed increases in mRNA levels of the catecholamine biosynthesis enzymes, tyrosine hydroxylase (TH) following combined treatment of sodium butyrate and SKF. Yet, chromatin immunoprecipitation studies revealed no recognizable pattern of open-chromatin-associated histone acetylation for histone H3 or H4 at the TH promoter region. Interestingly, a recent report has revealed that a butyrate-dependent cis-element within the TH promoter region directly regulates transcription (Patel et al., 2005). Moreover, the effects of butyrate on TH may be mediated indirectly via altering expression and binding of the TH-transcription factor DJ-

1 as this factor was shown elevate expression of the dopamine transporter (DAT) (Manning-Bog et al., 2007), potentially altering the relative dopaminergic signaling capacity of the brain without a concomitant increase in TH mRNA or activity (Goldberg et al., 2005). We plan to test this hypothesis directly by addressing a similar set of SB/stimulant experiments in mice deficient for DJ-1; if the enhancing effects of SB on stimulant-induced behavior (Chapter III) are mediated via TH, mice deficient for DJ-1 will reveal a comparatively attenuated response. As such, our colony of DJ-1 deficient mice, a generous gift from Dr. Jie Shen, is currently under expansion.

Furthermore, increased levels of TH mRNA may have been observed via butyrate-mediated increases in post-transcriptional stability of TH mRNA; that increased mRNA levels may represent an accumulated of transcript. To a similar end, a recent report has shown dramatic regulatory effects of HDACi treatment on the expression of microRNAs (miRNA), short, noncoding RNAs that direct mRNA degradation (Scott et al., 2006). Indeed, although we found no correlative treatment-associated difference in the ventral midbrain expression of select miRNAs predicted to target TH (preliminary, unpublished experiments), the possibility for changes in an unexamined miRNA or miRNA impact on a secondary TH effector-molecules cannot be ruled out.

Closing Remarks

Finally, it is clear that future experiments will be needed to detail the extended mechanisms of sodium butyrate on histone modification, transcriptional regulation and gene expression. The results outlined above highlight an HDACi that is by now, very close to my heart. Further, a now-growing record of publications, including those under my own surname, provide evidence that the impact of systemic treatment with histone-modifying drugs, including as sodium butyrate, are sufficient to induce dramatic, potentially efficacious effects on a behavioral and molecular level in the context of depression and stimulant drug abuse. Moreover, the effects of co-administration with antidepressant and stimulant drugs are particularly exciting in the context of experimental pharmacology and the development of novel treatment paradigms. However, considering the broad-action, high relative dosing (mM range) and known pleiotropic effects of sodium butyrate, it is my opinion that this drug will likely remain a *model* for examining more specific, novel HDAC inhibitors in the context of a variety of neuropsychiatric diseases before generic endorsements for this natural compound are given.

REFERENCES

Akbarian, S., 2003. The neurobiology of Rett syndrome. Neuroscientist. 9, 57-63.

Alarcon, J. M., Malleret, G., Touzani, K., Vronskaya, S., Ishii, S., Kandel, E. R. and Barco, A., 2004. Chromatin acetylation, memory, and LTP are impaired in CBP+/- mice: a model for the cognitive deficit in Rubinstein-Taybi syndrome and its amelioration. Neuron. 42, 947-959.

Alleweireldt, A. T., Weber, S. M., Kirschner, K. F., Bullock, B. L. and Neisewander, J. L., 2002. Blockade or stimulation of D1 dopamine receptors attenuates cue reinstatement of extinguished cocaine-seeking behavior in rats. Psychopharmacology (Berl). 159, 284-293.

Allfrey, V. G., Pogo, B. G., Littau, V. C., Gershey, E. L. and Mirsky, A. E., 1968. Histone acetylation in insect chromosomes. Science. 159, 314-316.

Altar, C. A., 1999. Neurotrophins and depression. Trends Pharmacol Sci. 20, 59-61.

Altar, C. A., Whitehead, R. E., Chen, R., Wortwein, G. and Madsen, T. M., 2003. Effects of electroconvulsive seizures and antidepressant drugs on brain-derived neurotrophic factor protein in rat brain. Biol Psychiatry. 54, 703-709.

Amann, B., Grunze, H., Vieta, E. and Trimble, M., 2007. Antiepileptic drugs and mood stability. Clin EEG Neurosci. 38, 116-123.

Amir, R. E., Van den Veyver, I. B., Wan, M., Tran, C. Q., Francke, U. and Zoghbi, H. Y., 1999. Rett syndrome is caused by mutations in X-linked MECP2, encoding methyl-CpG-binding protein 2. Nat Genet. 23, 185-188.

Anderson, S. M., Bari, A. A. and Pierce, R. C., 2003. Administration of the D1-like dopamine receptor antagonist SCH-23390 into the medial nucleus accumbens shell attenuates cocaine priming-induced reinstatement of drug-seeking behavior in rats. Psychopharmacology (Berl). 168, 132-138.

Angelucci, F., Aloe, L., Jimenez-Vasquez, P. and Mathe, A. A., 2002. Electroconvulsive stimuli alter the regional concentrations of nerve growth factor, brain-derived neurotrophic factor, and glial cell line-derived neurotrophic factor in adult rat brain. J Ect. 18, 138-143.

Baker, S. A., Stanford, L. E., Brown, R. E. and Hagg, T., 2005. Maturation but not survival of dopaminergic nigrostriatal neurons is affected in developing and aging BDNF-deficient mice. Brain Res. 1039, 177-188.

Balasubramanyam, K., Varier, R. A., Altaf, M., Swaminathan, V., Siddappa, N. B., Ranga, U. and Kundu, T. K., 2004. Curcumin, a novel p300/CREB-binding protein-specific inhibitor of acetyltransferase, represses the acetylation of histone/nonhistone proteins and histone acetyltransferase-dependent chromatin transcription. J Biol Chem. 279, 51163-51171.

Belin, D., Deroche-Gamonet, V. and Jaber, M., 2007. Cocaine-induced sensitization is associated with altered dynamics of transcriptional responses of the dopamine transporter, tyrosine hydroxylase, and dopamine D2 receptors in C57Bl/6J mice. Psychopharmacology (Berl). 193, 567-578.

Berke, J. D., Paletzki, R. F., Aronson, G. J., Hyman, S. E. and Gerfen, C. R., 1998. A complex program of striatal gene expression induced by dopaminergic stimulation. J Neurosci. 18, 5301-5310.

Berton, O., McClung, C. A., Dileone, R. J., Krishnan, V., Renthal, W., Russo, S. J., Graham, D., Tsankova, N. M., Bolanos, C. A., Rios, M., Monteggia, L. M., Self, D. W. and Nestler, E. J., 2006. Essential role of BDNF in the mesolimbic dopamine pathway in social defeat stress. Science. 311, 864-868.

Berton, O. and Nestler, E. J., 2006. New approaches to antidepressant drug discovery: beyond monoamines. Nat Rev Neurosci. 7, 137-151.

Black, J. C., Choi, J. E., Lombardo, S. R. and Carey, M., 2006a. A mechanism for coordinating chromatin modification and preinitiation complex assembly. Mol Cell. 23, 809-818.

Black, Y. D., Maclaren, F. R., Naydenov, A. V., Carlezon, W. A., Jr., Baxter, M. G. and Konradi, C., 2006b. Altered attention and prefrontal cortex gene expression in rats after binge-like exposure to cocaine during adolescence. J Neurosci. 26, 9656-9665.

Bockting, C. L., ten Doesschate, M. C., Spijker, J., Spinhoven, P., Koeter, M. W. and Schene, A. H., 2008. Continuation and maintenance use of antidepressants in recurrent depression. Psychother Psychosom. 77, 17-26.

Brami-Cherrier, K., Valjent, E., Herve, D., Darragh, J., Corvol, J. C., Pages, C., Arthur, S. J., Girault, J. A. and Caboche, J., 2005. Parsing molecular and behavioral effects of cocaine in mitogen- and stress-activated protein kinase-1-deficient mice. J Neurosci. 25, 11444-11454.

Branchi, I., D'Andrea, I., Fiore, M., Di Fausto, V., Aloe, L. and Alleva, E., 2006. Early Social Enrichment Shapes Social Behavior and Nerve Growth Factor and Brain-Derived Neurotrophic Factor Levels in the Adult Mouse Brain. Biol Psychiatry.

Bredy, T. W., Wu, H., Crego, C., Zellhoefer, J., Sun, Y. E. and Barad, M., 2007. Histone modifications around individual BDNF gene promoters in prefrontal cortex are associated with extinction of conditioned fear. Learn Mem. 14, 268-276.

Brevard, M. E., Duong, T. Q., King, J. A. and Ferris, C. F., 2003. Changes in MRI signal intensity during hypercapnic challenge under conscious and anesthetized conditions. Magn Reson Imaging. 21, 995-1001.

Browman, K. E., Badiani, A. and Robinson, T. E., 1998. The influence of environment on the induction of sensitization to the psychomotor activating effects of intravenous cocaine in rats is dose-dependent. Psychopharmacology (Berl). 137, 90-98.

Brown, C. E., Lechner, T., Howe, L. and Workman, J. L., 2000. The many HATs of transcription coactivators. Trends Biochem Sci. 25, 15-19.

Butler, R. and Bates, G. P., 2006. Histone deacetylase inhibitors as therapeutics for polyglutamine disorders. Nat Rev Neurosci. 7, 784-796.

Caine, S. B., Negus, S. S. and Mello, N. K., 2000. Effects of dopamine D(1-like) and D(2-like) agonists on cocaine self-administration in rhesus monkeys: rapid assessment of cocaine dose-effect functions. Psychopharmacology (Berl). 148, 41-51.

Caine, S. B., Negus, S. S., Mello, N. K. and Bergman, J., 1999. Effects of dopamine D(1-like) and D(2-like) agonists in rats that self-administer cocaine. J Pharmacol Exp Ther. 291, 353-360.

Caldarone, B. J., Karthigeyan, K., Harrist, A., Hunsberger, J. G., Wittmack, E., King, S. L., Jatlow, P. and Picciotto, M. R., 2003. Sex differences in response to oral amitriptyline in three animal models of depression in C57BL/6J mice. Psychopharmacology (Berl). 170, 94-101.

Canales, J. J. and Graybiel, A. M., 2000. Patterns of gene expression and behavior induced by chronic dopamine treatments. Ann Neurol. 47, S53-59.

Carlezon, W. A., Jr., Duman, R. S. and Nestler, E. J., 2005. The many faces of CREB. Trends Neurosci. 28, 436-445.

Cassel, S., Carouge, D., Gensburger, C., Anglard, P., Burgun, C., Dietrich, J. B., Aunis, D. and Zwiller, J., 2006. Fluoxetine and cocaine induce the epigenetic factors MeCP2 and MBD1 in adult rat brain. Mol Pharmacol. 70, 487-492.

Chan, J. P., Unger, T. J., Byrnes, J. and Rios, M., 2006. Examination of behavioral deficits triggered by targeting Bdnf in fetal or postnatal brains of mice. Neuroscience. 142, 49-58.

Chandramohan, Y., Droste, S. K. and Reul, J. M., 2007. Novelty stress induces phospho-acetylation of histone H3 in rat dentate gyrus granule neurons through coincident signalling via the N-methyl-D-aspartate receptor and the glucocorticoid receptor: relevance for c-fos induction. J Neurochem. 101, 815-828.

Chausmer, A. L. and Katz, J. L., 2002. Comparison of interactions of D1-like agonists, SKF 81297, SKF 82958 and A-77636, with cocaine: locomotor activity and drug discrimination studies in rodents. Psychopharmacology (Berl). 159, 145-153.

Chen, B. and Cepko, C. L., 2007. Requirement of histone deacetylase activity for the expression of critical photoreceptor genes. BMC Dev Biol. 7, 78.

Chen, B., Dowlatshahi, D., MacQueen, G. M., Wang, J. F. and Young, L. T., 2001. Increased hippocampal BDNF immunoreactivity in subjects treated with antidepressant medication. Biol Psychiatry. 50, 260-265.

Chen, P. S., Peng, G. S., Li, G., Yang, S., Wu, X., Wang, C. C., Wilson, B., Lu, R. B., Gean, P. W., Chuang, D. M. and Hong, J. S., 2006. Valproate protects dopaminergic neurons in midbrain neuron/glia cultures by stimulating the release of neurotrophic factors from astrocytes. Mol Psychiatry. 11, 1116-1125.

Cherry, D. K., 2007. National Ambulatory Medical Care Survey: 2005 Summary. In: Advance Data From Vital and Health Statistics). no. 387, pp. 40. National Center for Health Statistics, Hyattsville, MD.

Chwang, W. B., Arthur, J. S., Schumacher, A. and Sweatt, J. D., 2007. The nuclear kinase mitogen- and stress-activated protein kinase 1 regulates hippocampal chromatin remodeling in memory formation. J Neurosci. 27, 12732-12742.

Ciechanowski, P. S., Katon, W. J. and Russo, J. E., 2000. Depression and diabetes: impact of depressive symptoms on adherence, function, and costs. Arch Intern Med. 160, 3278-3285.

Cohen, E. R., Ugurbil, K. and Kim, S. G., 2002. Effect of basal conditions on the magnitude and dynamics of the blood oxygenation level-dependent fMRI response. J Cereb Blood Flow Metab. 22, 1042-1053.

Conti, A. C., Cryan, J. F., Dalvi, A., Lucki, I. and Blendy, J. A., 2002. cAMP response element-binding protein is essential for the upregulation of brain-derived neurotrophic factor transcription, but not the behavioral or endocrine responses to antidepressant drugs. J Neurosci. 22, 3262-3268.

Coppell, A. L., Pei, Q. and Zetterstrom, T. S., 2003. Bi-phasic change in BDNF gene expression following antidepressant drug treatment. Neuropharmacology. 44, 903-910.

Corominas, M., Roncero, C., Ribases, M., Castells, X. and Casas, M., 2007. Brain-derived neurotrophic factor and its intracellular signaling pathways in cocaine addiction. Neuropsychobiology. 55, 2-13.

Coyle, J. T. and Duman, R. S., 2003. Finding the intracellular signaling pathways affected by mood disorder treatments. Neuron. 38, 157-160.

Crandall, J. E., Hackett, H. E., Tobet, S. A., Kosofsky, B. E. and Bhide, P. G., 2004. Cocaine exposure decreases GABA neuron migration from the ganglionic eminence to the cerebral cortex in embryonic mice. Cereb Cortex. 14, 665-675.

Crawley, J. N., 1999. Behavioral phenotyping of transgenic and knockout mice: experimental design and evaluation of general health, sensory functions, motor abilities, and specific behavioral tests. Brain Res. 835, 18-26.

Crosio, C., Heitz, E., Allis, C. D., Borrelli, E. and Sassone-Corsi, P., 2003. Chromatin remodeling and neuronal response: multiple signaling pathways induce specific histone H3 modifications and early gene expression in hippocampal neurons. J Cell Sci. 116, 4905-4914.

Cryan, J. F. and Mombereau, C., 2004. In search of a depressed mouse: utility of models for studying depression-related behavior in genetically modified mice. Mol Psychiatry. 9, 326-357.

Das, G., 1993. Cocaine abuse in North America: a milestone in history. J Clin Pharmacol. 33, 296-310.

Davie, J. R., 2003. Inhibition of histone deacetylase activity by butyrate. J Nutr. 133, 2485S-2493S.

De Foubert, G., Carney, S. L., Robinson, C. S., Destexhe, E. J., Tomlinson, R., Hicks, C. A., Murray, T. K., Gaillard, J. P., Deville, C., Xhenseval, V., Thomas, C. E., O'Neill, M. J. and Zetterstrom, T. S., 2004. Fluoxetine-induced change in rat brain expression of brain-derived neurotrophic factor varies depending on length of treatment. Neuroscience. 128, 597-604.

de Lima, M. S., de Oliveira Soares, B. G., Reisser, A. A. and Farrell, M., 2002. Pharmacological treatment of cocaine dependence: a systematic review. Addiction. 97, 931-949.

De Vries, T. J., Cools, A. R. and Shippenberg, T. S., 1998. Infusion of a D-1 receptor agonist into the nucleus accumbens enhances cocaine-induced behavioural sensitization. Neuroreport. 9, 1763-1768.

De Wit, H. and Wise, R. A., 1977. Blockade of cocaine reinforcement in rats with the dopamine receptor blocker pimozide, but not with the noradrenergic blockers phentolamine or phenoxybenzamine. Can J Psychol. 31, 195-203.

Dehm, S. M., Hilton, T. L., Wang, E. H. and Bonham, K., 2004. SRC proximal and core promoter elements dictate TAF1 dependence and transcriptional repression by histone deacetylase inhibitors. Mol Cell Biol. 24, 2296-2307.

Dias, B. G., Banerjee, S. B., Duman, R. S. and Vaidya, V. A., 2003. Differential regulation of brain derived neurotrophic factor transcripts by antidepressant treatments in the adult rat brain. Neuropharmacology. 45, 553-563.

Dluzen, D. E., Gao, X., Story, G. M., Anderson, L. I., Kucera, J. and Walro, J. M., 2001. Evaluation of nigrostriatal dopaminergic function in adult +/+ and +/- BDNF mutant mice. Exp Neurol. 170, 121-128.

Dokmanovic, M., Clarke, C. and Marks, P. A., 2007a. Histone deacetylase inhibitors: overview and perspectives. Mol Cancer Res. 5, 981-989.

Dokmanovic, M., Perez, G., Xu, W., Ngo, L., Clarke, C., Parmigiani, R. B. and Marks, P. A., 2007b. Histone deacetylase inhibitors selectively suppress expression of HDAC7. Mol Cancer Ther. 6, 2525-2534.

Dong, E., Agis-Balboa, R. C., Simonini, M. V., Grayson, D. R., Costa, E. and Guidotti, A., 2005. Reelin and glutamic acid decarboxylase67 promoter remodeling in an epigenetic methionine-induced mouse model of schizophrenia. Proc Natl Acad Sci U S A. 102, 12578-12583.

Dong, Y., Green, T., Saal, D., Marie, H., Neve, R., Nestler, E. J. and Malenka, R. C., 2006. CREB modulates excitability of nucleus accumbens neurons. Nat Neurosci. 9, 475-477.

Drevets, W. C., 2000. Neuroimaging studies of mood disorders. Biol Psychiatry. 48, 813-829.

Drouin, C. and Waterhouse, B. D., 2004. Cocaine-induced vs. behaviour-related alterations of spontaneous and evoked discharge of somatosensory cortical neurons. Eur J Neurosci. 19, 1016-1026.

Duman, R. S., 2004a. Depression: a case of neuronal life and death? Biol Psychiatry. 56, 140-145.

Duman, R. S., 2004b. Role of neurotrophic factors in the etiology and treatment of mood disorders. Neuromolecular Med. 5, 11-25.

Duman, R. S., Heninger, G. R. and Nestler, E. J., 1997. A molecular and cellular theory of depression. Arch Gen Psychiatry. 54, 597-606.

Duman, R. S. and Monteggia, L. M., 2006. A neurotrophic model for stress-related mood disorders. Biol Psychiatry. 59, 1116-1127.

Dunn, A. L., Trivedi, M. H., Kampert, J. B., Clark, C. G. and Chambliss, H. O., 2005. Exercise treatment for depression: efficacy and dose response. Am J Prev Med. 28, 1-8.

Dwivedi, Y., Rizavi, H. S., Conley, R. R., Roberts, R. C., Tamminga, C. A. and Pandey, G. N., 2003. Altered gene expression of brain-derived neurotrophic factor and receptor tyrosine kinase B in postmortem brain of suicide subjects. Arch Gen Psychiatry. 60, 804-815.

Egorin, M. J., Yuan, Z. M., Sentz, D. L., Plaisance, K. and Eiseman, J. L., 1999. Plasma pharmacokinetics of butyrate after intravenous administration of sodium butyrate or oral administration of tributyrin or sodium butyrate to mice and rats. Cancer Chemother Pharmacol. 43, 445-453.

Einat, H. and Manji, H. K., 2006. Cellular plasticity cascades: genes-to-behavior pathways in animal models of bipolar disorder. Biol Psychiatry. 59, 1160-1171.

Einat, H., Yuan, P., Gould, T. D., Li, J., Du, J., Zhang, L., Manji, H. K. and Chen, G., 2003. The role of the extracellular signal-regulated kinase signaling pathway in mood modulation. J Neurosci. 23, 7311-7316.

Eisch, A. J., Bolanos, C. A., de Wit, J., Simonak, R. D., Pudiak, C. M., Barrot, M., Verhaagen, J. and Nestler, E. J., 2003. Brain-derived neurotrophic factor in the ventral midbrain-nucleus accumbens pathway: a role in depression. Biol Psychiatry. 54, 994-1005.

Fava, M., 2003. Diagnosis and definition of treatment-resistant depression. Biol Psychiatry. 53, 649-659.

Febo, M., Segarra, A. C., Nair, G., Schmidt, K., Duong, T. Q. and Ferris, C. F., 2005. The neural consequences of repeated cocaine exposure revealed by functional MRI in awake rats. Neuropsychopharmacology. 30, 936-943.

Febo, M., Segarra, A. C., Tenney, J. R., Brevard, M. E., Duong, T. Q. and Ferris, C. F., 2004. Imaging cocaine-induced changes in the mesocorticolimbic dopaminergic system of conscious rats. J Neurosci Methods. 139, 167-176.

Ferguson, J. N., Aldag, J. M., Insel, T. R. and Young, L. J., 2001. Oxytocin in the medial amygdala is essential for social recognition in the mouse. J Neurosci. 21, 8278-8285.

Ferrante, R. J., Kubilus, J. K., Lee, J., Ryu, H., Beesen, A., Zucker, B., Smith, K., Kowall, N. W., Ratan, R. R., Luthi-Carter, R. and Hersch, S. M., 2003. Histone deacetylase inhibition by sodium butyrate chemotherapy ameliorates the neurodegenerative phenotype in Huntington's disease mice. J Neurosci. 23, 9418-9427.

Ferris, C. F., Kulkarni, P., Sullivan, J. M., Jr., Harder, J. A., Messenger, T. L. and Febo, M., 2005. Pup suckling is more rewarding than cocaine: evidence from functional magnetic resonance imaging and three-dimensional computational analysis. J Neurosci. 25, 149-156.

Filip, M., Faron-Gorecka, A., Kusmider, M., Golda, A., Frankowska, M. and Dziedzicka-Wasylewska, M., 2006. Alterations in BDNF and trkB mRNAs following acute or sensitizing cocaine treatments and withdrawal. Brain Res. 1071, 218-225.

Fischer, A., Sananbenesi, F., Wang, X., Dobbin, M. and Tsai, L. H., 2007. Recovery of learning and memory is associated with chromatin remodelling. Nature. 447, 178-182.

Frazer, A., 1997. Pharmacology of antidepressants. J Clin Psychopharmacol. 17 Suppl 1, 2S-18S.

Fukumoto, T., Morinobu, S., Okamoto, Y., Kagaya, A. and Yamawaki, S., 2001. Chronic lithium treatment increases the expression of brain-derived neurotrophic factor in the rat brain. Psychopharmacology (Berl). 158, 100-106.

Gainetdinov, R. R., Bohn, L. M., Sotnikova, T. D., Cyr, M., Laakso, A., Macrae, A. D., Torres, G. E., Kim, K. M., Lefkowitz, R. J., Caron, M. G. and Premont, R. T., 2003. Dopaminergic supersensitivity in G protein-coupled receptor kinase 6-deficient mice. Neuron. 38, 291-303.

Gardian, G., Browne, S. E., Choi, D. K., Klivenyi, P., Gregorio, J., Kubilus, J. K., Ryu, H., Langley, B., Ratan, R. R., Ferrante, R. J. and Beal, M. F., 2005. Neuroprotective effects of phenylbutyrate in the N171-82Q transgenic mouse model of Huntington's disease. J Biol Chem. 280, 556-563.

Gardian, G., Yang, L., Cleren, C., Calingasan, N. Y., Klivenyi, P. and Beal, M. F., 2004. Neuroprotective effects of phenylbutyrate against MPTP neurotoxicity. Neuromolecular Med. 5, 235-241.

Geddes, J. R., Burgess, S., Hawton, K., Jamison, K. and Goodwin, G. M., 2004. Long-term lithium therapy for bipolar disorder: systematic review and meta-analysis of randomized controlled trials. Am J Psychiatry. 161, 217-222.

Genovese, C. R., Lazar, N. A. and Nichols, T., 2002. Thresholding of statistical maps in functional neuroimaging using the false discovery rate. Neuroimage. 15, 870-878.

Giros, B., Jaber, M., Jones, S. R., Wightman, R. M. and Caron, M. G., 1996. Hyperlocomotion and indifference to cocaine and amphetamine in mice lacking the dopamine transporter. Nature. 379, 606-612.

Glozak, M. A., Sengupta, N., Zhang, X. and Seto, E., 2005. Acetylation and deacetylation of non-histone proteins. Gene. 363, 15-23.

Goldberg, M. S., Pisani, A., Haburcak, M., Vortherms, T. A., Kitada, T., Costa, C., Tong, Y., Martella, G., Tscherter, A., Martins, A., Bernardi, G., Roth, B. L., Pothos, E. N., Calabresi, P. and Shen, J., 2005. Nigrostriatal dopaminergic deficits and hypokinesia caused by inactivation of the familial Parkinsonism-linked gene DJ-1. Neuron. 45, 489-496.

Gonzalez Castro, F., Barrington, E. H., Walton, M. A. and Rawson, R. A., 2000. Cocaine and methamphetamine: differential addiction rates. Psychol Addict Behav. 14, 390-396.

Graham, D. L., Hoppenot, R., Hendryx, A. and Self, D. W., 2007. Differential ability of D1 and D2 dopamine receptor agonists to induce and modulate expression and reinstatement of cocaine place preference in rats. Psychopharmacology (Berl). 191, 719-730.

Graybiel, A. M., Moratalla, R. and Robertson, H. A., 1990. Amphetamine and cocaine induce drug-specific activation of the c-fos gene in striosome-matrix compartments and limbic subdivisions of the striatum. Proc Natl Acad Sci U S A. 87, 6912-6916.

Greenberg, P. E., Kessler, R. C., Birnbaum, H. G., Leong, S. A., Lowe, S. W., Berglund, P. A. and Corey-Lisle, P. K., 2003. The economic burden of depression in the United States: how did it change between 1990 and 2000? J Clin Psychiatry. 64, 1465-1475.

Grimm, J. W., Lu, L., Hayashi, T., Hope, B. T., Su, T. P. and Shaham, Y., 2003. Time-dependent increases in brain-derived neurotrophic factor protein levels within the

mesolimbic dopamine system after withdrawal from cocaine: implications for incubation of cocaine craving. J Neurosci. 23, 742-747.
Grozinger, C. M. and Schreiber, S. L., 2002. Deacetylase enzymes: biological functions and the use of small-molecule inhibitors. Chem Biol. 9, 3-16.
Grunstein, M., 1990. Histone function in transcription. Annu Rev Cell Biol. 6, 643-678.
Guillin, O., Diaz, J., Carroll, P., Griffon, N., Schwartz, J. C. and Sokoloff, P., 2001. BDNF controls dopamine D3 receptor expression and triggers behavioural sensitization. Nature. 411, 86-89.
Gunne, L. M., Anggard, E. and Jonsson, L. E., 1972. Clinical trials with amphetamine-blocking drugs. Psychiatr Neurol Neurochir. 75, 225-226.
Halikas, J. A., Center, B. A., Pearson, V. L., Carlson, G. A. and Crea, F., 2001. A pilot, open clinical study of depakote in the treatment of cocaine abuse. Hum Psychopharmacol. 16, 257-264.
Hall, F. S., Drgonova, J., Goeb, M. and Uhl, G. R., 2003. Reduced behavioral effects of cocaine in heterozygous brain-derived neurotrophic factor (BDNF) knockout mice. Neuropsychopharmacology. 28, 1485-1490.
Hall, F. S., Li, X. F., Sora, I., Xu, F., Caron, M., Lesch, K. P., Murphy, D. L. and Uhl, G. R., 2002. Cocaine mechanisms: enhanced cocaine, fluoxetine and nisoxetine place preferences following monoamine transporter deletions. Neuroscience. 115, 153-161.
Hammer, R. P., Jr. and Cooke, E. S., 1994. Gradual tolerance of metabolic activity is produced in mesolimbic regions by chronic cocaine treatment, while subsequent cocaine challenge activates extrapyramidal regions of rat brain. J Neurosci. 14, 4289-4298.
Haney, M., Collins, E. D., Ward, A. S., Foltin, R. W. and Fischman, M. W., 1999. Effect of a selective dopamine D1 agonist (ABT-431) on smoked cocaine self-administration in humans. Psychopharmacology (Berl). 143, 102-110.
Haney, M., Ward, A. S., Foltin, R. W. and Fischman, M. W., 2001. Effects of ecopipam, a selective dopamine D1 antagonist, on smoked cocaine self-administration by humans. Psychopharmacology (Berl). 155, 330-337.
Hansen, J. C., 2002. Conformational dynamics of the chromatin fiber in solution: determinants, mechanisms, and functions. Annu Rev Biophys Biomol Struct. 31, 361-392.
Heidbreder, C. A. and Hagan, J. J., 2005. Novel pharmacotherapeutic approaches for the treatment of drug addiction and craving. Curr Opin Pharmacol. 5, 107-118.
Henn, F. A. and Vollmayr, B., 2005. Stress models of depression: forming genetically vulnerable strains. Neurosci Biobehav Rev. 29, 799-804.
Herzog, C. J., Miot, S., Mansuy, I. M., Giros, B. and Tzavara, E. T., 2007. Chronic valproate normalizes behavior in mice overexpressing calcineurin. Eur J Pharmacol.
Hockly, E., Richon, V. M., Woodman, B., Smith, D. L., Zhou, X., Rosa, E., Sathasivam, K., Ghazi-Noori, S., Mahal, A., Lowden, P. A., Steffan, J. S., Marsh, J. L., Thompson, L. M., Lewis, C. M., Marks, P. A. and Bates, G. P., 2003. Suberoylanilide hydroxamic acid, a histone deacetylase inhibitor, ameliorates

motor deficits in a mouse model of Huntington's disease. Proc Natl Acad Sci U S A. 100, 2041-2046.

Hope, B., Kosofsky, B., Hyman, S. E. and Nestler, E. J., 1992. Regulation of immediate early gene expression and AP-1 binding in the rat nucleus accumbens by chronic cocaine. Proc Natl Acad Sci U S A. 89, 5764-5768.

Hope, B. T., Nye, H. E., Kelz, M. B., Self, D. W., Iadarola, M. J., Nakabeppu, Y., Duman, R. S. and Nestler, E. J., 1994. Induction of a long-lasting AP-1 complex composed of altered Fos-like proteins in brain by chronic cocaine and other chronic treatments. Neuron. 13, 1235-1244.

Horger, B. A., Iyasere, C. A., Berhow, M. T., Messer, C. J., Nestler, E. J. and Taylor, J. R., 1999. Enhancement of locomotor activity and conditioned reward to cocaine by brain-derived neurotrophic factor. J Neurosci. 19, 4110-4122.

Hoshaw, B. A., Malberg, J. E. and Lucki, I., 2005. Central administration of IGF-I and BDNF leads to long-lasting antidepressant-like effects. Brain Res. 1037, 204-208.

Hsieh, J., Nakashima, K., Kuwabara, T., Mejia, E. and Gage, F. H., 2004. Histone deacetylase inhibition-mediated neuronal differentiation of multipotent adult neural progenitor cells. Proc Natl Acad Sci U S A. 101, 16659-16664.

Huang, H. S., Matevossian, A., Jiang, Y. and Akbarian, S., 2006. Chromatin immunoprecipitation in postmortem brain. J Neurosci Methods. 156, 284-292.

Huang, Y., Doherty, J. J. and Dingledine, R., 2002. Altered histone acetylation at glutamate receptor 2 and brain-derived neurotrophic factor genes is an early event triggered by status epilepticus. J Neurosci. 22, 8422-8428.

Hummel, M. and Unterwald, E. M., 2002. D1 dopamine receptor: a putative neurochemical and behavioral link to cocaine action. J Cell Physiol. 191, 17-27.

Huntley, G. W., Benson, D. L., Jones, E. G. and Isackson, P. J., 1992. Developmental expression of brain derived neurotrophic factor mRNA by neurons of fetal and adult monkey prefrontal cortex. Brain Res Dev Brain Res. 70, 53-63.

Hwang, J. P., Tsai, S. J., Hong, C. J., Yang, C. H., Lirng, J. F. and Yang, Y. M., 2006. The Val66Met polymorphism of the brain-derived neurotrophic-factor gene is associated with geriatric depression. Neurobiol Aging. 27, 1834-1837.

Hyman, S. E., 1999. Selective gene expression increases behavioral sensitivity to cocaine. Nat Neurosci. 2, 855-856.

Isackson, P. J., Huntsman, M. M., Murray, K. D. and Gall, C. M., 1991. BDNF mRNA expression is increased in adult rat forebrain after limbic seizures: temporal patterns of induction distinct from NGF. Neuron. 6, 937-948.

Jenkins, T. A., Dias, R., Amin, E. and Aggleton, J. P., 2002. Changes in Fos expression in the rat brain after unilateral lesions of the anterior thalamic nuclei. Eur J Neurosci. 16, 1425-1432.

Jenuwein, T. and Allis, C. D., 2001. Translating the histone code. Science. 293, 1074-1080.

Kalda, A., Heidmets, L. T., Shen, H. Y., Zharkovsky, A. and Chen, J. F., 2007. Histone deacetylase inhibitors modulates the induction and expression of amphetamine-induced behavioral sensitization partially through an associated learning of the environment in mice. Behav Brain Res. 181, 76-84.

Kalivas, P. W. and Volkow, N. D., 2005. The neural basis of addiction: a pathology of motivation and choice. Am J Psychiatry. 162, 1403-1413.

Kang, H. J., Adams, D. H., Simen, A., Simen, B. B., Rajkowska, G., Stockmeier, C. A., Overholser, J. C., Meltzer, H. Y., Jurjus, G. J., Konick, L. C., Newton, S. S. and Duman, R. S., 2007. Gene expression profiling in postmortem prefrontal cortex of major depressive disorder. J Neurosci. 27, 13329-13340.

Karege, F., Perret, G., Bondolfi, G., Schwald, M., Bertschy, G. and Aubry, J. M., 2002. Decreased serum brain-derived neurotrophic factor levels in major depressed patients. Psychiatry Res. 109, 143-148.

Kassell, N. F., Sprowell, J. A., Boarini, D. J. and Olin, J. J., 1983. Effect of dimethyl sulfoxide on the cerebral and systemic circulations of the dog. Neurosurgery. 12, 24-28.

Katz, J. L. and Witkin, J. M., 1992. Selective effects of the D1 dopamine receptor agonist, SKF 38393, on behavior maintained by cocaine injection in squirrel monkeys. Psychopharmacology (Berl). 109, 241-244.

Keller, M., Meurisse, M. and Levy, F., 2004. Mapping the neural substrates involved in maternal responsiveness and lamb olfactory memory in parturient ewes using Fos imaging. Behav Neurosci. 118, 1274-1284.

Kessler, R. C., Berglund, P., Demler, O., Jin, R., Koretz, D., Merikangas, K. R., Rush, A. J., Walters, E. E. and Wang, P. S., 2003. The epidemiology of major depressive disorder: results from the National Comorbidity Survey Replication (NCS-R). Jama. 289, 3095-3105.

King, J. A., Garelick, T. S., Brevard, M. E., Chen, W., Messenger, T. L., Duong, T. Q. and Ferris, C. F., 2005. Procedure for minimizing stress for fMRI studies in conscious rats. J Neurosci Methods. 148, 154-160.

Konradi, C., Leveque, J. C. and Hyman, S. E., 1996. Amphetamine and dopamine-induced immediate early gene expression in striatal neurons depends on postsynaptic NMDA receptors and calcium. J Neurosci. 16, 4231-4239.

Korzus, E., Rosenfeld, M. G. and Mayford, M., 2004. CBP histone acetyltransferase activity is a critical component of memory consolidation. Neuron. 42, 961-972.

Kouzarides, T., 2007. Chromatin modifications and their function. Cell. 128, 693-705.

Kreek, M. J., LaForge, K. S. and Butelman, E., 2002. Pharmacotherapy of addictions. Nat Rev Drug Discov. 1, 710-726.

Kumar, A., Choi, K. H., Renthal, W., Tsankova, N. M., Theobald, D. E., Truong, H. T., Russo, S. J., Laplant, Q., Sasaki, T. S., Whistler, K. N., Neve, R. L., Self, D. W. and Nestler, E. J., 2005. Chromatin remodeling is a key mechanism underlying cocaine-induced plasticity in striatum. Neuron. 48, 303-314.

Le Moine, C., Svenningsson, P., Fredholm, B. B. and Bloch, B., 1997. Dopamine-adenosine interactions in the striatum and the globus pallidus: inhibition of striatopallidal neurons through either D2 or A2A receptors enhances D1 receptor-mediated effects on c-fos expression. J Neurosci. 17, 8038-8048.

Lee, D. Y., Hayes, J. J., Pruss, D. and Wolffe, A. P., 1993. A positive role for histone acetylation in transcription factor access to nucleosomal DNA. Cell. 72, 73-84.

Legault, M., Rompre, P. P. and Wise, R. A., 2000. Chemical stimulation of the ventral hippocampus elevates nucleus accumbens dopamine by activating dopaminergic neurons of the ventral tegmental area. J Neurosci. 20, 1635-1642.

Levenson, J. M., O'Riordan, K. J., Brown, K. D., Trinh, M. A., Molfese, D. L. and Sweatt, J. D., 2004. Regulation of histone acetylation during memory formation in the hippocampus. J Biol Chem. 279, 40545-40559.

Levine, A. A., Guan, Z., Barco, A., Xu, S., Kandel, E. R. and Schwartz, J. H., 2005. CREB-binding protein controls response to cocaine by acetylating histones at the fosB promoter in the mouse striatum. Proc Natl Acad Sci U S A. 102, 19186-19191.

Li, J., Guo, Y., Schroeder, F. A., Youngs, R. M., Schmidt, T. W., Ferris, C., Konradi, C. and Akbarian, S., 2004. Dopamine D2-like antagonists induce chromatin remodeling in striatal neurons through cyclic AMP-protein kinase A and NMDA receptor signaling. J Neurochem. 90, 1117-1131.

Lindsay, R. M., Wiegand, S. J., Altar, C. A. and DiStefano, P. S., 1994. Neurotrophic factors: from molecule to man. Trends Neurosci. 17, 182-190.

Lindvall, O. and Odin, P., 1994. Clinical application of cell transplantation and neurotrophic factors in CNS disorders. Curr Opin Neurobiol. 4, 752-757.

Lippmann, M., Bress, A., Nemeroff, C. B., Plotsky, P. M. and Monteggia, L. M., 2007. Long-term behavioural and molecular alterations associated with maternal separation in rats. Eur J Neurosci. 25, 3091-3098.

Liu, Q. R., Lu, L., Zhu, X. G., Gong, J. P., Shaham, Y. and Uhl, G. R., 2006. Rodent BDNF genes, novel promoters, novel splice variants, and regulation by cocaine. Brain Res. 1067, 1-12.

Lopez-Leon, S., Janssens, A. C., Gonzalez-Zuloeta Ladd, A. M., Del-Favero, J., Claes, S. J., Oostra, B. A. and van Duijn, C. M., 2007. Meta-analyses of genetic studies on major depressive disorder. Mol Psychiatry.

Lu, L., Dempsey, J., Liu, S. Y., Bossert, J. M. and Shaham, Y., 2004. A single infusion of brain-derived neurotrophic factor into the ventral tegmental area induces long-lasting potentiation of cocaine seeking after withdrawal. J Neurosci. 24, 1604-1611.

Lu, L., Grimm, J. W., Shaham, Y. and Hope, B. T., 2003. Molecular neuroadaptations in the accumbens and ventral tegmental area during the first 90 days of forced abstinence from cocaine self-administration in rats. J Neurochem. 85, 1604-1613.

Lucki, I., Dalvi, A. and Mayorga, A. J., 2001. Sensitivity to the effects of pharmacologically selective antidepressants in different strains of mice. Psychopharmacology (Berl). 155, 315-322.

Luger, K., Mader, A. W., Richmond, R. K., Sargent, D. F. and Richmond, T. J., 1997. Crystal structure of the nucleosome core particle at 2.8 A resolution. Nature. 389, 251-260.

Luo, F., Wu, G., Li, Z. and Li, S. J., 2003. Characterization of effects of mean arterial blood pressure induced by cocaine and cocaine methiodide on BOLD signals in rat brain. Magn Reson Med. 49, 264-270.

Lyons, W. E., Mamounas, L. A., Ricaurte, G. A., Coppola, V., Reid, S. W., Bora, S. H., Wihler, C., Koliatsos, V. E. and Tessarollo, L., 1999. Brain-derived neurotrophic factor-deficient mice develop aggressiveness and hyperphagia in conjunction with brain serotonergic abnormalities. Proc Natl Acad Sci U S A. 96, 15239-15244.

Mackler, S. A. and Eberwine, J. H., 1991. The molecular biology of addictive drugs. Mol Neurobiol. 5, 45-58.

MacQueen, G. M., Ramakrishnan, K., Croll, S. D., Siuciak, J. A., Yu, G., Young, L. T. and Fahnestock, M., 2001. Performance of heterozygous brain-derived neurotrophic factor knockout mice on behavioral analogues of anxiety, nociception, and depression. Behav Neurosci. 115, 1145-1153.

Mah, L., Zarate, C. A., Jr., Singh, J., Duan, Y. F., Luckenbaugh, D. A., Manji, H. K. and Drevets, W. C., 2007. Regional cerebral glucose metabolic abnormalities in bipolar II depression. Biol Psychiatry. 61, 765-775.

Manaye, K. F., Lei, D. L., Tizabi, Y., Davila-Garcia, M. I., Mouton, P. R. and Kelly, P. H., 2005. Selective neuron loss in the paraventricular nucleus of hypothalamus in patients suffering from major depression and bipolar disorder. J Neuropathol Exp Neurol. 64, 224-229.

Manji, H. K., Drevets, W. C. and Charney, D. S., 2001. The cellular neurobiology of depression. Nat Med. 7, 541-547.

Manji, H. K. and Duman, R. S., 2001. Impairments of neuroplasticity and cellular resilience in severe mood disorders: implications for the development of novel therapeutics. Psychopharmacol Bull. 35, 5-49.

Manji, H. K., McNamara, R., Chen, G. and Lenox, R. H., 1999. Signalling pathways in the brain: cellular transduction of mood stabilisation in the treatment of manic-depressive illness. Aust N Z J Psychiatry. 33 Suppl, S65-83.

Manning-Bog, A. B., Caudle, W. M., Perez, X. A., Reaney, S. H., Paletzki, R., Isla, M. Z., Chou, V. P., McCormack, A. L., Miller, G. W., Langston, J. W., Gerfen, C. R. and Dimonte, D. A., 2007. Increased vulnerability of nigrostriatal terminals in DJ-1-deficient mice is mediated by the dopamine transporter. Neurobiol Dis. 27, 141-150.

Mariadason, J. M., Corner, G. A. and Augenlicht, L. H., 2000. Genetic reprogramming in pathways of colonic cell maturation induced by short chain fatty acids: comparison with trichostatin A, sulindac, and curcumin and implications for chemoprevention of colon cancer. Cancer Res. 60, 4561-4572.

Marks, P. A., Miller, T. and Richon, V. M., 2003. Histone deacetylases. Curr Opin Pharmacol. 3, 344-351.

Marks, P. A., Richon, V. M., Breslow, R. and Rifkind, R. A., 2001. Histone deacetylase inhibitors as new cancer drugs. Curr Opin Oncol. 13, 477-483.

Martens, J. A. and Winston, F., 2003. Recent advances in understanding chromatin remodeling by Swi/Snf complexes. Curr Opin Genet Dev. 13, 136-142.

Masana, Y., Wanaka, A., Kato, H., Asai, T. and Tohyama, M., 1993. Localization of trkB mRNA in postnatal brain development. J Neurosci Res. 35, 468-479.

Matsuzaki, M., Takagi, H. and Tokizane, T., 1964. Paradoxical Phase of Sleep: Its Artificial Induction in the Cat by Sodium Butyrate. Science. 146, 1328-1329.

McClung, C. A. and Nestler, E. J., 2003. Regulation of gene expression and cocaine reward by CREB and DeltaFosB. Nat Neurosci. 6, 1208-1215.

McClung, C. A., Ulery, P. G., Perrotti, L. I., Zachariou, V., Berton, O. and Nestler, E. J., 2004. DeltaFosB: a molecular switch for long-term adaptation in the brain. Brain Res Mol Brain Res. 132, 146-154.

Michelson, D., Stratakis, C., Hill, L., Reynolds, J., Galliven, E., Chrousos, G. and Gold, P., 1996. Bone mineral density in women with depression. N Engl J Med. 335, 1176-1181.

Miller, A. A., Kurschel, E., Osieka, R. and Schmidt, C. G., 1987. Clinical pharmacology of sodium butyrate in patients with acute leukemia. Eur J Cancer Clin Oncol. 23, 1283-1287.

Minamiyama, M., Katsuno, M., Adachi, H., Waza, M., Sang, C., Kobayashi, Y., Tanaka, F., Doyu, M., Inukai, A. and Sobue, G., 2004. Sodium butyrate ameliorates phenotypic expression in a transgenic mouse model of spinal and bulbar muscular atrophy. Hum Mol Genet. 13, 1183-1192.

Miro, X., Perez-Torres, S., Artigas, F., Puigdomenech, P., Palacios, J. M. and Mengod, G., 2002. Regulation of cAMP phosphodiesterase mRNAs expression in rat brain by acute and chronic fluoxetine treatment. An in situ hybridization study. Neuropharmacology. 43, 1148-1157.

Mitchell, A. S., Dalrymple-Alford, J. C. and Christie, M. A., 2002. Spatial working memory and the brainstem cholinergic innervation to the anterior thalamus. J Neurosci. 22, 1922-1928.

Monteggia, L. M., Barrot, M., Powell, C. M., Berton, O., Galanis, V., Gemelli, T., Meuth, S., Nagy, A., Greene, R. W. and Nestler, E. J., 2004. Essential role of brain-derived neurotrophic factor in adult hippocampal function. Proc Natl Acad Sci U S A. 101, 10827-10832.

Montgomery, S. A., 2006. Why do we need new and better antidepressants? Int Clin Psychopharmacol. 21 Suppl 1, S1-S10.

Moratalla, R., Elibol, B., Vallejo, M. and Graybiel, A. M., 1996. Network-level changes in expression of inducible Fos-Jun proteins in the striatum during chronic cocaine treatment and withdrawal. Neuron. 17, 147-156.

Moratalla, R., Vickers, E. A., Robertson, H. A., Cochran, B. H. and Graybiel, A. M., 1993. Coordinate expression of c-fos and jun B is induced in the rat striatum by cocaine. J Neurosci. 13, 423-433.

Moy, L. Y. and Tsai, L. H., 2004. Cyclin-dependent kinase 5 phosphorylates serine 31 of tyrosine hydroxylase and regulates its stability. J Biol Chem. 279, 54487-54493.

Murray, C. J. and Lopez, A. D., 1997. Alternative projections of mortality and disability by cause 1990-2020: Global Burden of Disease Study. Lancet. 349, 1498-1504.

Musselman, D. L., Evans, D. L. and Nemeroff, C. B., 1998. The relationship of depression to cardiovascular disease: epidemiology, biology, and treatment. Arch Gen Psychiatry. 55, 580-592.

Musto, D. F., 1992. Cocaine's history, especially the American experience. Ciba Found Symp. 166, 7-14; discussion 14-19.

Myers, M. B. and Donovan, W., 1975. Effect of dimethyl sulfoxide and hydrogen peroxide on tissue gas tensions. Ann N Y Acad Sci. 243, 320-324.

Nan, X., Campoy, F. J. and Bird, A., 1997. MeCP2 is a transcriptional repressor with abundant binding sites in genomic chromatin. Cell. 88, 471-481.

Naoe, Y., Shinkai, T., Hori, H., Fukunaka, Y., Utsunomiya, K., Sakata, S., Matsumoto, C., Shimizu, K., Hwang, R., Ohmori, O. and Nakamura, J., 2007. No association between the brain-derived neurotrophic factor (BDNF) Val66Met polymorphism and schizophrenia in Asian populations: Evidence from a case-control study and meta-analysis. Neurosci Lett. 415, 108-112.

Nelson, J. C., 1999. A review of the efficacy of serotonergic and noradrenergic reuptake inhibitors for treatment of major depression. Biol Psychiatry. 46, 1301-1308.

Nergardh, R., Oerther, S. and Fredholm, B. B., 2005. Differences between A 68930 and SKF 82958 could suggest synergistic roles of D1 and D5 receptors. Pharmacol Biochem Behav. 82, 495-505.

Nestler, E. J., 1992. Molecular mechanisms of drug addiction. J Neurosci. 12, 2439-2450.

Nestler, E. J., 2005. Is there a common molecular pathway for addiction? Nat Neurosci. 8, 1445-1449.

Nestler, E. J., Barrot, M., DiLeone, R. J., Eisch, A. J., Gold, S. J. and Monteggia, L. M., 2002. Neurobiology of depression. Neuron. 34, 13-25.

Nestler, E. J., Barrot, M. and Self, D. W., 2001. DeltaFosB: a sustained molecular switch for addiction. Proc Natl Acad Sci U S A. 98, 11042-11046.

Nibuya, M., Morinobu, S. and Duman, R. S., 1995. Regulation of BDNF and trkB mRNA in rat brain by chronic electroconvulsive seizure and antidepressant drug treatments. J Neurosci. 15, 7539-7547.

Nibuya, M., Nestler, E. J. and Duman, R. S., 1996. Chronic antidepressant administration increases the expression of cAMP response element binding protein (CREB) in rat hippocampus. J Neurosci. 16, 2365-2372.

North, B. J., Schwer, B., Ahuja, N., Marshall, B. and Verdin, E., 2005. Preparation of enzymatically active recombinant class III protein deacetylases. Methods. 36, 338-345.

Nusinzon, I. and Horvath, C. M., 2005. Histone deacetylases as transcriptional activators? Role reversal in inducible gene regulation. Sci STKE. 2005, re11.

Ongur, D., Drevets, W. C. and Price, J. L., 1998. Glial reduction in the subgenual prefrontal cortex in mood disorders. Proc Natl Acad Sci U S A. 95, 13290-13295.

Ooi, L., Belyaev, N. D., Miyake, K., Wood, I. C. and Buckley, N. J., 2006. BRG1 chromatin remodeling activity is required for efficient chromatin binding by repressor element 1-silencing transcription factor (REST) and facilitates REST-mediated repression. J Biol Chem. 281, 38974-38980.

Parab, S., Nankova, B. B. and La Gamma, E. F., 2007. Differential regulation of the tyrosine hydroxylase and enkephalin neuropeptide transmitter genes in rat PC12 cells by short chain fatty acids: concentration-dependent effects on transcription and RNA stability. Brain Res. 1132, 42-50.

Park, S. K., Nguyen, M. D., Fischer, A., Luke, M. P., Affar el, B., Dieffenbach, P. B., Tseng, H. C., Shi, Y. and Tsai, L. H., 2005. Par-4 links dopamine signaling and depression. Cell. 122, 275-287.

Patel, P., Nankova, B. B. and LaGamma, E. F., 2005. Butyrate, a gut-derived environmental signal, regulates tyrosine hydroxylase gene expression via a novel promoter element. Brain Res Dev Brain Res. 160, 53-62.

Paxinos, G. and Franklin, K., 2001a. The Mouse Brain in Stereotaxic Coordinates, 2nd Ed. Academic Press, San Diego.

Paxinos, G. and Franklin, K. B. J., 2001b. The Mouse Brain in Stereotaxic Coordinates. Academic Press, San Diego.

Paxinos, G., Watson, C., 1997. The Rat Brain in Stereotaxic Coordinates, 3rd Edition. Academic Press., Boston.

Peterson, C. L. and Laniel, M. A., 2004. Histones and histone modifications. Curr Biol. 14, R546-551.

Petrij, F., Giles, R. H., Dauwerse, H. G., Saris, J. J., Hennekam, R. C., Masuno, M., Tommerup, N., van Ommen, G. J., Goodman, R. H., Peters, D. J. and et al., 1995. Rubinstein-Taybi syndrome caused by mutations in the transcriptional co-activator CBP. Nature. 376, 348-351.

Pierce, R. C., Born, B., Adams, M. and Kalivas, P. W., 1996. Repeated intra-ventral tegmental area administration of SKF-38393 induces behavioral and neurochemical sensitization to a subsequent cocaine challenge. J Pharmacol Exp Ther. 278, 384-392.

Pierce, R. C., Pierce-Bancroft, A. F. and Prasad, B. M., 1999. Neurotrophin-3 contributes to the initiation of behavioral sensitization to cocaine by activating the Ras/Mitogen-activated protein kinase signal transduction cascade. J Neurosci. 19, 8685-8695.

Pincus, H. A. and Pettit, A. R., 2001. The societal costs of chronic major depression. J Clin Psychiatry. 62 Suppl 6, 5-9.

Porsolt, R. D., Bertin, A. and Jalfre, M., 1977a. Behavioral despair in mice: a primary screening test for antidepressants. Arch Int Pharmacodyn Ther. 229, 327-336.

Porsolt, R. D., Le Pichon, M. and Jalfre, M., 1977b. Depression: a new animal model sensitive to antidepressant treatments. Nature. 266, 730-732.

Pu, L., Liu, Q. S. and Poo, M. M., 2006. BDNF-dependent synaptic sensitization in midbrain dopamine neurons after cocaine withdrawal. Nat Neurosci. 9, 605-607.

Rada-Iglesias, A., Enroth, S., Ameur, A., Koch, C. M., Clelland, G. K., Respuela-Alonso, P., Wilcox, S., Dovey, O. M., Ellis, P. D., Langford, C. F., Dunham, I., Komorowski, J. and Wadelius, C., 2007. Butyrate mediates decrease of histone acetylation centered on transcription start sites and down-regulation of associated genes. Genome Res. 17, 708-719.

Rajadhyaksha, A., Leveque, J., Macias, W., Barczak, A. and Konradi, C., 1998. Molecular components of striatal plasticity: the various routes of cyclic AMP pathways. Dev Neurosci. 20, 204-215.

Rajkowska, G., 2000. Postmortem studies in mood disorders indicate altered numbers of neurons and glial cells. Biol Psychiatry. 48, 766-777.

Rajkowska, G., Miguel-Hidalgo, J. J., Wei, J., Dilley, G., Pittman, S. D., Meltzer, H. Y., Overholser, J. C., Roth, B. L. and Stockmeier, C. A., 1999. Morphometric evidence for neuronal and glial prefrontal cell pathology in major depression. Biol Psychiatry. 45, 1085-1098.

Renthal, W., Maze, I., Krishnan, V., Covington, H. E., 3rd, Xiao, G., Kumar, A., Russo, S. J., Graham, A., Tsankova, N., Kippin, T. E., Kerstetter, K. A., Neve, R. L., Haggarty, S. J., McKinsey, T. A., Bassel-Duby, R., Olson, E. N. and Nestler, E. J., 2007. Histone deacetylase 5 epigenetically controls behavioral adaptations to chronic emotional stimuli. Neuron. 56, 517-529.

Rihmer, Z., 2007. Drug-placebo difference: in antidepressant drug trials could be 50% greater than previously believed. Neuropsychopharmacol Hung. 9, 35-37.

Rios, M., Fan, G., Fekete, C., Kelly, J., Bates, B., Kuehn, R., Lechan, R. M. and Jaenisch, R., 2001. Conditional deletion of brain-derived neurotrophic factor in the postnatal brain leads to obesity and hyperactivity. Mol Endocrinol. 15, 1748-1757.

Rios, M., Lambe, E. K., Liu, R., Teillon, S., Liu, J., Akbarian, S., Roffler-Tarlov, S., Jaenisch, R. and Aghajanian, G. K., 2006. Severe deficits in 5-HT(2A)-mediated neurotransmission in BDNF conditional mutant mice. J Neurobiol. 66, 408-420.

Ritz, M. C., Lamb, R. J., Goldberg, S. R. and Kuhar, M. J., 1988. Cocaine self-administration appears to be mediated by dopamine uptake inhibition. Prog Neuropsychopharmacol Biol Psychiatry. 12, 233-239.

Roberts, D. C., Corcoran, M. E. and Fibiger, H. C., 1977. On the role of ascending catecholaminergic systems in intravenous self-administration of cocaine. Pharmacol Biochem Behav. 6, 615-620.

Roberts, D. C. and Koob, G. F., 1982. Disruption of cocaine self-administration following 6-hydroxydopamine lesions of the ventral tegmental area in rats. Pharmacol Biochem Behav. 17, 901-904.

Roberts, D. C., Koob, G. F., Klonoff, P. and Fibiger, H. C., 1980. Extinction and recovery of cocaine self-administration following 6-hydroxydopamine lesions of the nucleus accumbens. Pharmacol Biochem Behav. 12, 781-787.

Rocha, B. A., Fumagalli, F., Gainetdinov, R. R., Jones, S. R., Ator, R., Giros, B., Miller, G. W. and Caron, M. G., 1998a. Cocaine self-administration in dopamine-transporter knockout mice. Nat Neurosci. 1, 132-137.

Rocha, B. A., Scearce-Levie, K., Lucas, J. J., Hiroi, N., Castanon, N., Crabbe, J. C., Nestler, E. J. and Hen, R., 1998b. Increased vulnerability to cocaine in mice lacking the serotonin-1B receptor. Nature. 393, 175-178.

Romach, M. K., Glue, P., Kampman, K., Kaplan, H. L., Somer, G. R., Poole, S., Clarke, L., Coffin, V., Cornish, J., O'Brien, C. P. and Sellers, E. M., 1999. Attenuation of the euphoric effects of cocaine by the dopamine D1/D5 antagonist ecopipam (SCH 39166). Arch Gen Psychiatry. 56, 1101-1106.

Russo-Neustadt, A. A., Beard, R. C., Huang, Y. M. and Cotman, C. W., 2000. Physical activity and antidepressant treatment potentiate the expression of specific brain-derived neurotrophic factor transcripts in the rat hippocampus. Neuroscience. 101, 305-312.

Ryu, H., Smith, K., Camelo, S. I., Carreras, I., Lee, J., Iglesias, A. H., Dangond, F., Cormier, K. A., Cudkowicz, M. E., Brown, R. H., Jr. and Ferrante, R. J., 2005. Sodium phenylbutyrate prolongs survival and regulates expression of anti-apoptotic genes in transgenic amyotrophic lateral sclerosis mice. J Neurochem. 93, 1087-1098.

Sanchez, C. J., Bailie, T. M., Wu, W. R., Li, N. and Sorg, B. A., 2003. Manipulation of dopamine d1-like receptor activation in the rat medial prefrontal cortex alters stress- and cocaine-induced reinstatement of conditioned place preference behavior. Neuroscience. 119, 497-505.

Santini, E., Valjent, E., Usiello, A., Carta, M., Borgkvist, A., Girault, J. A., Herve, D., Greengard, P. and Fisone, G., 2007. Critical involvement of cAMP/DARPP-32 and extracellular signal-regulated protein kinase signaling in L-DOPA-induced dyskinesia. J Neurosci. 27, 6995-7005.

Schindler, C. W. and Carmona, G. N., 2002. Effects of dopamine agonists and antagonists on locomotor activity in male and female rats. Pharmacol Biochem Behav. 72, 857-863.

Schmauss, C., 2000. A single dose of methamphetamine leads to a long term reversal of the blunted dopamine D1 receptor-mediated neocortical c-fos responses in mice deficient for D2 and D3 receptors. J Biol Chem. 275, 38944-38948.

Schramm, N. L., McDonald, M. P. and Limbird, L. E., 2001. The alpha(2a)-adrenergic receptor plays a protective role in mouse behavioral models of depression and anxiety. J Neurosci. 21, 4875-4882.

Schroeder, F. A., Lin, C. L., Crusio, W. E. and Akbarian, S., 2007. Antidepressant-like effects of the histone deacetylase inhibitor, sodium butyrate, in the mouse. Biol Psychiatry. 62, 55-64.

Schroeder, F. A., Penta, K. L., Matevossian, A., Jones, S. R., Konradi, C., Tapper, A. R. and Akbarian, S., 2008. Drug-Induced Activation of Dopamine D(1) Receptor Signaling and Inhibition of Class I/II Histone Deacetylase Induce Chromatin Remodeling in Reward Circuitry and Modulate Cocaine-Related Behaviors. Neuropsychopharmacology.

Schulz, R., Beach, S. R., Ives, D. G., Martire, L. M., Ariyo, A. A. and Kop, W. J., 2000. Association between depression and mortality in older adults: the Cardiovascular Health Study. Arch Intern Med. 160, 1761-1768.

Scott, G. K., Mattie, M. D., Berger, C. E., Benz, S. C. and Benz, C. C., 2006. Rapid alteration of microRNA levels by histone deacetylase inhibition. Cancer Res. 66, 1277-1281.

Self, D. W., Choi, K. H., Simmons, D., Walker, J. R. and Smagula, C. S., 2004. Extinction training regulates neuroadaptive responses to withdrawal from chronic cocaine self-administration. Learn Mem. 11, 648-657.

Self, D. W., Karanian, D. A. and Spencer, J. J., 2000. Effects of the novel D1 dopamine receptor agonist ABT-431 on cocaine self-administration and reinstatement. Ann N Y Acad Sci. 909, 133-144.

Self, D. W. and Stein, L., 1992. The D1 agonists SKF 82958 and SKF 77434 are self-administered by rats. Brain Res. 582, 349-352.

Shah, P., Nankova, B. B., Parab, S. and La Gamma, E. F., 2006. Short chain fatty acids induce TH gene expression via ERK-dependent phosphorylation of CREB protein. Brain Res. 1107, 13-23.

Shaltiel, G., Chen, G. and Manji, H. K., 2007. Neurotrophic signaling cascades in the pathophysiology and treatment of bipolar disorder. Curr Opin Pharmacol. 7, 22-26.

Sheline, Y. I., Gado, M. H. and Kraemer, H. C., 2003. Untreated depression and hippocampal volume loss. Am J Psychiatry. 160, 1516-1518.

Shogren-Knaak, M., Ishii, H., Sun, J. M., Pazin, M. J., Davie, J. R. and Peterson, C. L., 2006. Histone H4-K16 acetylation controls chromatin structure and protein interactions. Science. 311, 844-847.

Sicard, K., Shen, Q., Brevard, M. E., Sullivan, R., Ferris, C. F., King, J. A. and Duong, T. Q., 2003. Regional cerebral blood flow and BOLD responses in conscious and anesthetized rats under basal and hypercapnic conditions: implications for functional MRI studies. J Cereb Blood Flow Metab. 23, 472-481.

Simonini, M. V., Camargo, L. M., Dong, E., Maloku, E., Veldic, M., Costa, E. and Guidotti, A., 2006. The benzamide MS-275 is a potent, long-lasting brain region-selective inhibitor of histone deacetylases. Proc Natl Acad Sci U S A. 103, 1587-1592.

Siuciak, J. A., Boylan, C., Fritsche, M., Altar, C. A. and Lindsay, R. M., 1996. BDNF increases monoaminergic activity in rat brain following intracerebroventricular or intraparenchymal administration. Brain Res. 710, 11-20.

Siuciak, J. A., Lewis, D. R., Wiegand, S. J. and Lindsay, R. M., 1997. Antidepressant-like effect of brain-derived neurotrophic factor (BDNF). Pharmacol Biochem Behav. 56, 131-137.

Sommer, A., Hilfenhaus, S., Menkel, A., Kremmer, E., Seiser, C., Loidl, P. and Luscher, B., 1997. Cell growth inhibition by the Mad/Max complex through recruitment of histone deacetylase activity. Curr Biol. 7, 357-365.

Sora, I., Hall, F. S., Andrews, A. M., Itokawa, M., Li, X. F., Wei, H. B., Wichems, C., Lesch, K. P., Murphy, D. L. and Uhl, G. R., 2001. Molecular mechanisms of cocaine reward: combined dopamine and serotonin transporter knockouts eliminate cocaine place preference. Proc Natl Acad Sci U S A. 98, 5300-5305.

Sora, I., Wichems, C., Takahashi, N., Li, X. F., Zeng, Z., Revay, R., Lesch, K. P., Murphy, D. L. and Uhl, G. R., 1998. Cocaine reward models: conditioned place preference can be established in dopamine- and in serotonin-transporter knockout mice. Proc Natl Acad Sci U S A. 95, 7699-7704.

Sorg, B. A., Li, N., Wu, W. and Bailie, T. M., 2004. Activation of dopamine D1 receptors in the medial prefrontal cortex produces bidirectional effects on cocaine-induced locomotor activity in rats: effects of repeated stress. Neuroscience. 127, 187-196.

Spealman, R. D., Madras, B. K. and Bergman, J., 1989. Effects of cocaine and related drugs in nonhuman primates. II. Stimulant effects on schedule-controlled behavior. J Pharmacol Exp Ther. 251, 142-149.

Stadler, F., Kolb, G., Rubusch, L., Baker, S. P., Jones, E. G. and Akbarian, S., 2005. Histone methylation at gene promoters is associated with developmental

regulation and region-specific expression of ionotropic and metabotropic glutamate receptors in human brain. J Neurochem. 94, 324-336.
Stein, E. A. and Fuller, S. A., 1993. Cocaine's time action profile on regional cerebral blood flow in the rat. Brain Res. 626, 117-126.
Steru, L., Chermat, R., Thierry, B., Mico, J. A., Lenegre, A., Steru, M., Simon, P. and Porsolt, R. D., 1987. The automated Tail Suspension Test: a computerized device which differentiates psychotropic drugs. Prog Neuropsychopharmacol Biol Psychiatry. 11, 659-671.
Stewart, W. F., Ricci, J. A., Chee, E., Hahn, S. R. and Morganstein, D., 2003. Cost of lost productive work time among US workers with depression. Jama. 289, 3135-3144.
Struhl, K., 1998. Histone acetylation and transcriptional regulatory mechanisms. Genes Dev. 12, 599-606.
Sun, W. and Rebec, G. V., 2003. Lidocaine inactivation of ventral subiculum attenuates cocaine-seeking behavior in rats. J Neurosci. 23, 10258-10264.
Swanson, L., 1999. Brain maps: structure of the rat brain, 2nd edition. Elsevier Science, Boston.
Tanis, K. Q. and Duman, R. S., 2007. Intracellular signaling pathways pave roads to recovery for mood disorders. Ann Med. 39, 531-544.
Tardito, D., Perez, J., Tiraboschi, E., Musazzi, L., Racagni, G. and Popoli, M., 2006. Signaling pathways regulating gene expression, neuroplasticity, and neurotrophic mechanisms in the action of antidepressants: a critical overview. Pharmacol Rev. 58, 115-134.
Thiagalingam, S., Cheng, K. H., Lee, H. J., Mineva, N., Thiagalingam, A. and Ponte, J. F., 2003. Histone deacetylases: unique players in shaping the epigenetic histone code. Ann N Y Acad Sci. 983, 84-100.
Thomson, S., Clayton, A. L., Hazzalin, C. A., Rose, S., Barratt, M. J. and Mahadevan, L. C., 1999. The nucleosomal response associated with immediate-early gene induction is mediated via alternative MAP kinase cascades: MSK1 as a potential histone H3/HMG-14 kinase. Embo J. 18, 4779-4793.
Timmusk, T., Palm, K., Metsis, M., Reintam, T., Paalme, V., Saarma, M. and Persson, H., 1993. Multiple promoters direct tissue-specific expression of the rat BDNF gene. Neuron. 10, 475-489.
Tremolizzo, L., Carboni, G., Ruzicka, W. B., Mitchell, C. P., Sugaya, I., Tueting, P., Sharma, R., Grayson, D. R., Costa, E. and Guidotti, A., 2002. An epigenetic mouse model for molecular and behavioral neuropathologies related to schizophrenia vulnerability. Proc Natl Acad Sci U S A. 99, 17095-17100.
Tsankova, N. M., Berton, O., Renthal, W., Kumar, A., Neve, R. L. and Nestler, E. J., 2006a. Sustained hippocampal chromatin regulation in a mouse model of depression and antidepressant action. Nat Neurosci. 9, 519-525.
Tsankova, N. M., Berton, O., Renthal, W., Kumar, A., Neve, R. L. and Nestler, E. J., 2006b. Sustained hippocampal chromatin regulation in a mouse model of depression and antidepressant action. Nat Neurosci.

Tsankova, N. M., Kumar, A. and Nestler, E. J., 2004. Histone modifications at gene promoter regions in rat hippocampus after acute and chronic electroconvulsive seizures. J Neurosci. 24, 5603-5610.

Tse, C., Sera, T., Wolffe, A. P. and Hansen, J. C., 1998. Disruption of higher-order folding by core histone acetylation dramatically enhances transcription of nucleosomal arrays by RNA polymerase III. Mol Cell Biol. 18, 4629-4638.

Turner, R., 1997. Signal sources in bold contrast fMRI. Adv Exp Med Biol. 413, 19-25.

Verdone, L., Caserta, M. and Di Mauro, E., 2005. Role of histone acetylation in the control of gene expression. Biochem Cell Biol. 83, 344-353.

Vermetten, E., Vythilingam, M., Southwick, S. M., Charney, D. S. and Bremner, J. D., 2003. Long-term treatment with paroxetine increases verbal declarative memory and hippocampal volume in posttraumatic stress disorder. Biol Psychiatry. 54, 693-702.

Vettese-Dadey, M., Grant, P. A., Hebbes, T. R., Crane- Robinson, C., Allis, C. D. and Workman, J. L., 1996. Acetylation of histone H4 plays a primary role in enhancing transcription factor binding to nucleosomal DNA in vitro. Embo J. 15, 2508-2518.

Vinet, J., Carra, S., Blom, J. M., Brunello, N., Barden, N. and Tascedda, F., 2004. Chronic treatment with desipramine and fluoxetine modulate BDNF, CaMKKalpha and CaMKKbeta mRNA levels in the hippocampus of transgenic mice expressing antisense RNA against the glucocorticoid receptor. Neuropharmacology. 47, 1062-1069.

Volkow, N. D., 2004. Cocaine Abuse and Addiction. In: National Insitute on Drug Abuse Research Report Series (ed. Volkow, N. D.).

Vorel, S. R., Liu, X., Hayes, R. J., Spector, J. A. and Gardner, E. L., 2001. Relapse to cocaine-seeking after hippocampal theta burst stimulation. Science. 292, 1175-1178.

Wang, G. G., Allis, C. D. and Chi, P., 2007a. Chromatin remodeling and cancer, Part I: Covalent histone modifications. Trends Mol Med. 13, 363-372.

Wang, G. G., Allis, C. D. and Chi, P., 2007b. Chromatin remodeling and cancer, Part II: ATP-dependent chromatin remodeling. Trends Mol Med. 13, 373-380.

Weaver, I. C., Cervoni, N., Champagne, F. A., D'Alessio, A. C., Sharma, S., Seckl, J. R., Dymov, S., Szyf, M. and Meaney, M. J., 2004. Epigenetic programming by maternal behavior. Nat Neurosci. 7, 847-854.

Weaver, I. C., Champagne, F. A., Brown, S. E., Dymov, S., Sharma, S., Meaney, M. J. and Szyf, M., 2005. Reversal of maternal programming of stress responses in adult offspring through methyl supplementation: altering epigenetic marking later in life. J Neurosci. 25, 11045-11054.

Wilson, M. C. and Schuster, C. R., 1972. The effects of chlorpromazine on psychomotor stimulant self-administration in the rhesus monkey. Psychopharmacologia. 26, 115-126.

Winder, D. G., Egli, R. E., Schramm, N. L. and Matthews, R. T., 2002. Synaptic plasticity in drug reward circuitry. Curr Mol Med. 2, 667-676.

Wittchen, H. U., Knauper, B. and Kessler, R. C., 1994. Lifetime risk of depression. Br J Psychiatry Suppl, 16-22.

Wolff, M., Gibb, S. J. and Dalrymple-Alford, J. C., 2006. Beyond spatial memory: the anterior thalamus and memory for the temporal order of a sequence of odor cues. J Neurosci. 26, 2907-2913.

Wong, M. L. and Licinio, J., 2004. From monoamines to genomic targets: a paradigm shift for drug discovery in depression. Nat Rev Drug Discov. 3, 136-151.

Wood, M. A., Kaplan, M. P., Park, A., Blanchard, E. J., Oliveira, A. M., Lombardi, T. L. and Abel, T., 2005. Transgenic mice expressing a truncated form of CREB-binding protein (CBP) exhibit deficits in hippocampal synaptic plasticity and memory storage. Learn Mem. 12, 111-119.

Wu, Z., Sullivan, JMJ., 2003. Multiple material marching cubes algorithm. International Journal for Numerical Methods in Engineering. 58, 189-207.

Xu, F., Gainetdinov, R. R., Wetsel, W. C., Jones, S. R., Bohn, L. M., Miller, G. W., Wang, Y. M. and Caron, M. G., 2000. Mice lacking the norepinephrine transporter are supersensitive to psychostimulants. Nat Neurosci. 3, 465-471.

Xu, Y., Ku, B., Cui, L., Li, X., Barish, P. A., Foster, T. C. and Ogle, W. O., 2007. Curcumin reverses impaired hippocampal neurogenesis and increases serotonin receptor 1A mRNA and brain-derived neurotrophic factor expression in chronically stressed rats. Brain Res. 1162, 9-18.

Xu, Y., Ku, B., Tie, L., Yao, H., Jiang, W., Ma, X. and Li, X., 2006. Curcumin reverses the effects of chronic stress on behavior, the HPA axis, BDNF expression and phosphorylation of CREB. Brain Res. 1122, 56-64.

Xu, Y., Ku, B. S., Yao, H. Y., Lin, Y. H., Ma, X., Zhang, Y. H. and Li, X. J., 2005. The effects of curcumin on depressive-like behaviors in mice. Eur J Pharmacol. 518, 40-46.

Yamada, M., Yamada, M. and Higuchi, T., 2005. Antidepressant-elicited changes in gene expression: remodeling of neuronal circuits as a new hypothesis for drug efficacy. Prog Neuropsychopharmacol Biol Psychiatry. 29, 999-1009.

Yamaguchi, M., Suzuki, T., Seki, T., Namba, T., Juan, R., Arai, H., Hori, T. and Asada, T., 2004. Repetitive cocaine administration decreases neurogenesis in adult rat hippocampus. Ann N Y Acad Sci. 1025, 351-362.

Yao, W. D., Gainetdinov, R. R., Arbuckle, M. I., Sotnikova, T. D., Cyr, M., Beaulieu, J. M., Torres, G. E., Grant, S. G. and Caron, M. G., 2004. Identification of PSD-95 as a regulator of dopamine-mediated synaptic and behavioral plasticity. Neuron. 41, 625-638.

Yasuda, S., Liang, M. H., Marinova, Z., Yahyavi, A. and Chuang, D. M., 2007. The mood stabilizers lithium and valproate selectively activate the promoter IV of brain-derived neurotrophic factor in neurons. Mol Psychiatry.

Yildirim, E., Zhang, Z., Uz, T., Chen, C. Q., Manev, R. and Manev, H., 2003. Valproate administration to mice increases histone acetylation and 5-lipoxygenase content in the hippocampus. Neurosci Lett. 345, 141-143.

Ying, M., Xu, R., Wu, X., Zhu, H., Zhuang, Y., Han, M. and Xu, T., 2005. Sodium butyrate ameliorates histone hypoacetylation and neurodegenerative phenotypes in a mouse model for DRPLA. J Biol Chem.

Yokel, R. A. and Wise, R. A., 1976. Attenuation of intravenous amphetamine reinforcement by central dopamine blockade in rats. Psychopharmacology (Berl). 48, 311-318.

Zarate, C. A., Jr. and Quiroz, J. A., 2003. Combination treatment in bipolar disorder: a review of controlled trials. Bipolar Disord. 5, 217-225.

Zarate, C. A., Jr., Singh, J. and Manji, H. K., 2006. Cellular Plasticity Cascades: Targets for the Development of Novel Therapeutics for Bipolar Disorder. Biol Psychiatry.

Zisook, S., Rush, A. J., Haight, B. R., Clines, D. C. and Rockett, C. B., 2006. Use of bupropion in combination with serotonin reuptake inhibitors. Biol Psychiatry. 59, 203-210.